Supporting information

Remodeling of N-Heterocyclic Iminato Ligand Frameworks for the Facile Synthesis of Isoureas from Alcohols and Carbodiimides Promoted by Organoactinide (Th, U) Complexes

Konstantin Makarov, Sayantani Saha, Tapas Ghatak, Natalia Fridman, and Moris S. Eisen*
Schulich Faculty of Chemistry, Technion − Israel Institute of Technology, Technion City, 3200008, Israel
E-mail: chmoris@ttechnion.ac.il
Fax: + 972-4-8295703; Tel: + 972-4-8292680

Table of Contents

1. Experimental Section

1.1. General Procedures and Materials. All manipulations of air-sensitive materials were performed with the rigorous exclusion of oxygen and moisture in flamed Schlenk-type glassware or J-Young Teflon valve-sealed NMR tubes on a dual manifold Schlenk line interfaced to a high vacuum (10^{-5} Torr) line, or in a nitrogen-filled Innovative Technologies glovebox with a medium-capacity recirculator (1 – 2 ppm of O_2). Argon and nitrogen were purified by passage through MnO oxygen-removal column and a Davison 4Å molecular sieve column. Hydrocarbon solvents benzene-d_6 (Cambridge Isotopes), were distilled under vacuum from Na/K alloy and degassed by three freeze-pump-thaw cycles prior to use. 1,3-diisopropyl carbodiimide (DIC) (Sigma Aldrich) was dried by vacuum transfer. 1,3-di-*p*-tolyl carbodiimide (DTC) (Sigma Aldrich) and 1,3-di-cyclohexyl carbodiimide (DCC) were dried overnight on a high vacuum line (10-5torr) and stored in a glovebox before use. Other carbodiimides, including 1,3-di-(2,4,6-trimethylphenyl) carbodiimide, 1,3-di-(2,6 diisopropylphenyl) carbodiimide, 1,3-di-p-methoxyphenyl carbodiimide, 1,3-di-*o*-tolyl carbodiimide, N-(2,6-diisopropylphenyl)-N'-phenyl carbodiimide, N-(2,4,6-trimethylphenyl)-N'- phenyl carbodiimide were synthesized according to previous reports.[1,2] liquid alcohols were distilled from CaH_2 prior to use and stored over 4Å molecular sieves. Solid alcohols (Sigma Aldrich) were dried overnight on a high vacuum line (10^{-5} torr). The actinide complex precursors, $[(Me_3Si)_2N]_2An[\kappa^2\text{-}(N,C)CH_2Si(CH_3)_2N(SiMe_3)]$, (An=Th, U), (thorium and uranium metallacycles), were prepared according to published procedures.[3] N^2-isopropyl-[1,1'-biphenyl]-2,2'-diamine and ligands L^1H and L^2H, actinide complexes Th-1, U-1, and Th-2, were synthesized according to our previous reports.[4–6] NMR spectra were recorded on Bruker Advance 300, and 500, Bruker Advance III 400, and 600 spectrometers on crude reaction mixtures. Chemical shifts for ^1H and ^{13}C NMR are referenced to internal protiosolvent and reported relative to tetramethylsilane. J-values are reported for ^1H NMR coupling constants in the unit of Hertz (Hz). MS experiments were performed at 200 °C (source temperature) on a Maxis Impact (Bruker) mass spectrometer with an APCI solid probe method. The single-crystal material was immersed in perfluoropolyalkylether and was quickly fished with a glass rod and mounted on a Kappa CCD diffractometer under a cold stream of nitrogen. Data collection was performed using monochromated Mo Kα radiation using φ and ω scans to cover the Ewald sphere. Accurate cell parameters were obtained with the amount of indicated reflections.[7] The structure was solved by SHELXS-97 direct methods and refined by the SHELXL97 program package.[8,9] The atoms were refined anisotropically. Hydrogen atoms were included using the riding model. Figures were drawn (50% probability thermal ellipsoids) using Diamond V3.1.

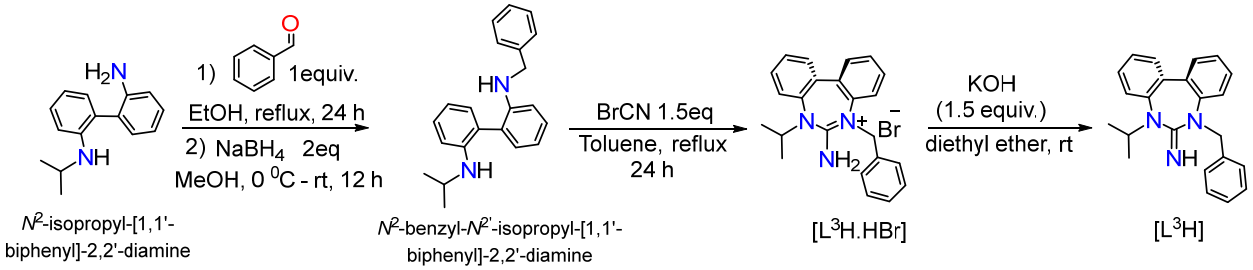

Scheme S1. Schematic diagram of synthesis of ligands L^3H.

1.2. Synthesis of N^2-benzyl-$N^{2'}$-isopropyl-[1,1'-biphenyl]-2,2'-diamine. A mixture of benzaldehyde (0.45 mL, 4.42 mmol) and N^2-isopropyl-[1,1'-biphenyl]-2,2'-diamine (a) (1 g, 4.42 mmol) in ethanol (50 mL) was refluxed for 24 h. Next, the solvent was removed, and the intermediate imine product was re-dissolved in MeOH (30 mL). The reaction mixture was then cooled to 0 °C and $NaBH_4$ (0.37 g, 9.72 mmol) was added slowly. The mixture was allowed to reach room temperature and stirred for 12 h. 2 M aqueous NaOH solution (50 mL) was added, and the aqueous and organic layers separated. The aqueous layer was extracted with EtOAc (3 x 20 mL). The combined organic layers were washed with brine, dried over anhydrous $MgSO_4$ and the solvent was removed under reduced pressure. The product was purified by column chromatography (neutral Al_2O_3) using hexane and ethyl acetate as eluant (85:15). Yield: 1.18 g (85%). ^{1}H NMR (400 MHz, $CDCl_3$) δ 7.34 (d, *J* = 4.4 Hz, 4H, Ar*H*), 7.30 – 7.21 (m, 3H, Ar*H*), 7.18 – 7.10 (m, 2H, Ar*H*), 6.80 (t, *J* = 7.7 Hz, 3H, Ar*H*), 6.68 (d, *J* = 8.1 Hz, 1H, Ar*H*), 4.39 (s, 2H, -*CH*-Bn), 4.30 (s, 1H, NH), 3.71 (sept, *J* = 7.7 Hz, 1H), 3.59 (s, 1H, NH), 1.19 (d, *J* = 7.7 Hz, 3H, -CH(*CH*$_3$)$_2$), 1.17 (d, *J* =7.7 Hz, 3H, -CH(*CH*$_3$)$_2$). ^{13}C NMR (100 MHz, $CDCl_3$, 294 K): δ 145.6, 145.2, 139.7, 1 1.3, 131.1, 129.1, 129.0, 128.5, 126.98, 126.96, 124.1, 117.3, 116.8, 111.2, 110.8, 47.8, 44.2, 22.9 ppm. ESI-MS: m/z, 317.2057 $[M+H]^+$. Anal. Calcd for $C_{22}H_{24}N_2$: C, 83.49; H, 7.65; N, 8.86; Found: C, 83.40; H, 7.56; N, 8.95.

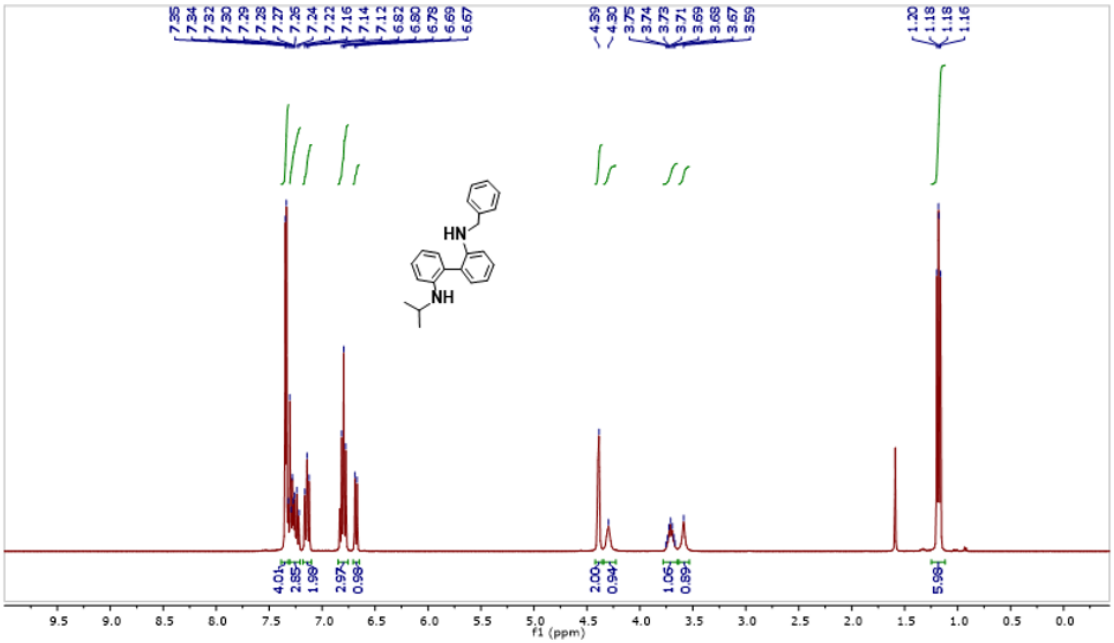

Figure S1. ^{1}H NMR of N^{2}-benzyl-$N^{2'}$-isopropyl-[1,1'-biphenyl]-2,2'-diamine in $CDCl_3$.

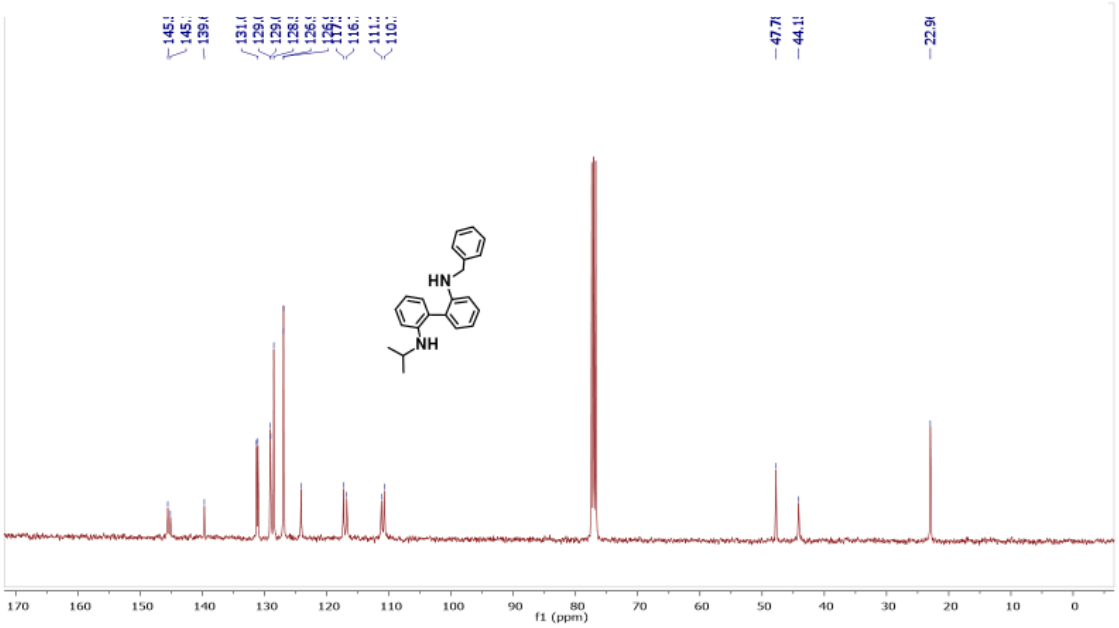

Figure S2. ^{13}C NMR of N^{2}-benzyl-$N^{2'}$-isopropyl-[1,1'-biphenyl]-2,2'-diamine in $CDCl_3$.

1.3. Synthesis of [L^{3}H.HBr]. A solution of cyanogen bromide (0.46 g, 4.34 mmol) in toluene (50 mL) was added dropwise to a stirred solution of N^2-benzyl-N$^{2'}$-isopropyl-[1,1'-biphenyl]-2,2'-diamine (0.92 g, 2.91 mmol) in toluene at 110 °C. After complete addition, the mixture was stirred at 110 °C for 12 h. The reaction mixture was cool to room temperature. The volume of toluene was reduced to about 5 mL by a rotary evaporator and 100 mL of diethyl ether was added to get solid precipitate. The precipitate was filtrated and washed with diethyl ether (3 × 30 mL) and dried in vacuum, to afford a white solid. Yield: 1.10 g (90%). ^{1}H NMR (400 MHz, $CDCl_3$, 294 K): δ 9.57 (br, 2H, -NH_2), 7.66 (d, J = 8.0 Hz, 1H, Ar*H*), 7.54-7.48 (m, 4H, Ar*H*), 7.44-7.39 (m, 2H, Ar*H*), 7.35-7.32 (m, 1H, Ar*H*), 7.06-7.02 (m, 1H, Ar*H*), 6.96 (t, J = 4.0 Hz, 2H, Ar*H*), 6.75 (d, J = 8.0 Hz, 2H, Ar*H*), 5.54 (d, J = 16.0 Hz, 1H, -*CH*$_2$-Bn), 5.17 (d, J = 16.0 Hz, 1H, -*CH*$_2$-Bn), 4.70 (sept, J = 8.0 Hz, 1H, -*CH*(CH_3)$_2$), 1.51 (d, J = 8.0 Hz, 3H, -CH(*CH*$_3$)$_2$), 0.86 (d, J = 8.0 Hz, 3H, -CH(*CH*$_3$)$_2$). ^{13}C NMR (100 MHz, $CDCl_3$, 294 K): δ 165.2, 142.2, 138.9, 136.6, 134.9, 133.9, 129.4, 128.9, 128.6, 128.5, 128.2, 127.9, 127.7, 127.6, 127.5, 127.4, 124.5, 55.7, 54.8, 23.9, 21.8 ppm. ESI-MS: m/z, 342.2007 $[M+H]^+$. Anal. Calcd for $C_{23}H_{24}N_3Br$: C, 65.54; H, 5.74; N, 9.98; Found: C, 64.95; H, 5.82; N, 9.77.

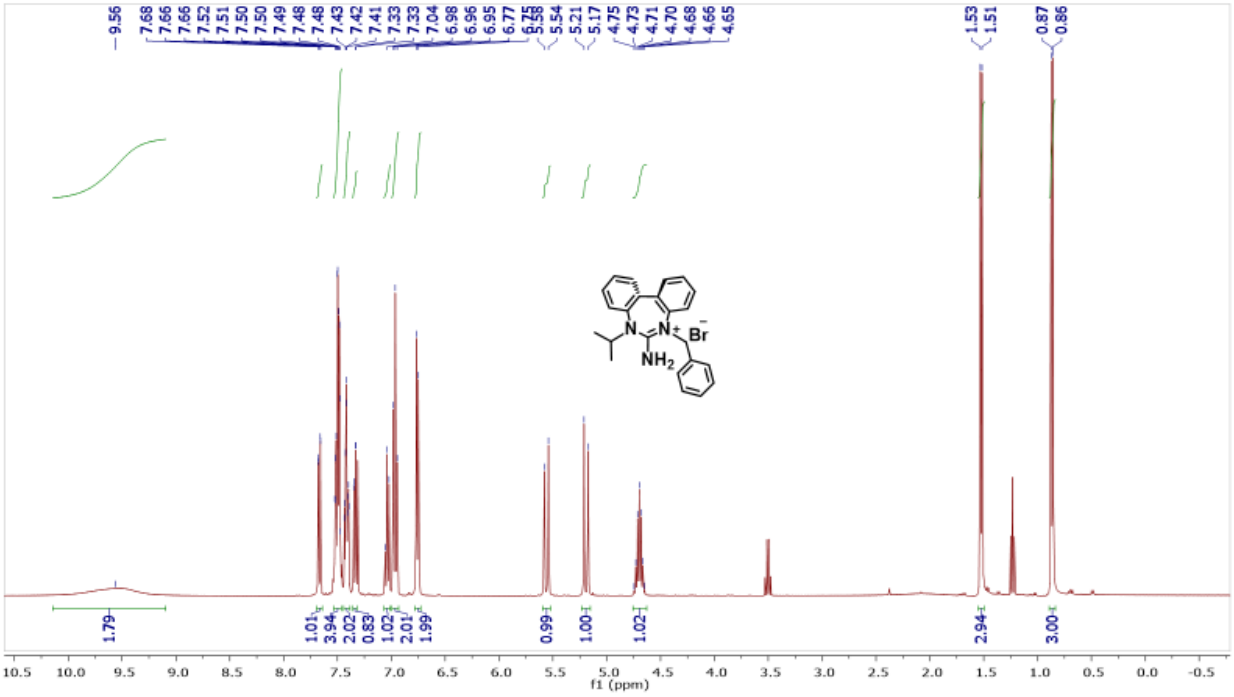

Figure S3. ^{1}H NMR of L^{3}H.HBr in $CDCl_3$.

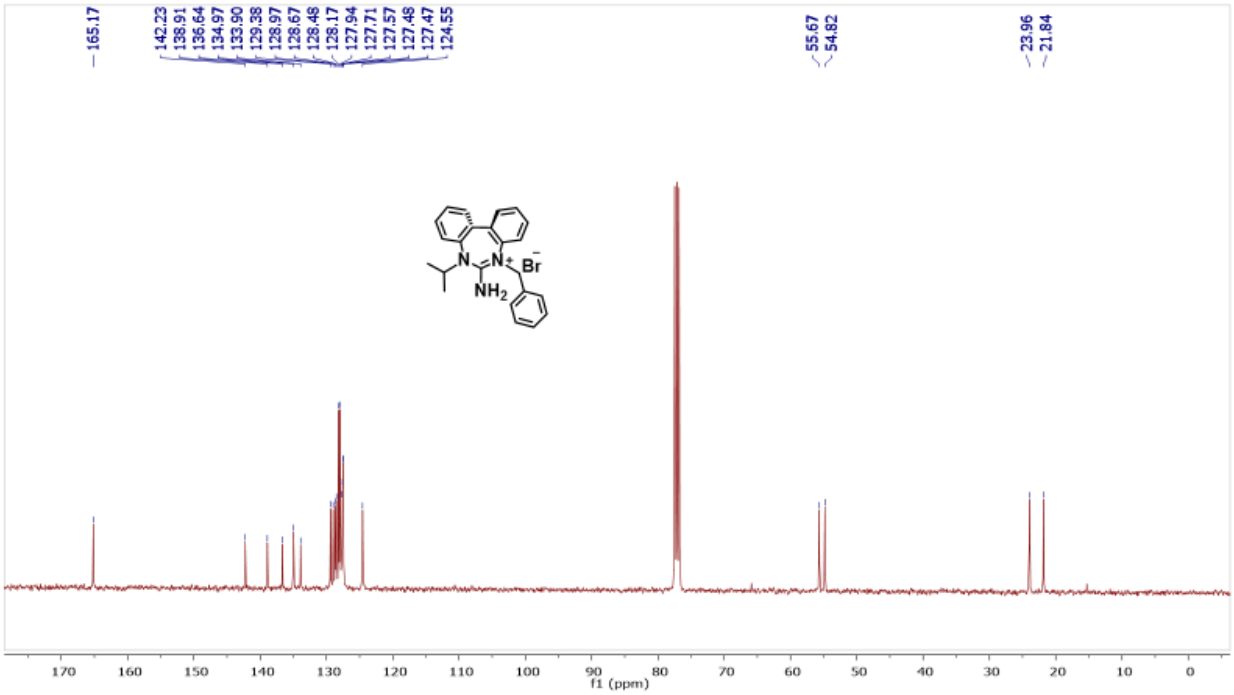

Figure S4. ^{13}C NMR of L^{3}H.HBr in $CDCl_3$.

1.4. Synthesis of L^{3}H. Aqueous KOH (0.25 g, 4.44 mmol) was added to a diethyl ether (50 mL) suspension of L^{3}H.HBr (1 g, 2.22 mmol), and the mixture was vigorously stirred for 30 min at room temperature. In a separatory funnel, the two layers were separated, and the ether layer was separated and washed with distilled water (3 x 20ml). The ether layer was dried over anhydrous $MgSO_4$ and the solvent was removed under reduced pressure. Yield: 0.72 g (95%). ^{1}H NMR (400 MHz, $CDCl_3$, 294 K): δ 7.38 (t, J = 7.5 Hz, 2H, Ar*H*), 7.34 – 7.26 (m, 2H, Ar*H*), 7.23 (m, 2H, Ar*H*), 7.15 (m, 2H, Ar*H*), 7.09 (m, 2H, Ar*H*), 6.98 (m, 3H, Ar*H*), 6.79 (m, 2H, Ar*H*), 5.01 (d, J = 15.4 Hz, 1H, -*CH*$_2$-Bn), 4.63 (d, J = 15.4 Hz, 1H, -*CH*$_2$-Bn), 3.99 (br, 1H, -*CH*$(CH_3)_2$), 1.27 (d, J = 6.5 Hz, 3H, -CH(*CH*$_3$)$_2$), 0.86 (d, J = 6.5 Hz, 3H, -CH(*CH*$_3$)$_2$). ^{13}C NMR (100 MHz, $CDCl_3$,294 K): δ 166.90, 144.58, 142.18, 138.06, 137.49, 135.15, 128.40, 128.22, 128.10, 127.78, 127.55, 127.12, 126.59, 125.94, 125.27, 124.84, 121.49, 52.62, 50.53, 23.63, 21.79. ESI-MS: m/z, 342.1974 [M+H]+. Anal. Calcd for $C_{23}H_{23}N_3$: C, 80.90; H, 6.79; N, 12.31; Found: C, 79.93; H, 7.13; N, 12.15.

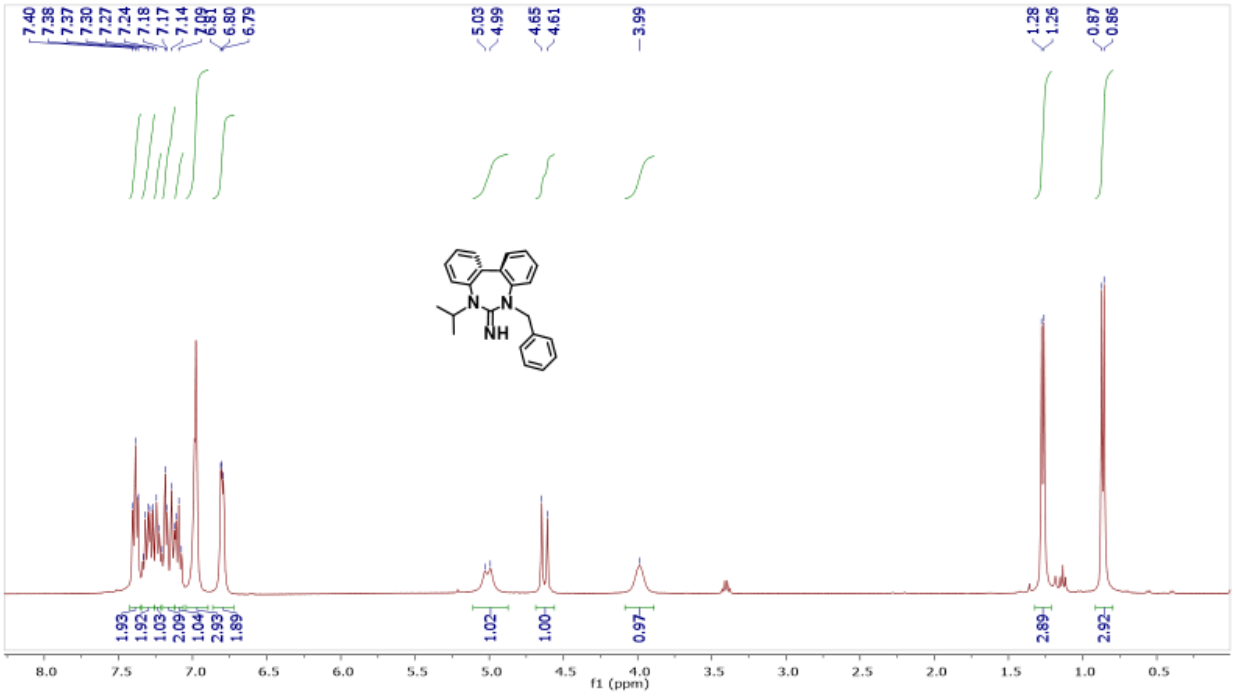

Figure S5. ^{1}H NMR of L^{3}H in $CDCl_3$.

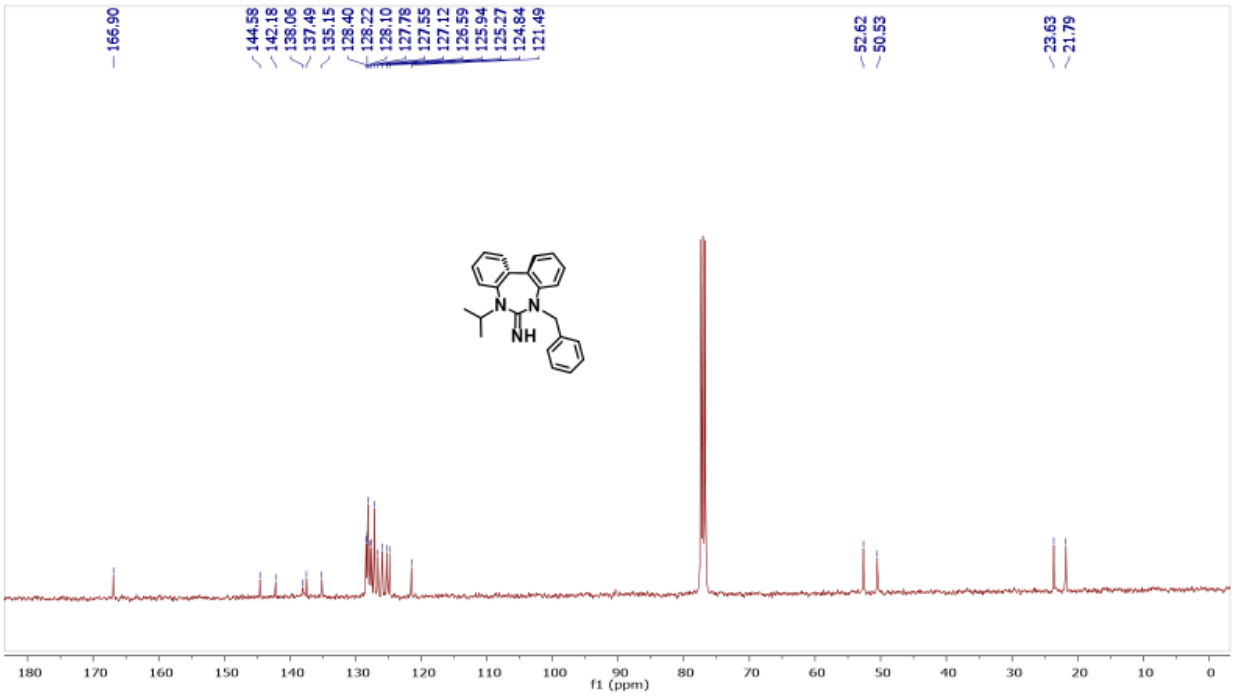

Figure S6. ^{13}C NMR of L^{3}H in $CDCl_3$.

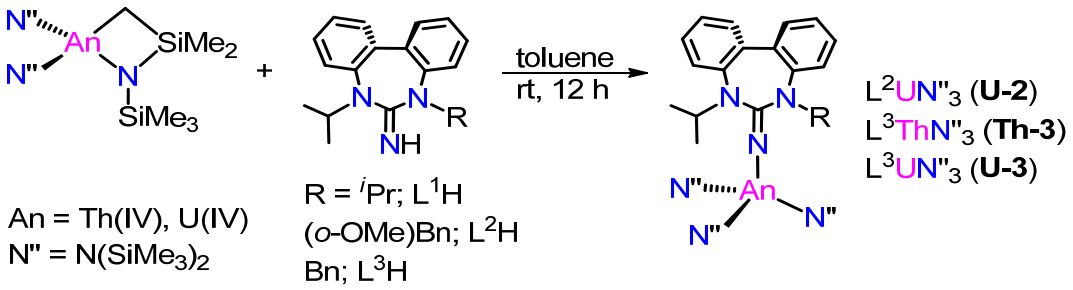

Scheme S2. General synthetic procedure for compounds **U-2, Th-3** and **U-3**.

1.5. Synthesis of Complex U-2 [(L²)U{N(SiMe₃)₂}₃]. To a solution of uranium metallacycle (0.10 g, 1.4 mmol) in 5 mL toluene was added dropwise a 5 mL toluene solution of the ligand L^2H (51.7 mg, 1.4 mmol). The reaction mixture was stirred at room temperature for 12 h and the solvent was removed under high vacuum. X-ray quality crystals of **U-2** were grown from a toluene/hexane mixture at −35 ºC. Yield: 134 mg (88%). ^{1}H NMR (500 MHz, C_6D_6) δ 25.30 (s, 1H, Ar*H*), 24.15 (s, 2H, Ar*H*), 13.57 (s, 1H, Ar*H*), 11.99 (t, *J* = 7.4 Hz, 1H, Ar*H*), 11.84 (d, *J* = 8.3 Hz, 1H, Ar*H*), 11.81 (d, *J* = 8.3 Hz, 1H, Ar*H*), 11.10 (d, *J* = 7.4 Hz, 1H, Ar*H*), 9.77 (t, *J* = 8.1 Hz, 1H, Ar*H*), 8.92 (dd, *J* = 8.1, 5.5 Hz, 1H, Ar*H*), 7.69 (s, 3H, Ar*H*), 6.63 (t, *J* = 5.5 Hz, 1H, Ar*H*), 0.15 (s, 3H, -O*CH*$_3$), -8.06 (s, 3H, -CH(*CH*$_3$)$_2$), -8.79 (s, 3H, -CH(*CH*$_3$)$_2$), -9.44 (s, 54H, -N(TMS)$_2$). ^{13}C NMR (126 MHz, C_6D_6) δ 169.89, 165.02, 159.24, 147.74, 146.33, 139.79, 139.15, 133.69, 132.06, 131.06, 129.32, 129.29, 128.56, 128.33, 125.69, 125.44, 121.78, 120.18, 59.42, 21.42, 14.30, 2.64. HRMS (APCI): m/z = 1088.5326 $(M+H)^+$.

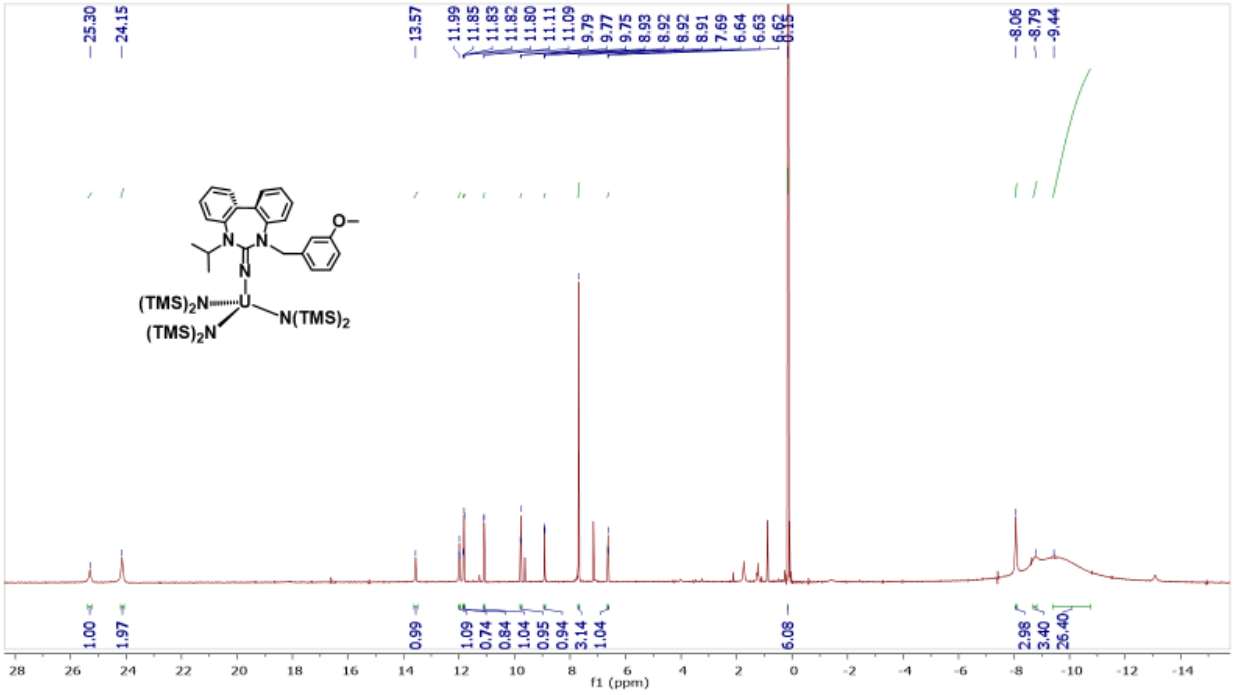

Figure S7. ^{1}H NMR of **U-2** in C_6D_6.

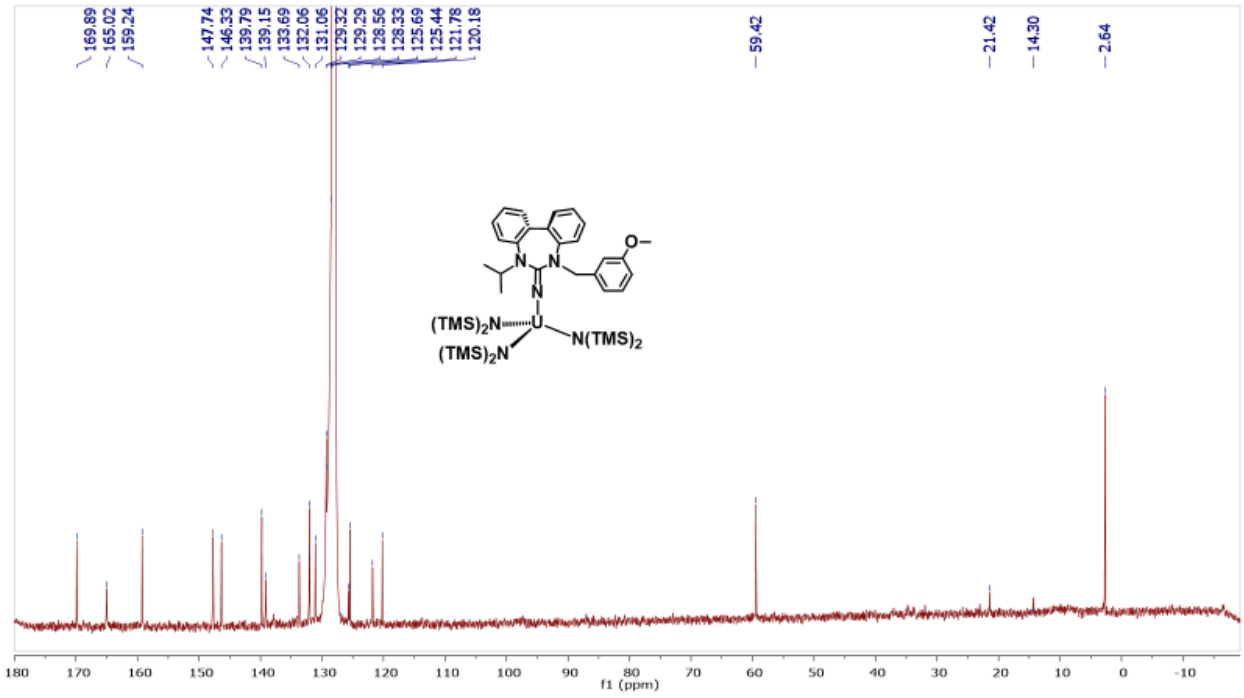

Figure S8. ^{13}C NMR of **U-2** in C_6D_6.

1.6. Synthesis of Complex Th-3 [(L^3)Th{N(SiMe$_3$)$_2$}$_3$]. The reaction of ligand L^3H (47.5 mg, 1.4 mmol) and thorium metallacycle (0.10 g, 1.4 mmol) was carried out following a similar procedure described for the synthesis of complex **U-2**. Yield: 133 mg (90%). ^{1}H NMR (300 MHz, C_6D_6) δ 7.37 – 7.22 (m, 3H, Ar*H*), 7.15 (m, 4H, Ar*H*), 6.97 (m, 3H, Ar*H*), 6.88 – 6.65 (m, 3H, Ar*H*), 5.56 (d, *J* = 15.2 Hz, 1H, -*CH*$_2$-Bn), 5.00 (d, *J* = 15.2 Hz, 1H, -*CH*$_2$-Bn), 4.71 (q, *J* = 6.5 Hz, 1H, -*CH*(CH$_3$)$_2$), 1.19 (d, *J* = 6.5 Hz, 3H, -CH(*CH*$_3$)$_2$), 0.62 (d, *J* = 6.5 Hz, 3H, -CH(*CH*$_3$)$_2$), 0.44 (s, 54H, -N(TMS)$_2$). ^{13}C NMR (126 MHz, C_6D_6) δ 156.30, 143.23, 140.36, 139.48, 137.88, 135.72, 129.34, 129.17, 128.61, 128.45, 128.35, 127.77, 127.41, 127.18, 127.11, 126.74, 125.70, 124.79, 121.86, 52.81, 51.02, 23.77, 22.95, 4.92, * = solvent impurity peaks. HRMS (APCI): m/z = 980.4727 $(M+H)^+$-SiMe$_3$.

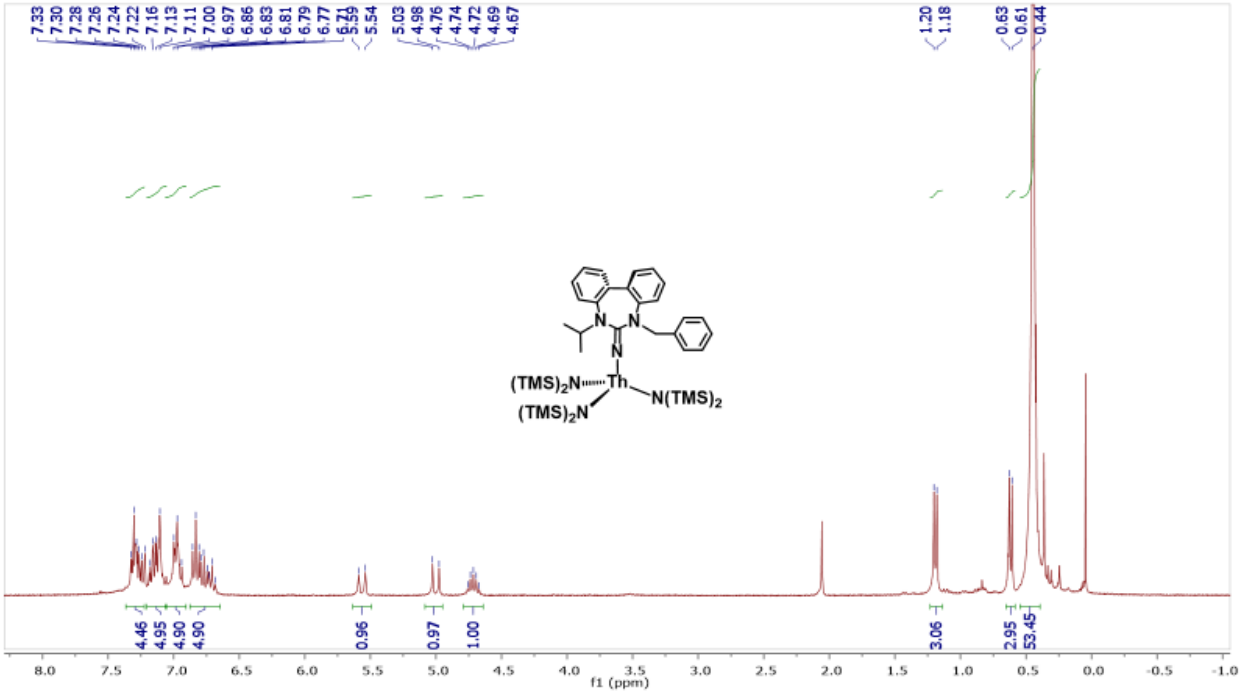

Figure S9. ^{1}H NMR of **Th-3** in C_6D_6.

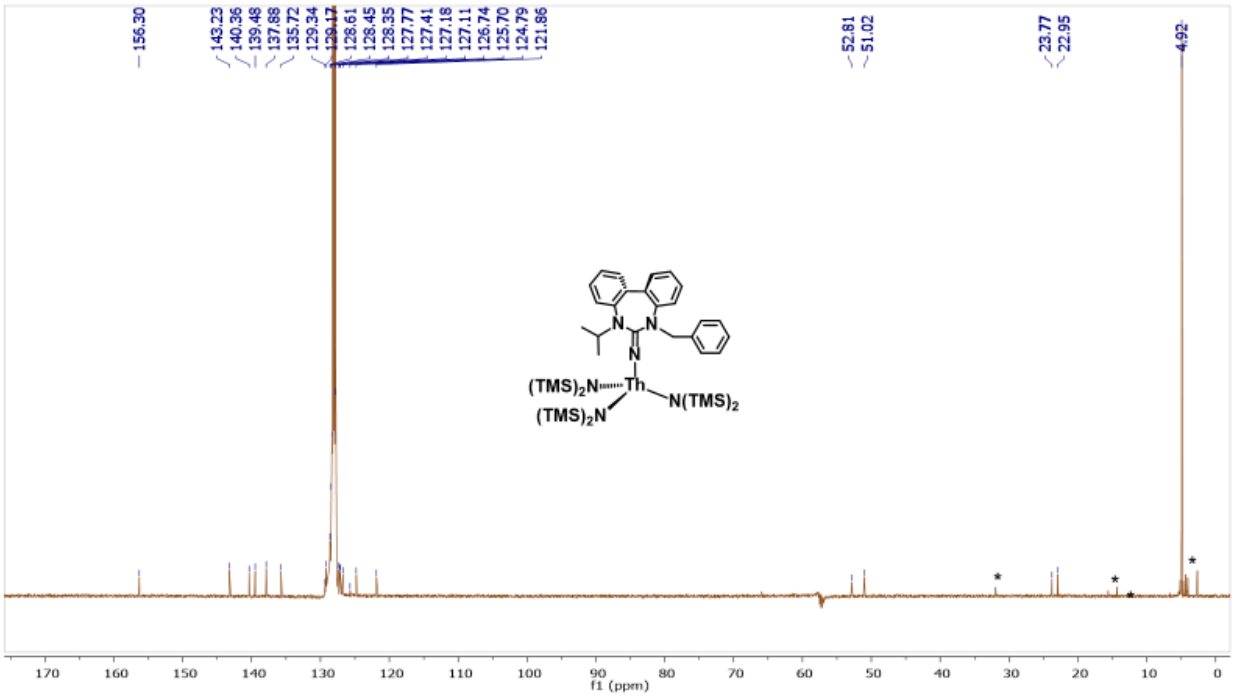

Figure S10. ^{13}C NMR of **Th-3** in C_6D_6.

1.7. Synthesis of Complex U-3 [(L^3)U{N(SiMe$_3$)$_2$}$_3$]. The reaction of ligand L^{3}H (47.5 mg, 1.4 mmol) and thorium metallacycle (0.10 g, 1.4 mmol) was carried out following a similar procedure described for the synthesis of complex **U-2**. Yield: 113 mg (76%). ^{1}H NMR (300 MHz, C_6D_6) δ 25.84 (s, 1H, Ar*H*), 24.88 (s, 2H, Ar*H*), 13.82 (t, *J* = 7.1 Hz, 2H, Ar*H*), 12.17 (dt, *J* = 14.9, 7.1 Hz, 2H, Ar*H*), 12.01 (dd, *J* = 7.7, 1.5 Hz, 1H, Ar*H*), 11.26 (dd, *J* = 7.7, 1.5 Hz, 1H, Ar*H*), 9.87 (t, *J* = 7.7 Hz, 1H, Ar*H*), 9.03 (t, *J* = 7.1 Hz, 1H, Ar*H*), 6.62 (t, *J* = 7.1 Hz, 1H, Ar*H*), 0.12 (s, 1H, -*CH*(CH$_3$)$_2$), -8.02 (s, 3H, -CH(*CH$_3$*)$_2$), -8.69 (s, 3H, -CH(*CH$_3$*)$_2$), -9.87, -12.01 (m, 54H, -N(TMS)$_2$). ^{13}C NMR (151 MHz, Tol-d$_8$) δ 163.31, 159.49, 147.91, 146.50, 144.50, 139.76, 137.68, 134.58, 133.41, 131.55, 130.76, 129.21, 119.88, 65.64, 31.69, 22.74, 15.20, 13.98, 13.98, 2.23. HRMS (APCI): m/z 1058.5203 (M+H)$^+$.

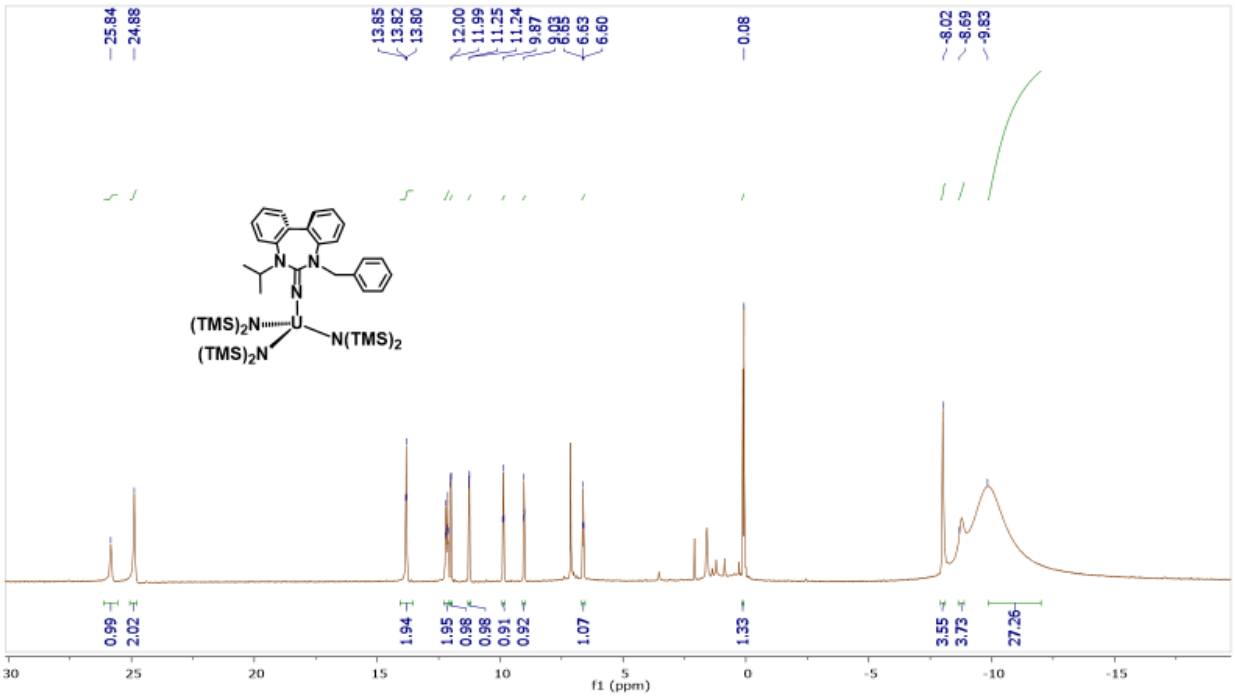

Figure S11. ^{1}H NMR of **U-3** in C_6D_6.

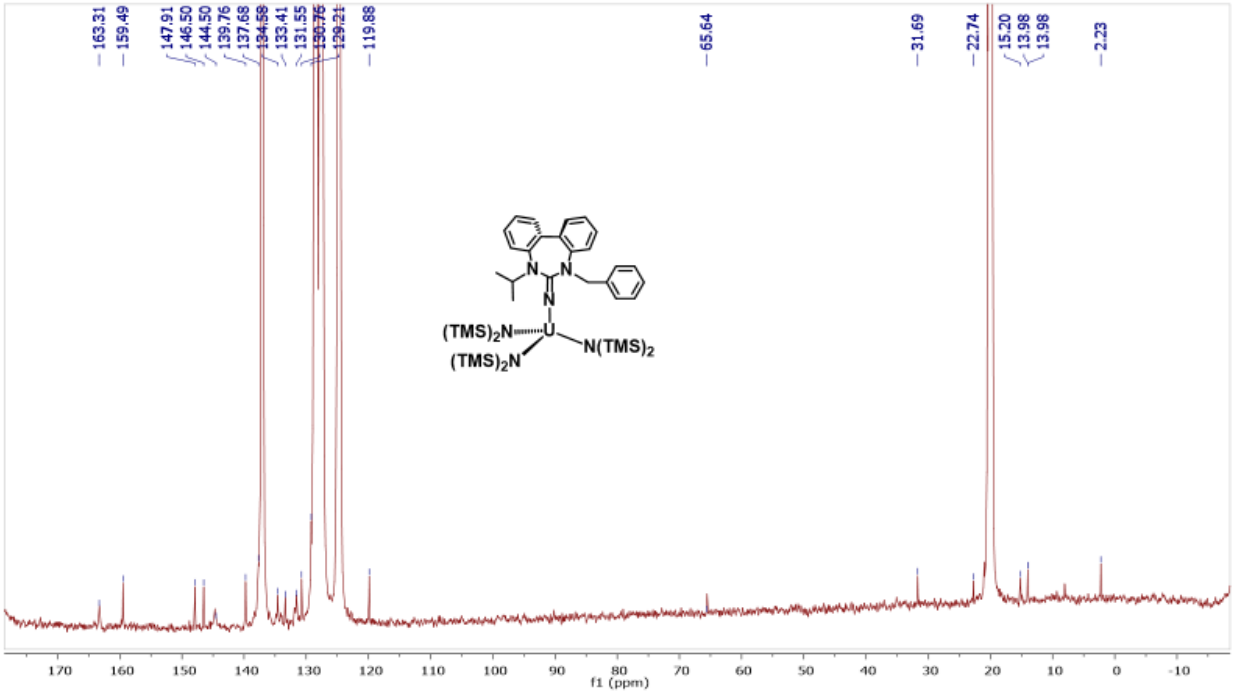

Figure S12. ^{13}C NMR of **U-3** in Tol-d_8.

1.8. Crystallographic data of U-2, Th-3 and U-3.

Table S1. Selected Bond Lengths (Å) and Angles (deg) for complexes **U-2**, **Th-3,** and **U-3**.

Complex	**U-2**	**Th-3**	**U-3**
An-N1	2.140(9)	2.129(7)	2.204(3)
An-N4	2.298(8)	2.285(7)	2.364(4)
An-N5	2.261(8)	2.287(8)	2.355(3)
An-N6	2.283(8)	2.309(7)	2.334(4)
C1-N1	1.292(12)	1.305(11)	1.271(5)
An-N1-C1	165.6(8)	165.6(7)	164.5(3)
N1-An-N4	103.1(3)	118.3(3)	114.27(13)
N1-An-N5	92.7(3)	92.2(3)	104.39(12)
N1-An-N6	117.7(3)	103.5(3)	93.66(13)
N4-An-N5	119.4(3)	117.6(3)	107.15(12)
N4-An-N6	107.2(3)	106.8(3)	117.46(12)
N5-An-N6	115.9(3)	117.5(3)	118.71(14)

Table S2. Crystallographic data of complexes **U-2**, **Th-3,** and **U-3**.

	U-2	**Th-3**	**U-3**
Empirical formula	$C_{42}H_{78}N_6OSi_6U$	$C_{41}H_{76}N_6Si_6Th$	$C_{41}H_{76}N_6Si_6U$
Formula weight	1089.67	1053.65	1059.64
Temperature/K	200.15	200.15	200.15
Crystal system	triclinic	triclinic	triclinic
Space group	P-1	P-1	P-1
a/Å	11.231(3)	11.2761(14)	11.202(3)
b/Å	13.900(5)	13.825(2)	13.817(4)
c/Å	19.161(5)	19.081(2)	19.030(7)
α/°	69.259(10)	69.338(4)	69.497(7)
β/°	83.307(7)	83.924(3)	83.942(6)
γ/°	71.538(6)	71.128(2)	71.051(5)
Volume/Å^3	2653.3(13)	2633.5(7)	2609.4(14)
Z	2	2	2
ρ_{calc}g/cm^3	1.364	1.329	1.349
μ/mm^{-1}	3.229	3.000	3.280
F(000)	1112.0	1076.0	1080.0
Crystal size/mm^3	0.09 × 0.06 × 0.06	0.21 × 0.12 × 0.09	0.24 × 0.09 × 0.09
Radiation	MoKα (λ = 0.71073)	MoKα (λ = 0.71073)	MoKα (λ = 0.71073)
2Θ range for data collection/°	2.272 to 50.752	3.308 to 50.562	2.284 to 50.52
Index ranges	-13 ≤ h ≤ 13, -16 ≤ k ≤ 16, -22 ≤ l ≤ 22	-13 ≤ h ≤ 13, -16 ≤ k ≤ 16, -22 ≤ l ≤ 22	-13 ≤ h ≤ 13, -16 ≤ k ≤ 16, -22 ≤ l ≤ 22
Reflections collected	22550	26293	29328
Independent reflections	9525 [R_{int} = 0.1176, R_{sigma} = 0.3473]	9476 [R_{int} = 0.1186, R_{sigma} = 0.1025]	9264 [R_{int} = 0.1199, R_{sigma} = 0.2070]
Data/restraints/parameters	9525/7/424	9476/0/507	9264/0/411
Goodness-of-fit on F^2	0.644	0.829	0.838
Final R indexes [I>=2σ (I)]	R_1 = 0.0564, wR_2 = 0.0965	R_1 = 0.0352, wR_2 = 0.0697	R_1 = 0.0645, wR_2 = 0.1206
Final R indexes [all data]	R_1 = 0.1601, wR_2 = 0.1285	R_1 = 0.0483, wR_2 = 0.0734	R_1 = 0.1120, wR_2 = 0.1372
Largest diff. peak/hole/e Å^{-3}	0.93/-1.70	1.64/-1.15	2.18/-2.67

[a] $R_1 = \Sigma ||F_o| - |F_c||/\Sigma|F_o|$ with $F_o^2 > 2\sigma(F_o^2)$. $wR_2 = [\Sigma w(|F_o^2| - |F_c^2|)^2/\Sigma|F_o^2|^2]^{1/2}$

1.9. General procedure for the catalytic addition of alcohols into carbodiimides. A sealable J. Young NMR tube was loaded with 2 μmol of the desired catalyst from a stock solution in C_6D_6 inside the glove box, followed by the addition of carbodiimide (100 equiv.) and alcohols (100 equiv.) the reaction was diluted to 550 μL with C_6D_6. Samples were taken out of the glove box and the reaction progress was monitored by ^{1}H NMR spectroscopy. The yields were determind from ^{1}H NMR versus 1,3,5-trimethoxybenzene (59.5 μmol) as internal standard. The crude mixtures were analyzed using ^{1}H NMR, the values were compared to previous literature.[10] Unreported products were characterized by ^{1}H, and ^{13}C- NMR, and MS. All isourea products are unstable under air and moisture sensitive, they should be stored under an inert atmosphere.

Scale-up reaction: In the glovebox, in a sealed vial, 9.0 mg of catalyst Th-1 (9.0 μmol, 1 mol %), DTC (0.200g, 0.9 mmol), and ^{i}PrOH (69 μL, 0.9 mmol) were disoloved in C_6D_6 (2 ml). the reaction was completed affter 3 hours of stiring at RT. The solvent was removed under reduced pressure. The residue dried to afford the final product (Entry c, Table 2) as yellowish oil in 92 % isolated yield.

1.10. Characterization data of the addition products.

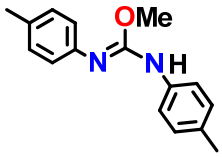

(Entry 1-6, Table 1): ^{1}H NMR (300 MHz, C_6D_6) δ 7.08 – 6.97 (m, 4H), 6.82 (t, *J* = 8.6 Hz, 2H), 6.73 (d, *J* = 7.8 Hz, 2H), 5.86 (s, 1H), 3.73 (s, 3H), 2.16 (s, 3H), 2.05 (s, 3H). The NMR spectra are matching with those reported in the literature.

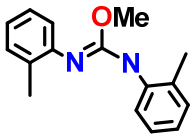

(Entry 8-9, Table 1): ^{1}H NMR (300 MHz, C_6D_6) δ 7.02 (d, *J* = 4.0 Hz, 4H), 6.82 (t, *J* = 8.5 Hz, 2H), 6.73 (d, *J* = 7.7 Hz, 2H), 5.87 (s, 1H), 3.73 (s, 3H), 2.16 (s, 3H), 2.05 (s, 3H). ^{13}C NMR (101 MHz, C_6D_6) δ 150.85, 146.34, 136.69, 132.52, 132.09, 130.69, 129.56, 122.96, 121.15, 53.68, 20.84, 20.68. MS (APCI): m/z 255.1522 (M+H)*.

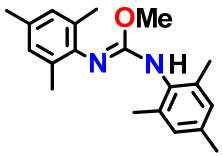

(Entry. 10-11, Table 1): ^{1}H NMR (300 MHz, C_6D_6) δ 6.95 (s, 2H), 6.66 (s, 2H), 4.55 (s, 1H), 3.66 (s, 3H), 2.36 (s, 6H), 2.28 (s, 3H), 2.09 (s, 3H), 2.04 (s, 6H). The NMR spectra are matching with those reported in the literature.

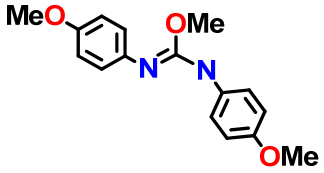

(Entry 14-15, Table 1): ^{1}H NMR (300 MHz, C_6D_6) δ 7.03 (dd, J = 9.5, 2.8 Hz, 2H), 6.84 (d, J = 8.4 Hz, 2H), 6.77 (d, J = 8.5 Hz, 2H), 6.68 – 6.59 (m, 2H), 5.79 (s, 1H), 3.75 (s, 3H), 3.37 (s, 3H), 3.27 (s, 3H). The NMR spectra are matching with those reported in the literature.

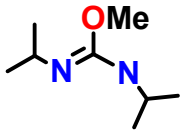

(Entry 16-17, Table 1): ^{1}H NMR (300 MHz, C_6D_6) δ 3.80 – 3.68 (m, 1H), 3.67 (s, 3H), 3.11 (m, 1H), 1.23 (d, J = 6.2 Hz, 6H), 0.89 (d, J = 6.2 Hz, 6H). The NMR spectra are matching with those reported in the literature.

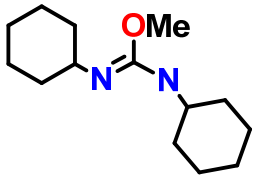

(Entry 18-19 , Table 1): ^{1}H NMR (300 MHz, C_6D_6) δ 3.69 (s, 3H), 3.47 (m, 1H), 2.95 (m, 1H), 1.83 (m, 2H), 1.57 (m, 2H), 1.38 – 1.20 (m, 2H), 1.03 (m, 2H), 0.84 m, 2H). The NMR spectra are matching with those reported in the literature.

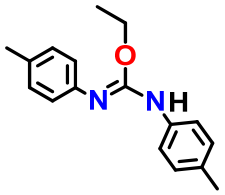

(Entry a, Table 2): ^{1}H NMR (300 MHz, C_6D_6) δ 7.02 (s, 4H), 6.81 (m, 4H), 5.89 (s, 1H), 4.36 (q, J = 7.1 Hz, 2H), 2.17 (s, 3H), 2.06 (s, 3H), 1.13 (t, J = 7.1 Hz, 3H). The NMR spectra are matching with those reported in the literature.

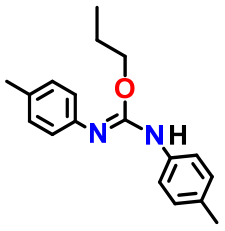

(Entry b, Table 2): ^{1}H NMR (300 MHz, C_6D_6) δ 7.04 (s, 4H), 6.81 (m, 4H), 5.90 (s, 1H), 4.33 (t, *J* = 6.6 Hz, 2H), 2.17 (s, 6H), 2.05 (s, 6H), 1.64 – 1.49 (m, 2H), 0.83 (t, *J* = 7.4 Hz, 3H). ^{13}C NMR (101 MHz, C_6D_6) δ 150.32, 146.54, 136.87, 132.31, 131.96, 130.69, 129.55, 122.95, 120.96, 68.51, 22.42, 20.69, 10.87. MS (APCI): m/z 283.1824 (M+H)*.

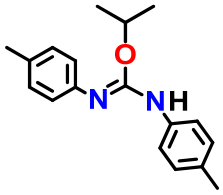

(Entry c, Table 2): ^{1}H NMR (300 MHz, C_6D_6) δ 7.03 (dd, *J* = 5.9, 2.0 Hz, 4H), 6.81 (d, *J* = 8.0 Hz, 4H), 5.89 (s, 1H), 5.59 – 5.38 (m, 1H), 2.17 (s, 3H), 2.05 (s, 3H), 1.26 (d, *J* = 6.2 Hz, 6H). The NMR spectra are matching with those reported in the literature.

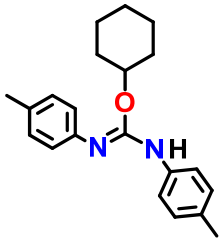

(Entry d, Table 2): ^{1}H NMR (300 MHz, C_6D_6) δ 7.02 (s, 4H), 6.89 – 6.77 (m, 4H), 5.91 (s, 1H), 5.45 – 5.28 (m, 1H), 2.17 (s, 3H), 2.06 (s, 3H), 1.60 (m, 4H), 1.27 – 1.08 (m, 4H). The NMR spectra are matching with those reported in the literature.

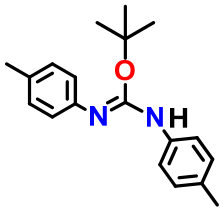

(Entry e, Table 2): ^{1}H NMR (300 MHz, C_6D_6) δ 7.01 (m, 4H), 6.81 (m, 4H), 5.82 (s, 1H), 2.17 (s, 3H), 2.07 (s, 3H), 1.61 (s, 9H). The NMR spectra are matching with those reported in the literature.

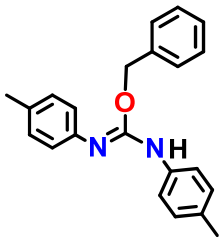

(Entry f, Table 2): ^{1}H NMR (300 MHz, C_6D_6) δ 7.26 (d, *J* = 7.1 Hz, 2H), 7.12 – 6.88 (m, 7H), 6.71 (s, 4H), 5.87 (s, 1H), 5.40 (s, 2H), 2.11 (s, 3H), 1.95 (s, 3H). The NMR spectra are matching with those reported in the literature.

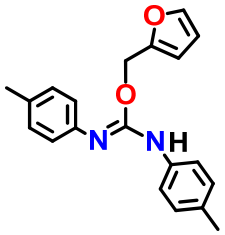

(Entry g, Table 2): ^{1}H NMR (300 MHz, C_6D_6) δ 7.01 (m, 5H), 6.74 (s, 4H), 6.25 (d, *J* = 3.1 Hz, 1H), 6.02 (dd, *J* = 3.1, 1.9 Hz, 1H), 5.86 (s, 1H), 5.38 (s, 2H), 2.16 (s, 3H), 1.99 (s, 3H). The NMR spectra are matching with those reported in the literature.

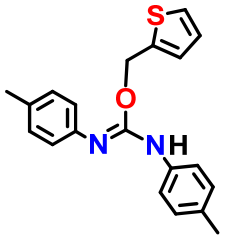

(Entry h, Table 2): ^{1}H NMR (300 MHz, C_6D_6) δ 7.06 (s, 5H), 6.91 – 6.82 (m, 1H), 6.75 (m, 4H), 6.66 (m, 1H), 5.87 (s, 1H), 5.50 (s, 2H), 2.17 (s, 3H), 2.00 (s, 3H). The NMR spectra are matching with those reported in the literature.

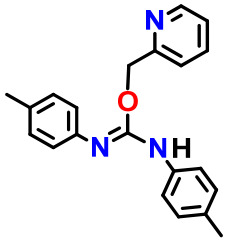

(Entry i, Table 2): ^{1}H NMR (300 MHz, C_6D_6) δ 8.43 (m, 1H), 7.22 (d, *J* = 7.8 Hz, 1H), 7.01 – 6.77 (m, 9H), 6.66 – 6.51 (m, 1H), 6.03 (s, 1H), 5.71 (s, 2H), 2.09 (br, 6H). The NMR spectra are matching with those reported in the literature.

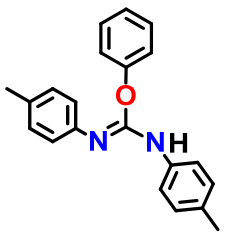

(Entry j, Table 2): ^{1}H NMR (300 MHz, C_6D_6) δ 7.12 – 6.64 (m, 13H), 2.01 (s, 6H). The NMR spectra are matching with those reported in the literature.

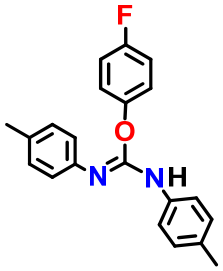

(Entry k, Table 2): ^{1}H NMR (300 MHz, C_6D_6) δ 7.13 – 7.04 (m, 2H), 6.93 (s, 6H), 6.81 (m, 2H), 6.68 (d, *J* = 8.5 Hz, 1H), 6.50 (dd, *J* = 8.5, 4.2 Hz, 1H), 6.08 (s, 1H), 2.08 (s, 6H). ^{13}C NMR (101 MHz, C_6D_6) δ 150.33, 146.55, 136.88, 132.32, 131.97, 130.70, 129.56, 122.96, 120.97, 68.52, 22.43, 20.84, 20.70, 10.88. MS (APCI): m/z 335.1566 (M+H)*.

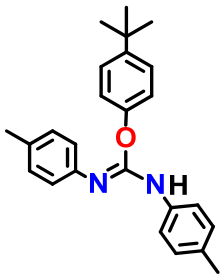

(Entry l, Table 2): ^{1}H NMR (300 MHz, C_6D_6) δ 7.06 (m, 4H), 6.97 (m, 6H), 6.76 (m, 2H), 6.08 (s, 1H), 2.08 (s, 6H), 1.14 (s, 9H). ^{13}C NMR (101 MHz, C_6D_6) δ 151.23, 147.52, 142.07, 132.46, 130.43, 129.82, 126.54, 126.34, 124.38, 121.59, 119.86, 115.33, 34.31, 31.46, 20.79. MS (APCI): m/z 373.2283 (M+H)*.

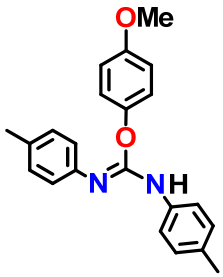

(Entry m, Table 2): ^{1}H NMR (400 MHz, $CDCl_3$) δ 7.11 – 6.77 (m, 10H), 6.65 (d, *J* = 7.2 Hz, 2H), 6.03 (s, 1H), 3.22 (s, 3H), 2.09 (s, 6H). ^{13}C NMR (101 MHz, $CDCl_3$) δ 157.06, 146.93, 132.52, 130.43, 129.97, 124.37, 121.77, 120.96, 114.66, 55.05, 20.80. MS (APCI): m/z 347.1769 (M+H)*.

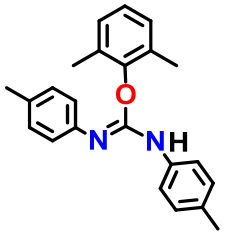

(Entry n, Table 2): ^{1}H NMR (300 MHz, C_6D_6) δ 7.05 – 6.79 (m, 11H), 5.95 (s, 1H), 2.31 (s, 6H), 2.13 (s, 3H), 2.07 (s, 3H). The NMR spectra are matching with those reported in the literature.

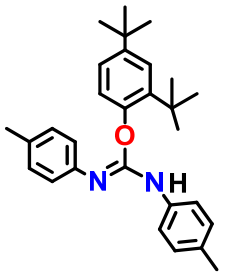

(Entry o, Table 2): ^{1}H NMR (300 MHz, C_6D_6) δ 7.51, 7.13, 7.04, 7.02, 6.98, 6.95, 6.95, 6.16, 6.13, 2.08, 1.45, 1.21. The NMR spectra are matching with those reported in the literature.

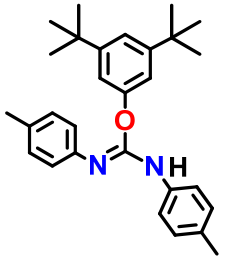

(Entry p, Table 2): ^{1}H NMR (400 MHz, C_6D_6) δ 7.27, 7.13, 7.11, 7.08, 7.06, 7.03, 6.91, 6.64, 6.06, 2.07, 1.21. ^{13}C NMR (101 MHz, C_6D_6) δ 156.96, 153.61, 152.47, 152.16, 132.46, 129.92, 129.33, 121.78, 118.63, 113.81, 110.41, 35.01, 34.89, 31.66, 31.45, 20.79. MS (APCI): m/z 429.2897 (M+H)*.

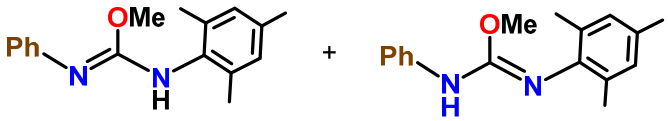

(Entry 1, Table 3): ^{1}H NMR (300 MHz, C_6D_6) δ 7.21 (t, J = 7.7 Hz, 7H), 7.12 (d, J = 7.3 Hz, 8H), 6.94 (s, 6H), 6.91 (s, 8H), 6.89 (s, 7H), 6.86 (s, 14H), 6.74 (t, J = 7.4 Hz, 7H), 6.66 (d, J = 7.7 Hz, 16H), 6.61 (s, 6H), 5.48 (s, 10H), 4.85 (s, 4H), 3.71 (s, 29H), 3.56 (s, 13H), 2.18 (s, 29H), 2.17 (s, 58H), 2.04 (s, 12H), 1.99 (s, 25H). ^{13}C NMR (101 MHz, C_6D_6) δ 152.09, 149.99, 149.05, 142.60, 140.88, 139.04, 136.22, 134.86, 133.01, 132.74, 131.98, 130.01, 129.80, 129.71, 129.68, 129.36, 128.98, 124.85, 124.11, 123.21, 123.10, 122.74, 120.83, 53.72, 53.65, 20.94, 20.84, 19.01, 18.27. MS (APCI): m/z 269.1675 (M+H)*.

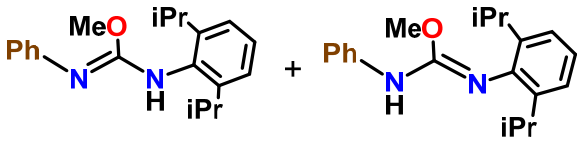

(Entry 2, Table 3): ^{1}H NMR (300 MHz, C_6D_6) δ 7.21 – 7.17 (m, 31H), 7.10 (dd, *J* = 8.7, 6.4 Hz, 19H), 6.90 (tt, *J* = 4.1, 2.1 Hz, 33H), 6.76 – 6.70 (m, 10H), 6.67 – 6.62 (m, 30H), 5.46 (s, 18H), 5.22 (s, 2H), 3.70 (s, 56H), 3.56 (s, 6H), 3.30 – 3.14 (m, 40H), 1.21 (d, *J* = 3.0 Hz, 117H), 1.19 (d, *J* = 3.0 Hz, 122H), 1.00 (s, 7H), 0.97 (s, 8H). ^{13}C NMR (101 MHz, C_6D_6) δ 152.55, 149.89, 148.88, 146.96, 145.28, 143.11, 142.63, 140.55, 138.83, 132.92, 130.15, 129.83, 129.33, 129.01, 128.57, 126.22, 124.88, 124.17, 124.13, 123.75, 123.53, 123.25, 123.10, 122.96, 120.91, 53.78, 53.52, 29.67, 28.63, 23.79, 23.72, 23.28.
MS (APCI): m/z 311.2122 (M+H)*.

1.11. ^{1}H-NMR spectra of the reaction mixture from the catalytic addition of alcohols to carbodiimides.

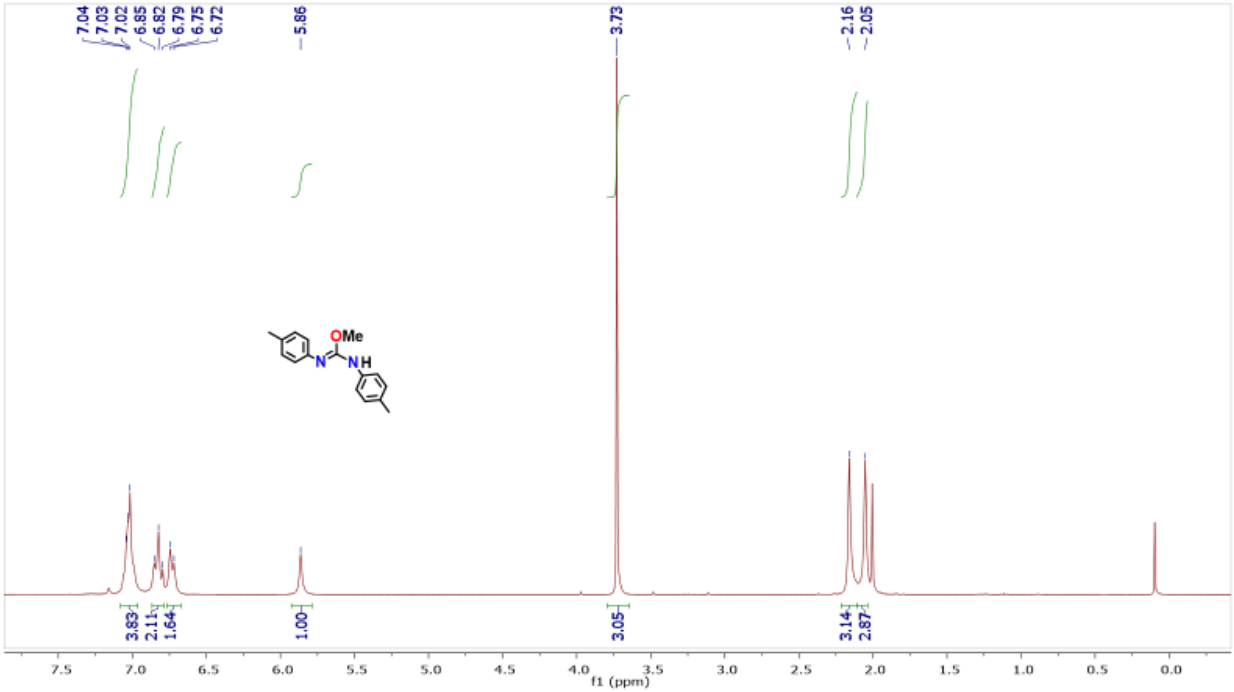

Figure S13. ^{1}H NMR of Entry 1, Table 1 in reaction mixture in C_6D_6.

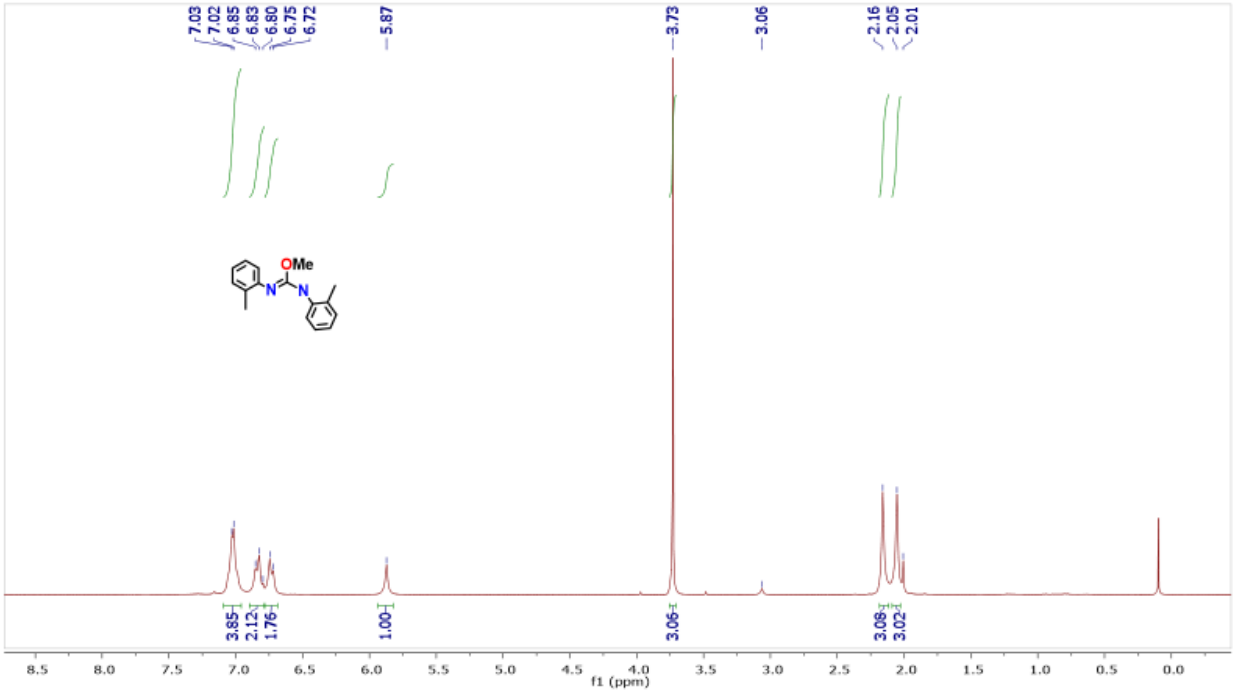

Figure S14. ^{1}H NMR of Entry 8, Table 1 in reaction mixture in C_6D_6.

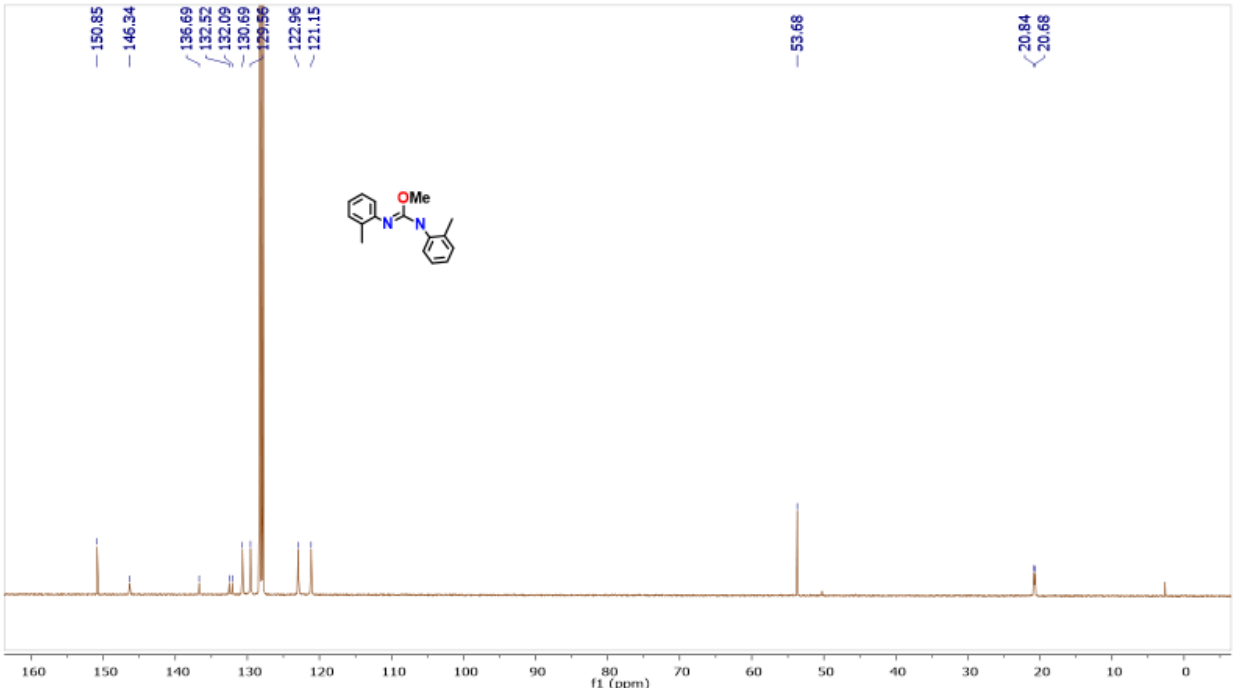

Figure S15. ^{13}C NMR of Entry 8, Table 1 in reaction mixture in C_6D_6.

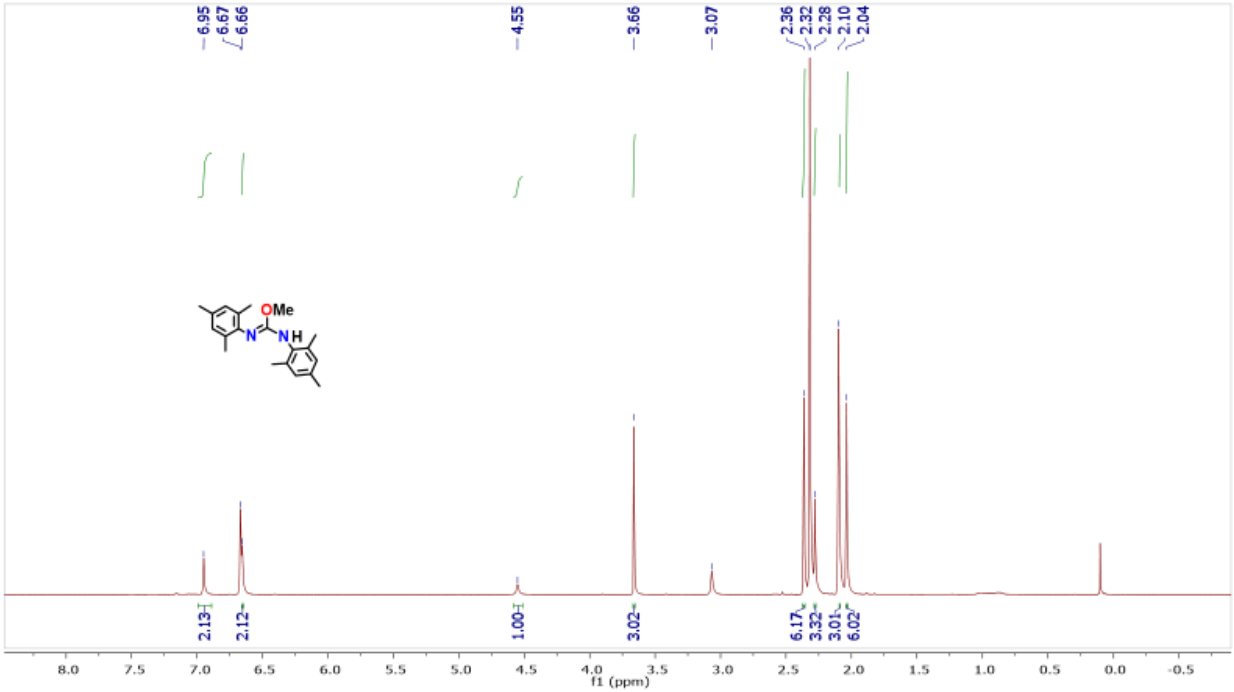

Figure S16. ^{1}H NMR of Entry 10, Table 1 in reaction mixture in C_6D_6.

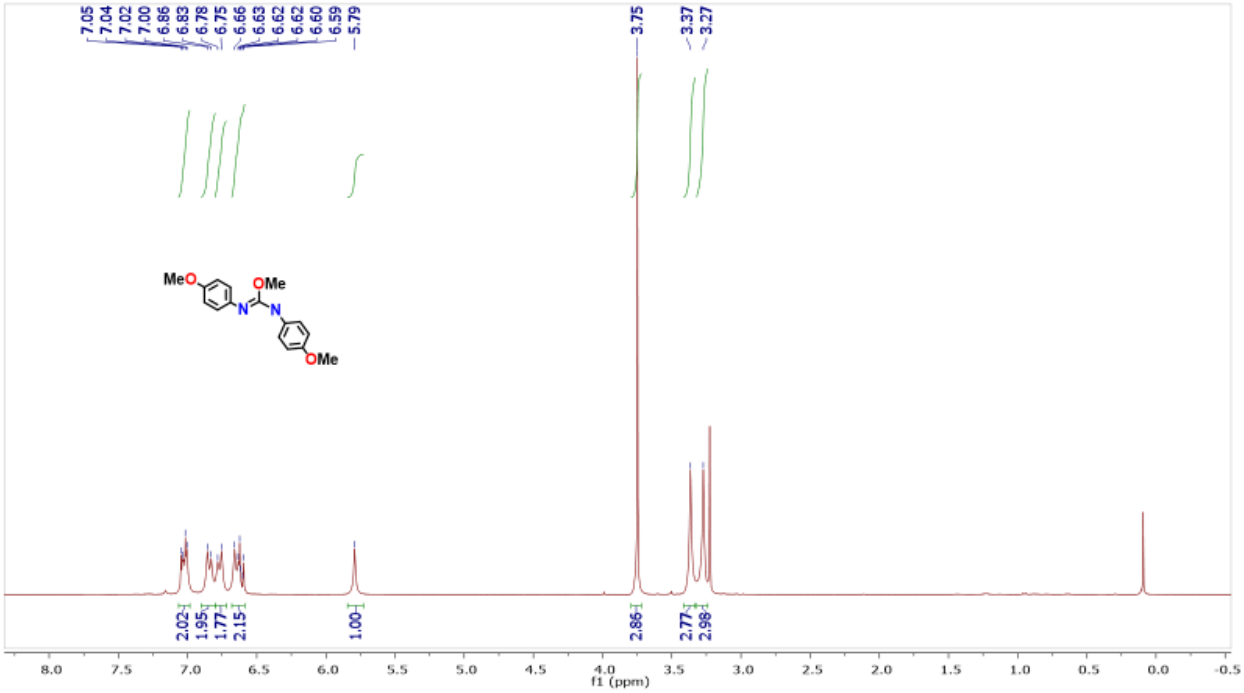

Figure S17. ^{1}H NMR of Entry 14, Table 1 in reaction mixture in C_6D_6.

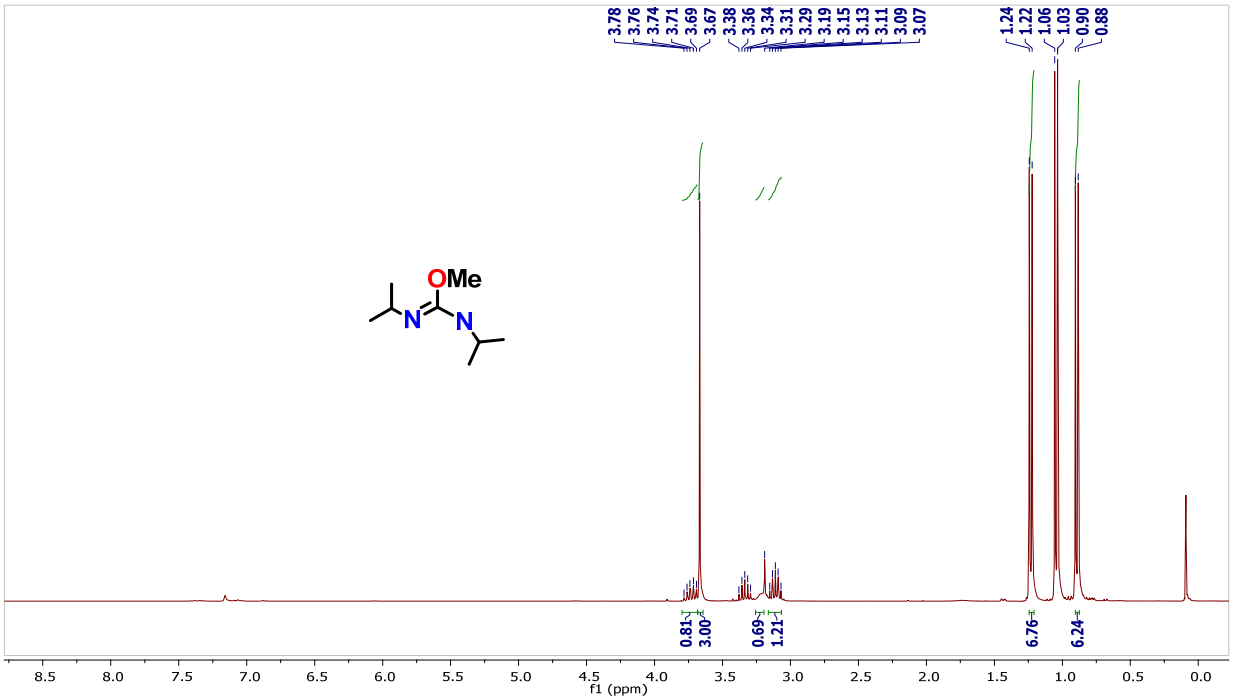

Figure S18. ^{1}H NMR of Entry 16, Table 1 in reaction mixture in C_6D_6.

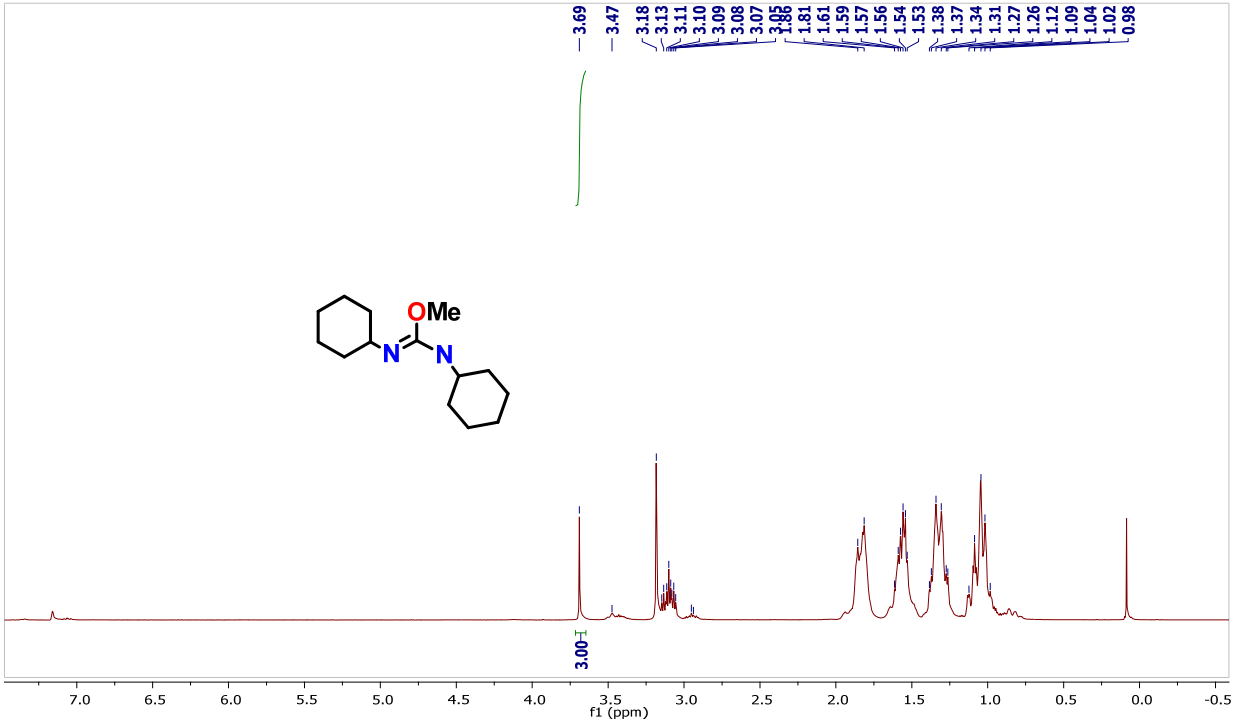

Figure S19. ^{1}H NMR of Entry 16, Table 1 in reaction mixture in C_6D_6

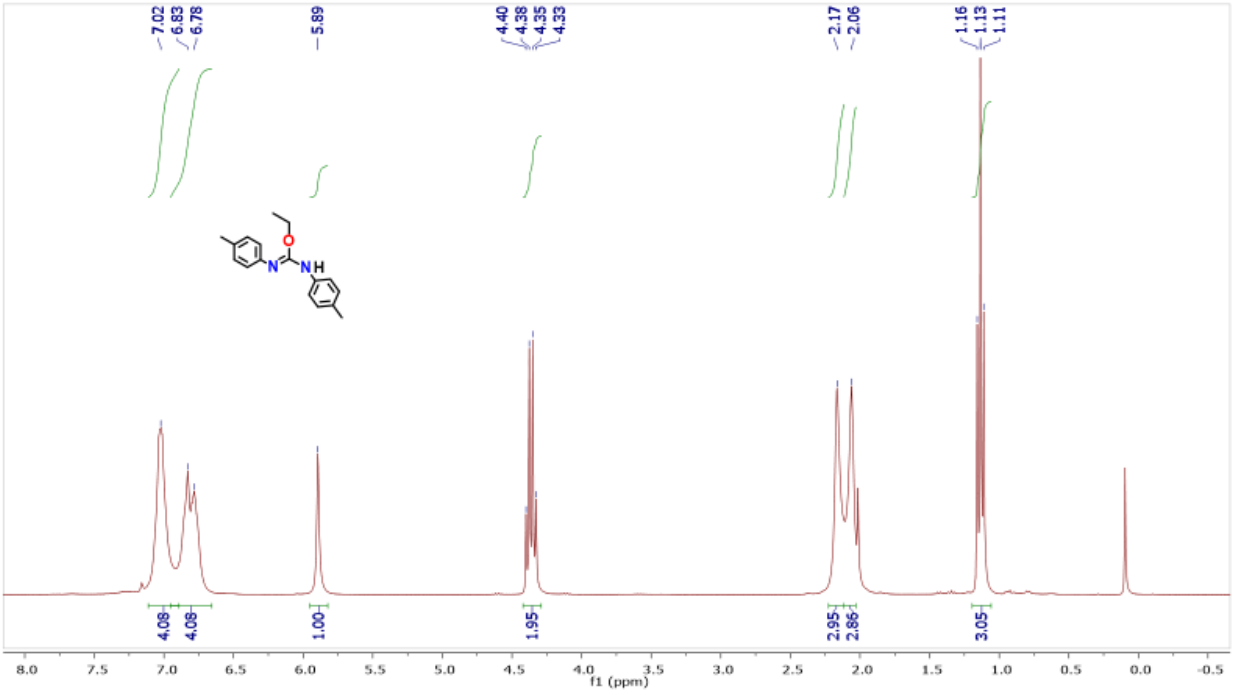

Figure S20. ^{1}H NMR of Entry a, Table 2 in reaction mixture in C_6D_6.

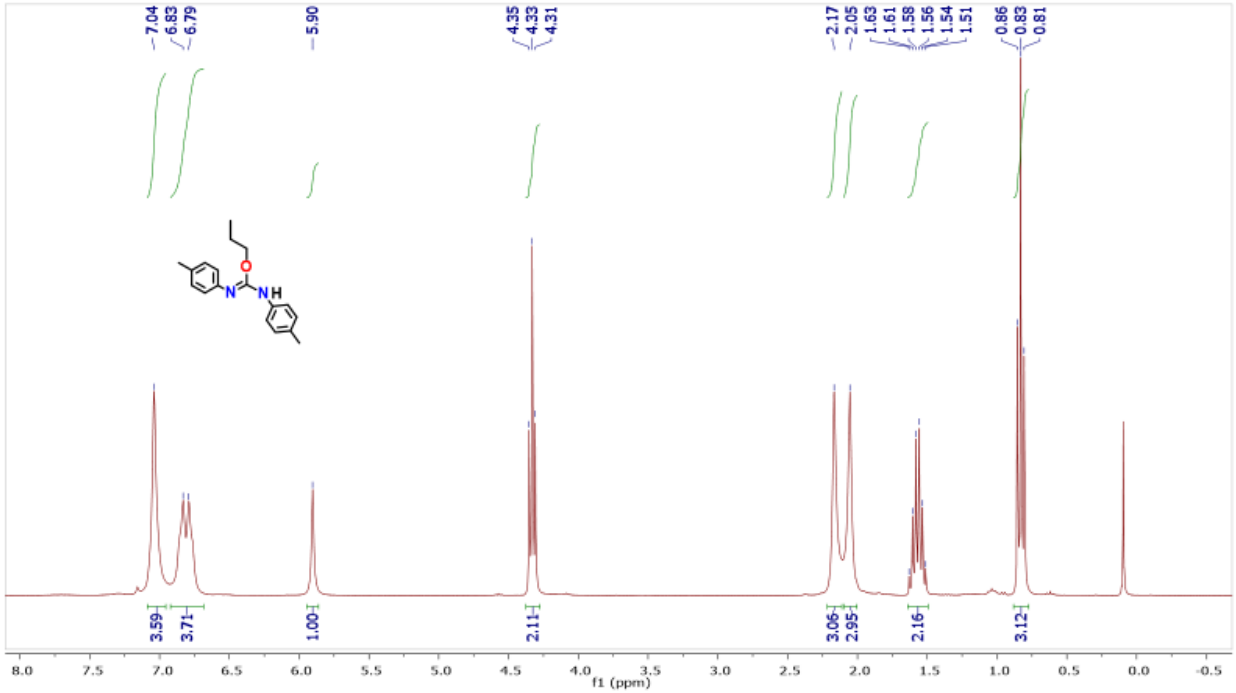

Figure S21. ^{1}H NMR of Entry b, Table 2 in reaction mixture in C_6D_6.

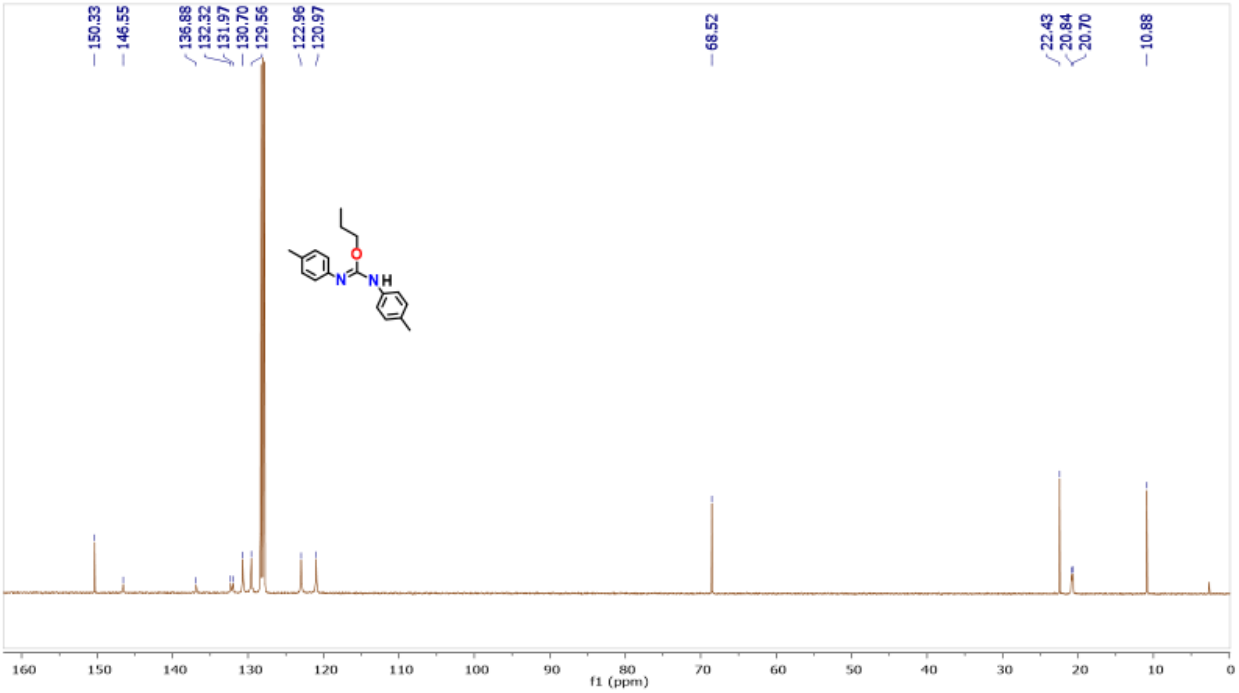

Figure S22. ^{13}C NMR of Entry b, Table 2 in reaction mixture in C_6D_6.

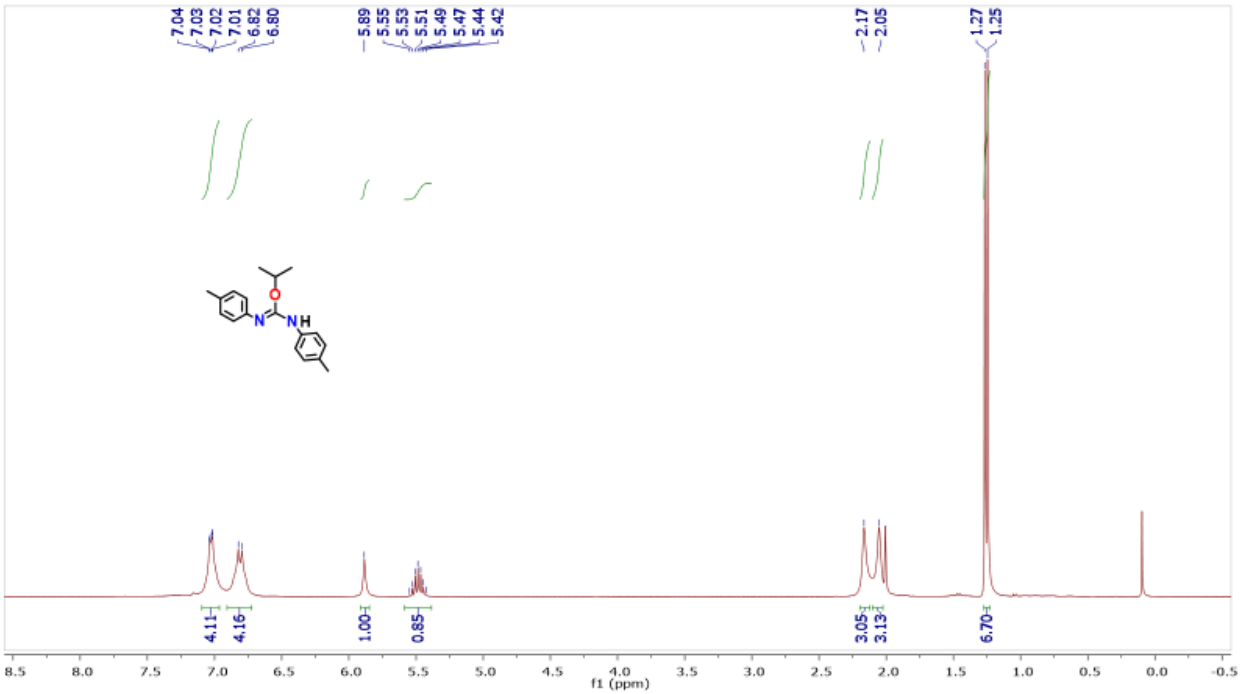

Figure S23. ^{1}H NMR of Entry c, Table 2 in reaction mixture in C_6D_6.

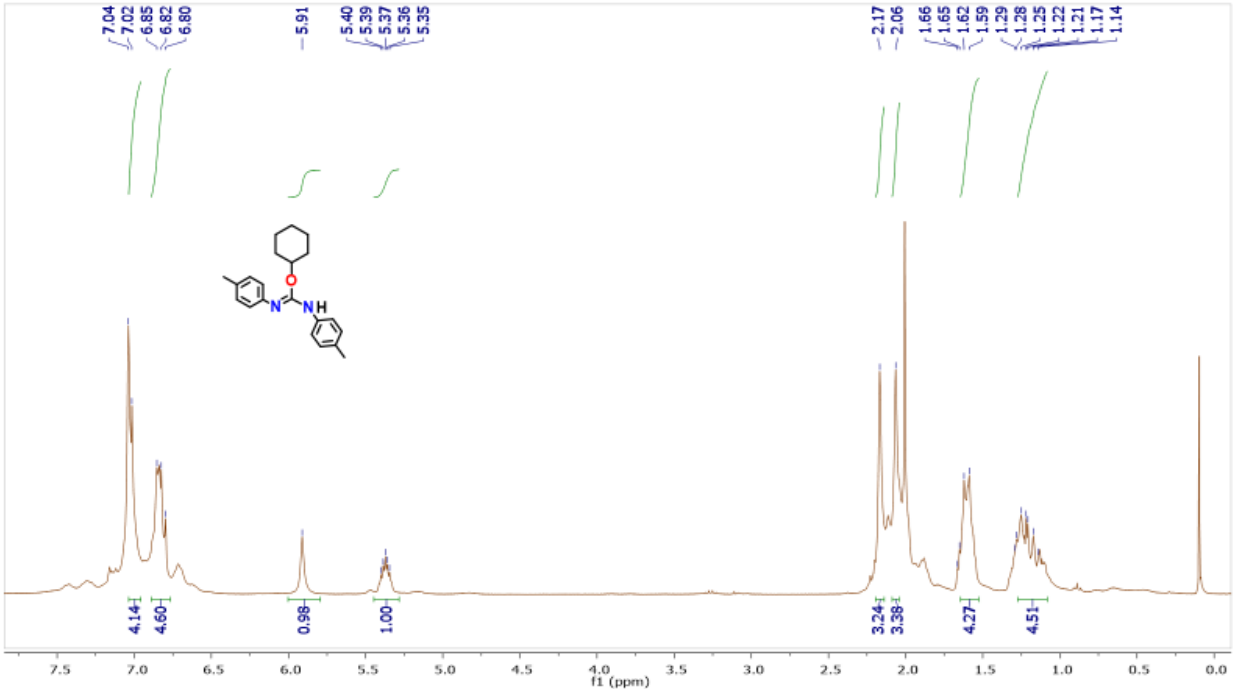

Figure S24. ^{1}H NMR of Entry d, Table 2 in reaction mixture in C_6D_6.

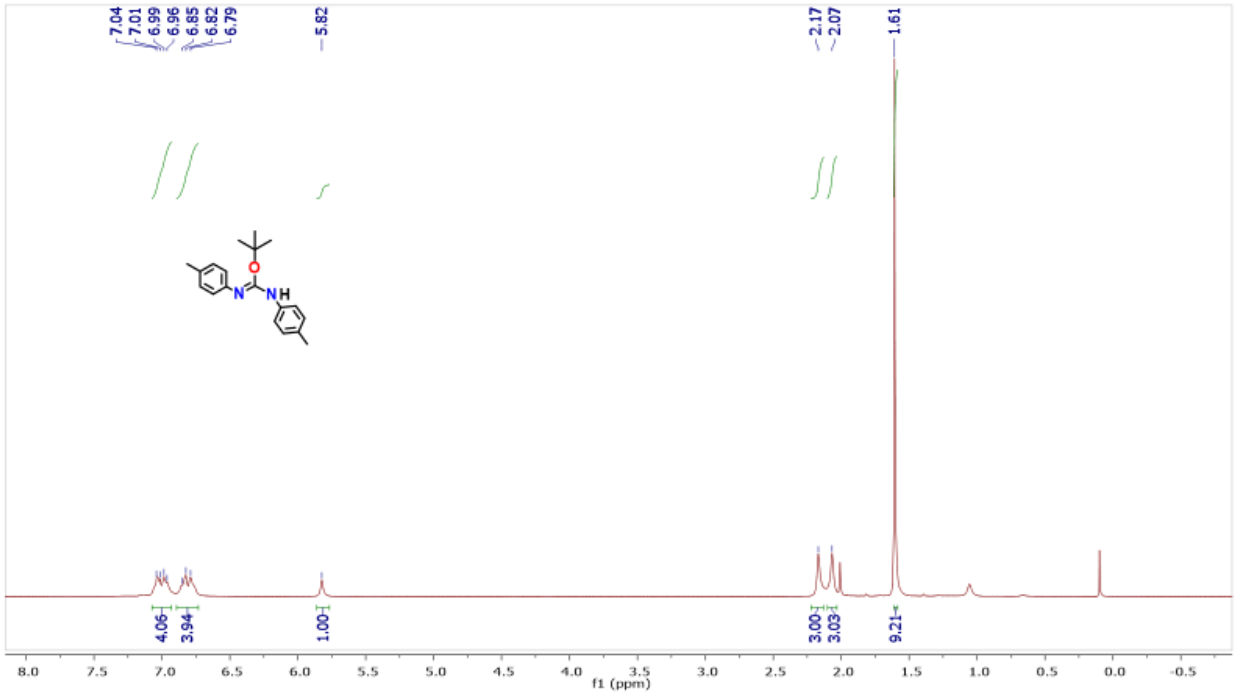

Figure S25. ^{1}H NMR of Entry e, Table 2 in reaction mixture in C_6D_6.

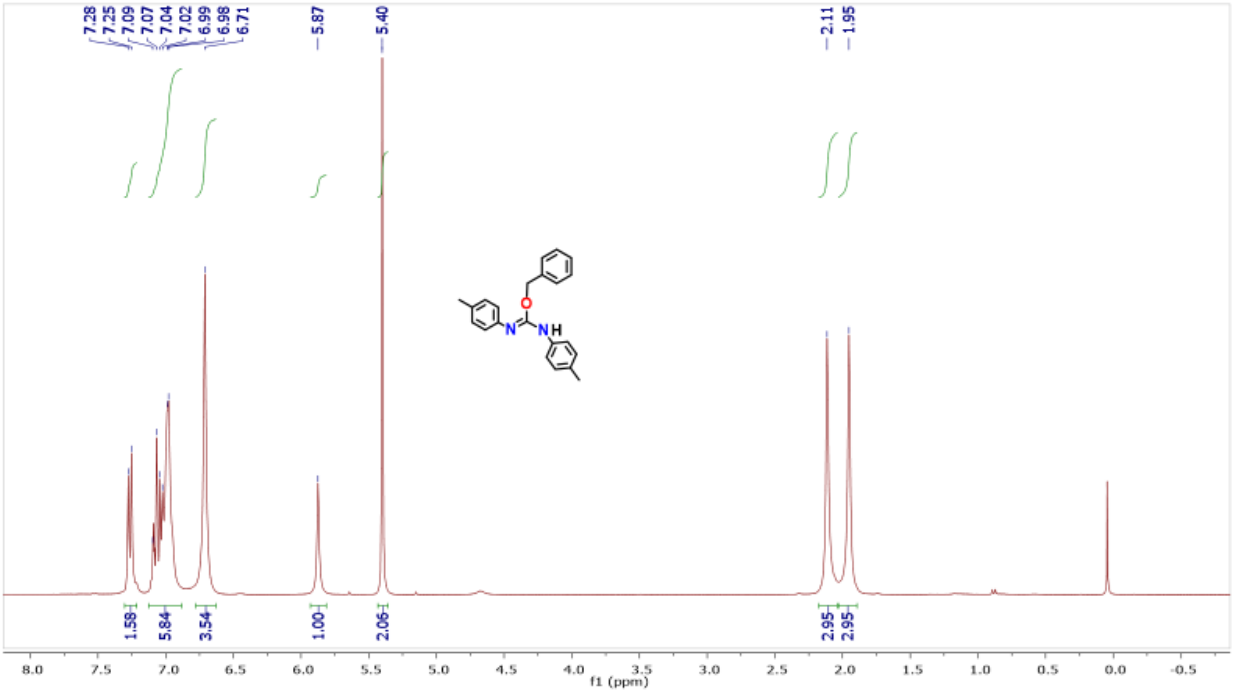

Figure S26. ^{1}H NMR of Entry f, Table 2 in reaction mixture in C_6D_6.

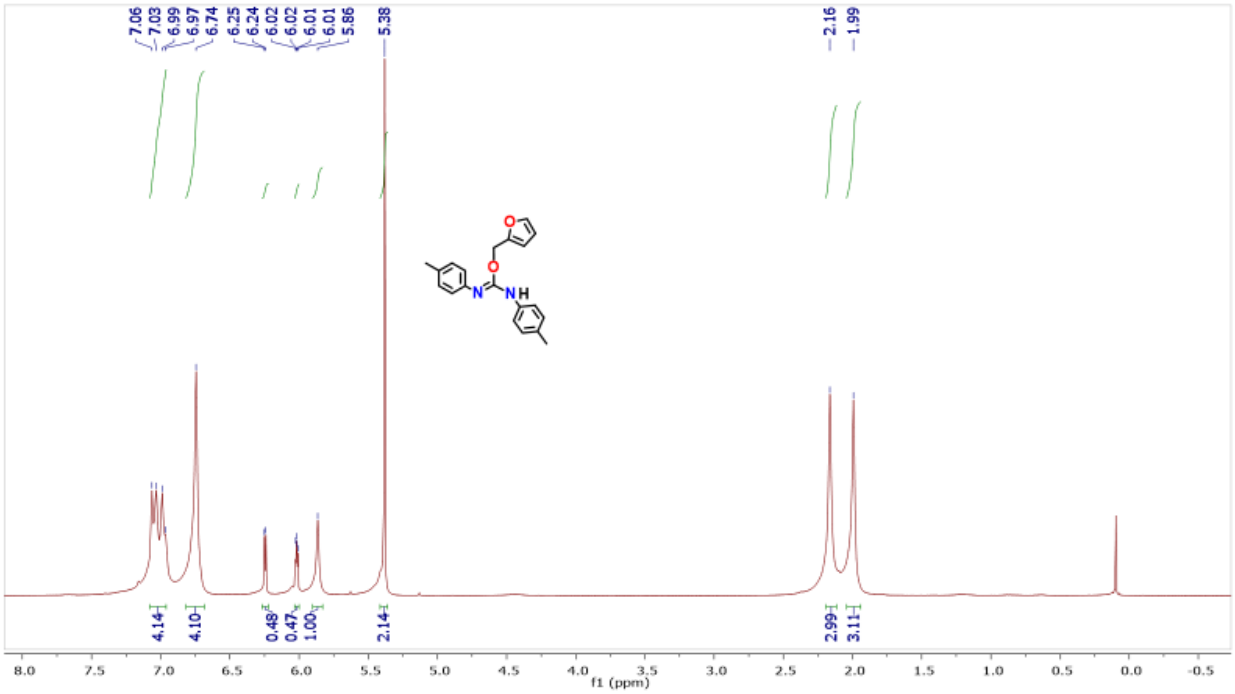

Figure S27. ^{1}H NMR of Entry g, Table 2 in reaction mixture in C_6D_6.

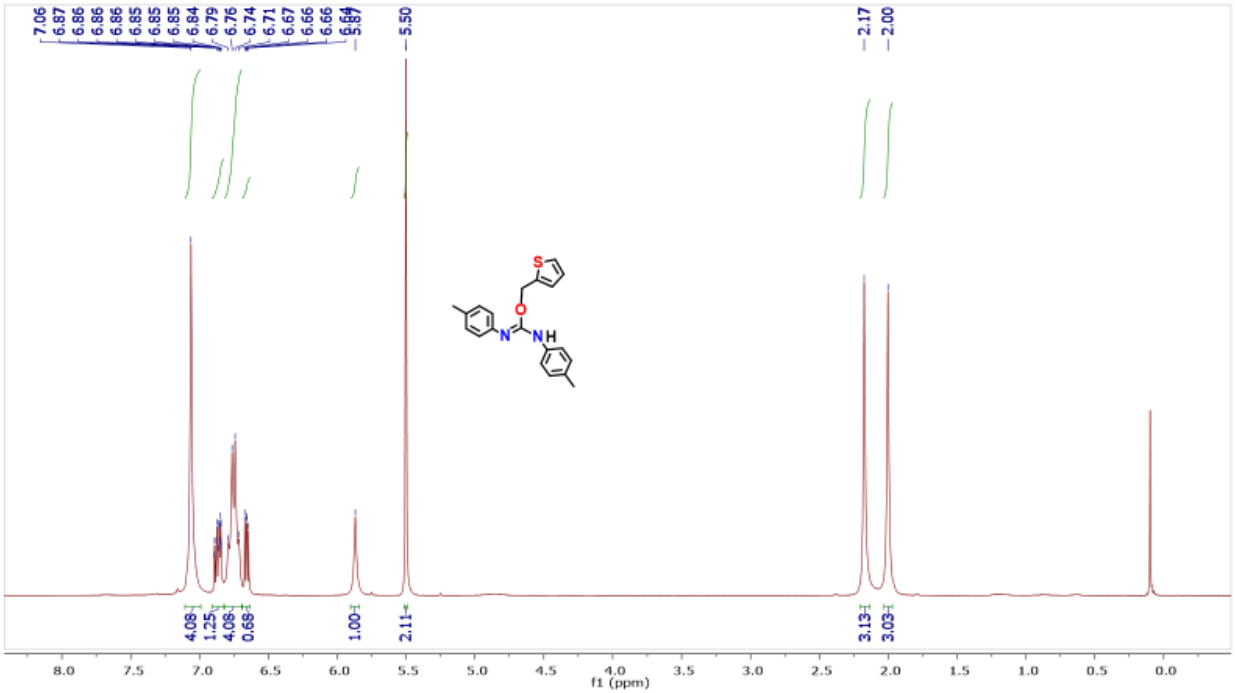

Figure S28. ^{1}H NMR of Entry h, Table 2 in reaction mixture in C_6D_6.

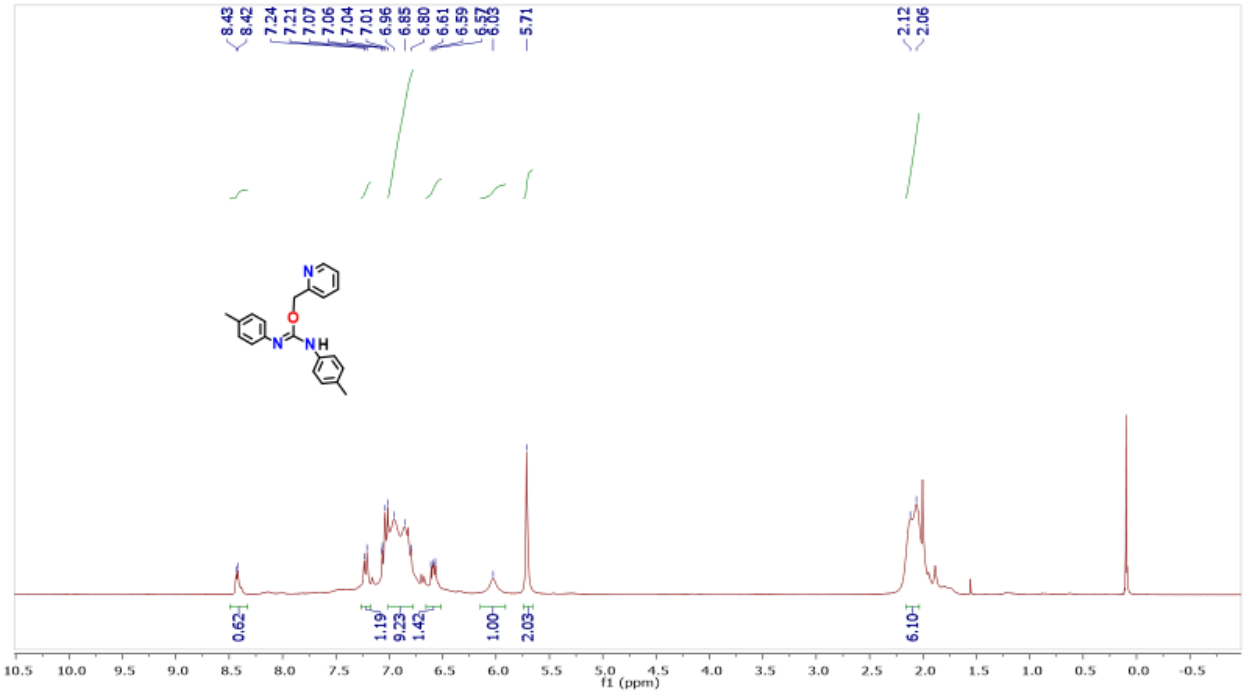

Figure S29. ^{1}H NMR of Entry i, Table 2 in reaction mixture in C_6D_6.

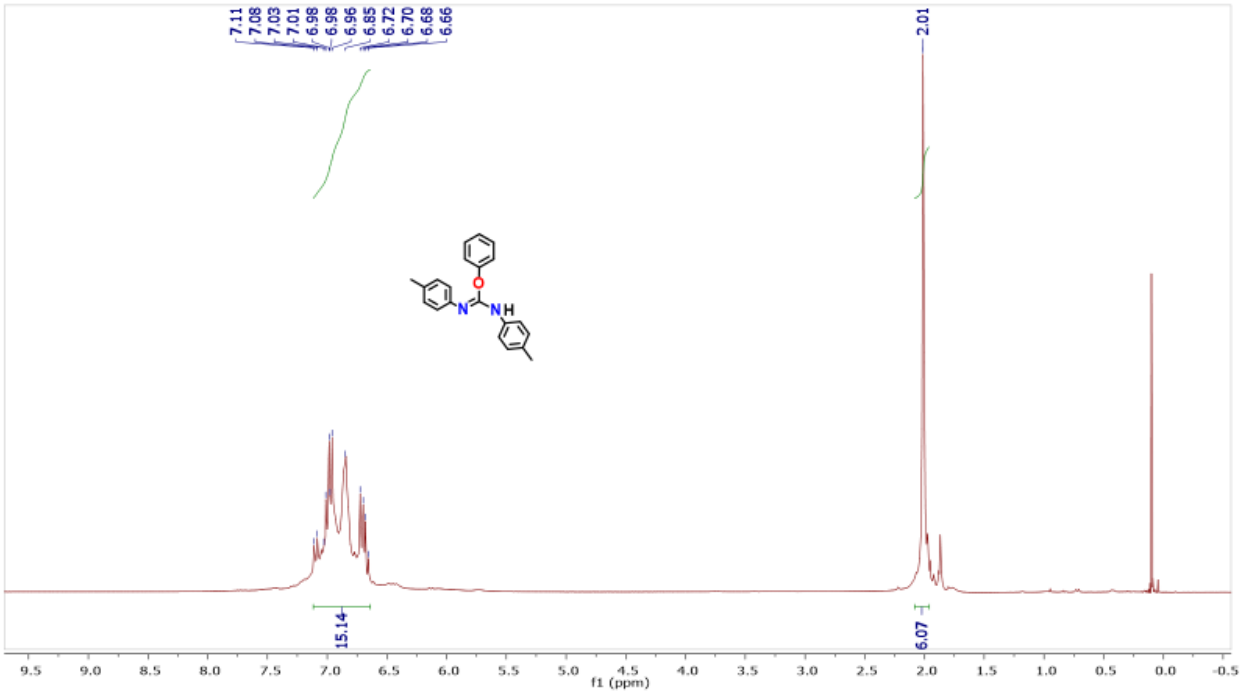

Figure S30. ^{1}H NMR of Entry j, Table 2 in reaction mixture in C_6D_6.

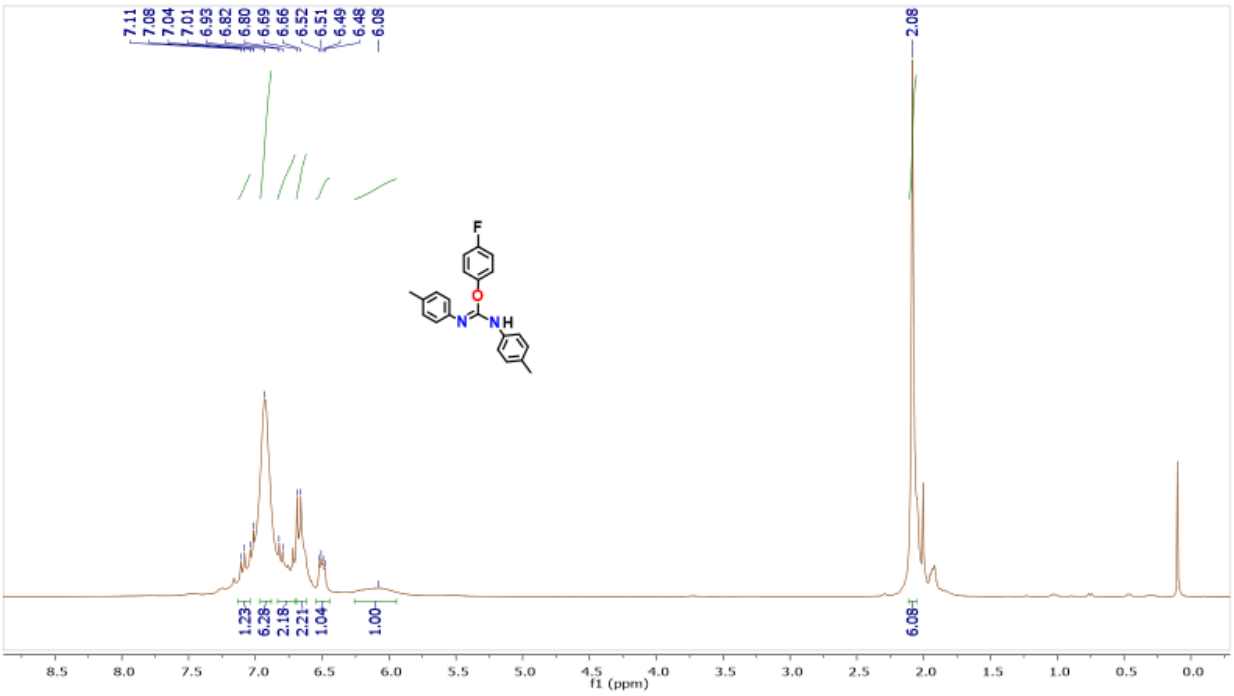

Figure S31. ^{1}H NMR of Entry k, Table 2 in reaction mixture in C_6D_6.

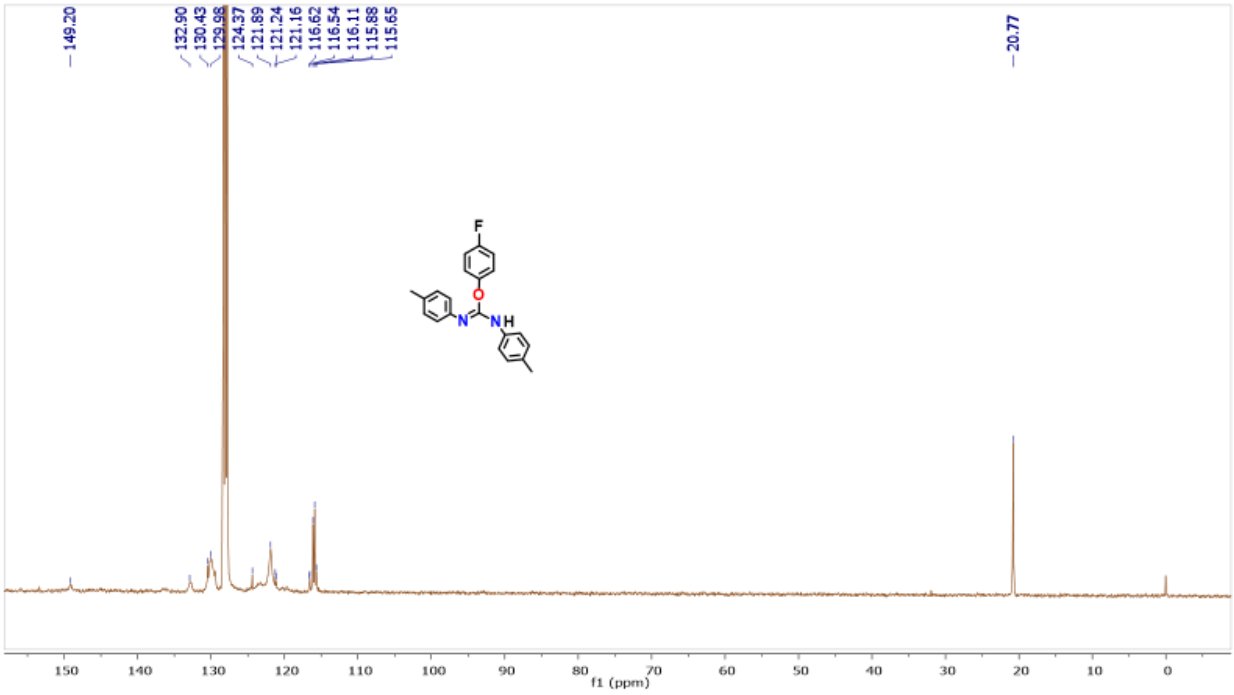

Figure S32. ^{13}C NMR of Entry f, Table 2 in reaction mixture in C_6D_6.

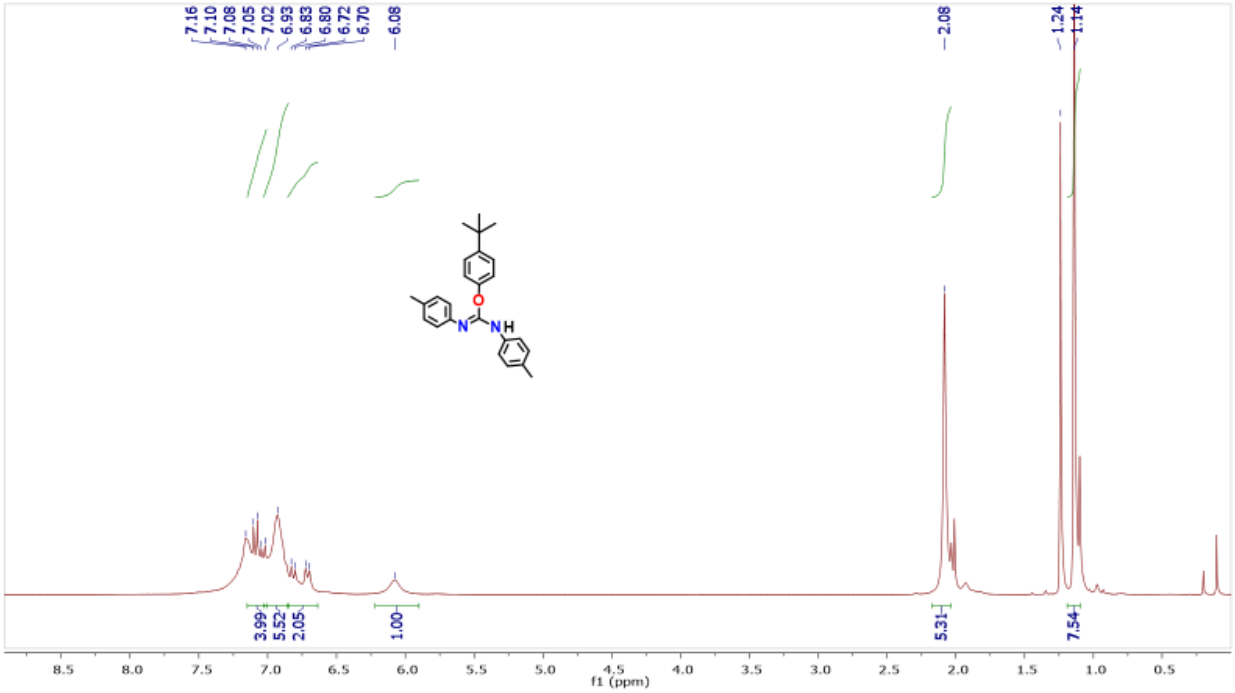

Figure S33. ^{1}H NMR of Entry l, Table 2 in reaction mixture in C_6D_6.

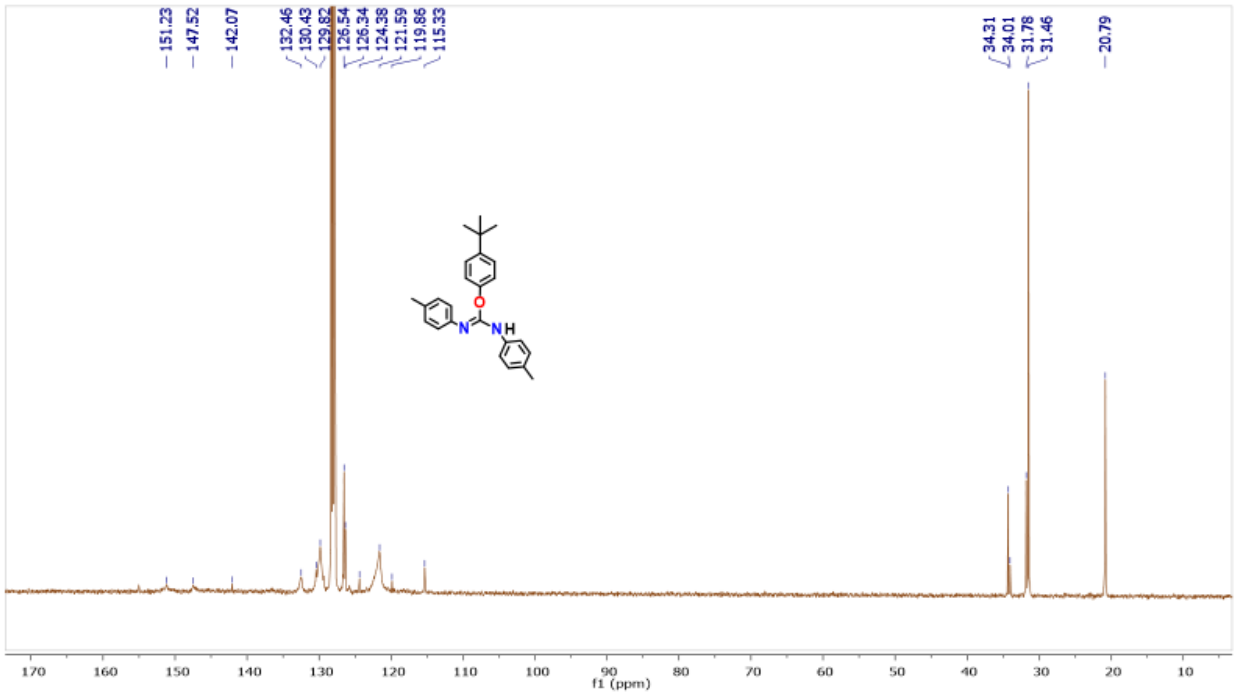

Figure S34. ^{13}C NMR of Entry l, Table 2 in reaction mixture in C_6D_6.

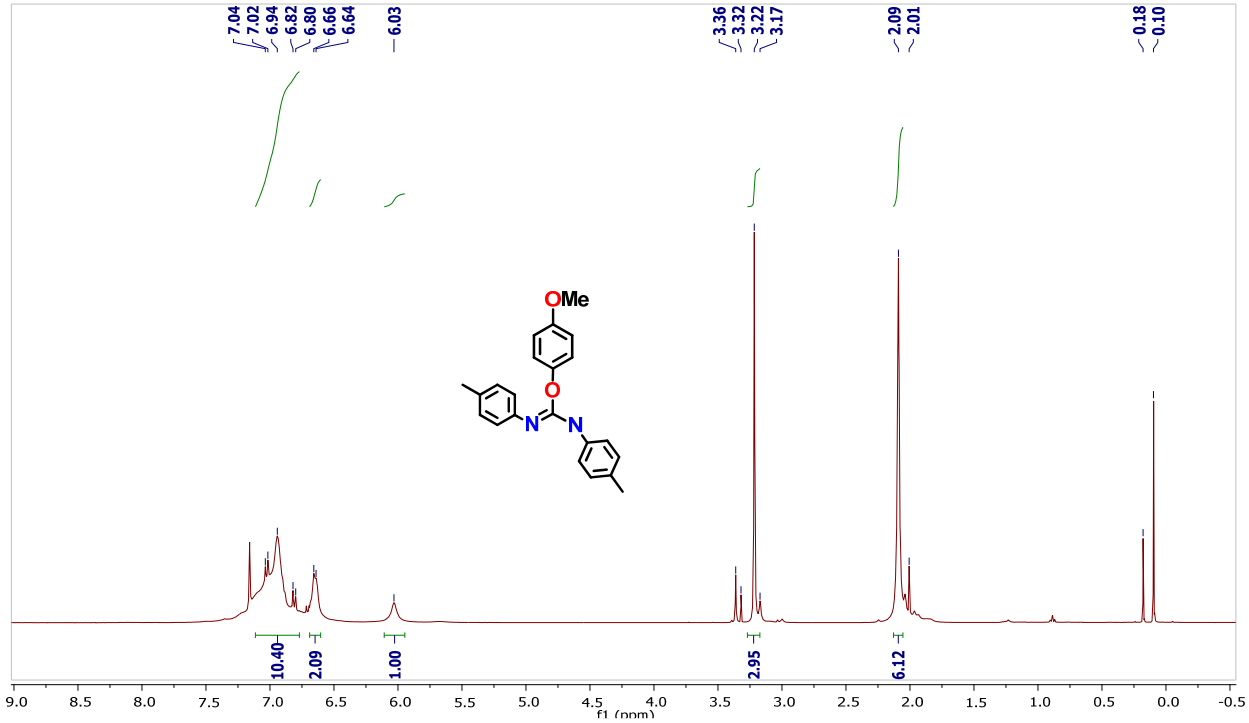

Figure S35. ^{1}H NMR of Entry m, Table 2 in reaction mixture in C_6D_6

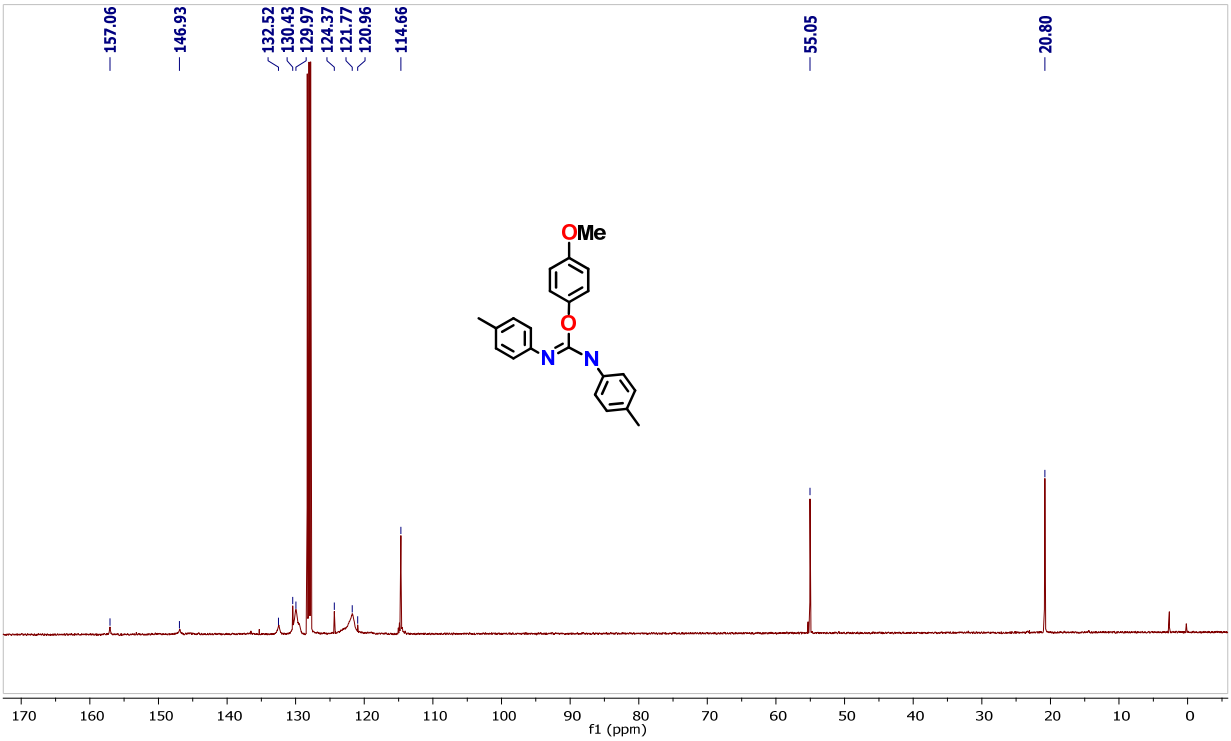

Figure S36. ^{13}C NMR of Entry m, Table 2 in reaction mixture in C_6D_6.

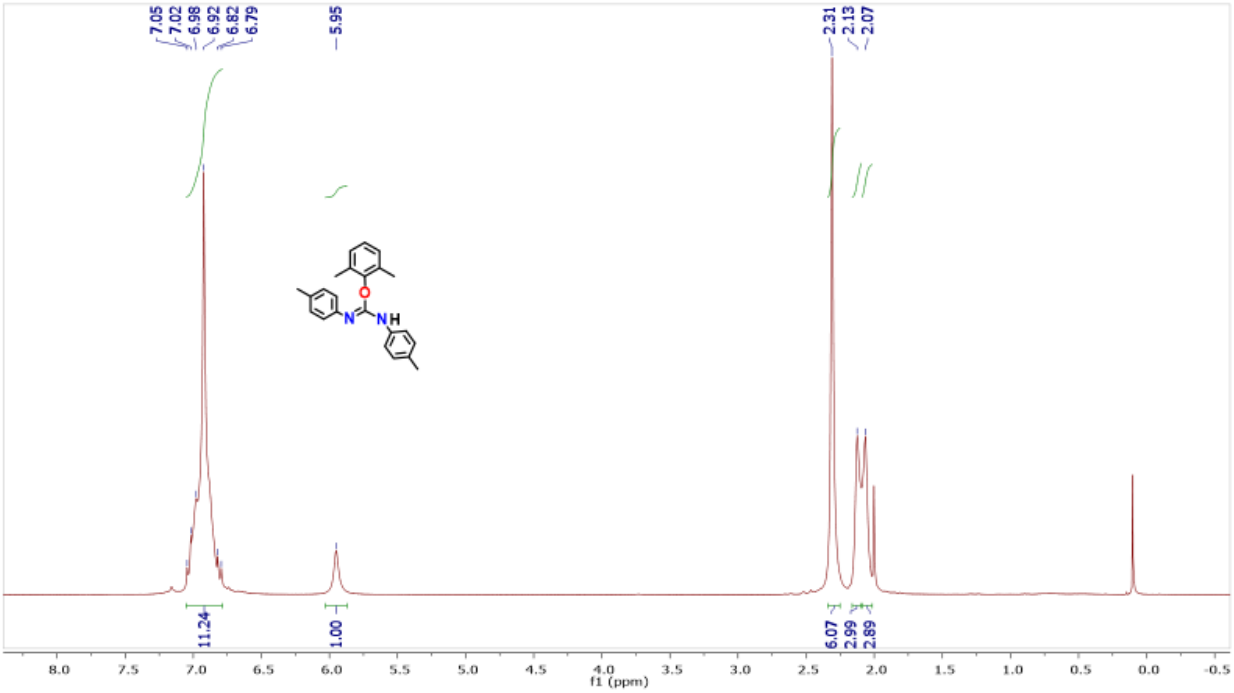

Figure S37. ^{1}H NMR of Entry n, Table 2 in reaction mixture in C_6D_6.

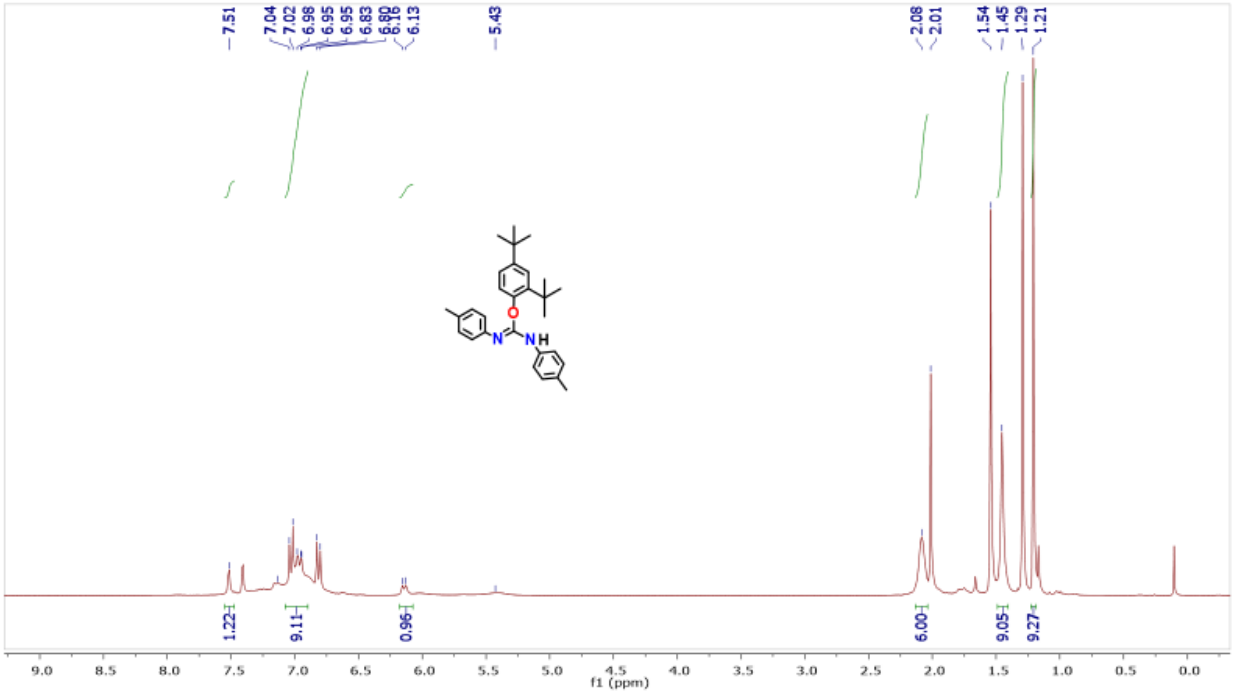

Figure S38. ^{1}H NMR of Entry o, Table 2 in reaction mixture in C_6D_6.

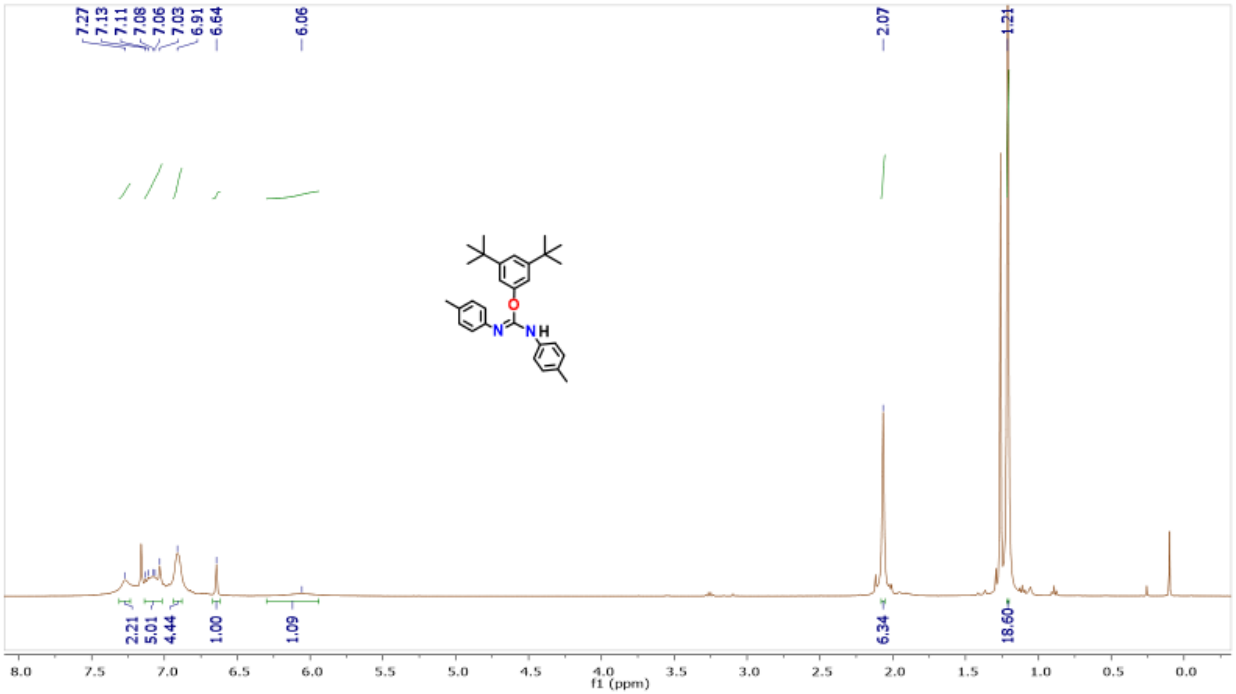

Figure S39. ^{1}H NMR of Entry p, Table 2 in reaction mixture in C_6D_6.

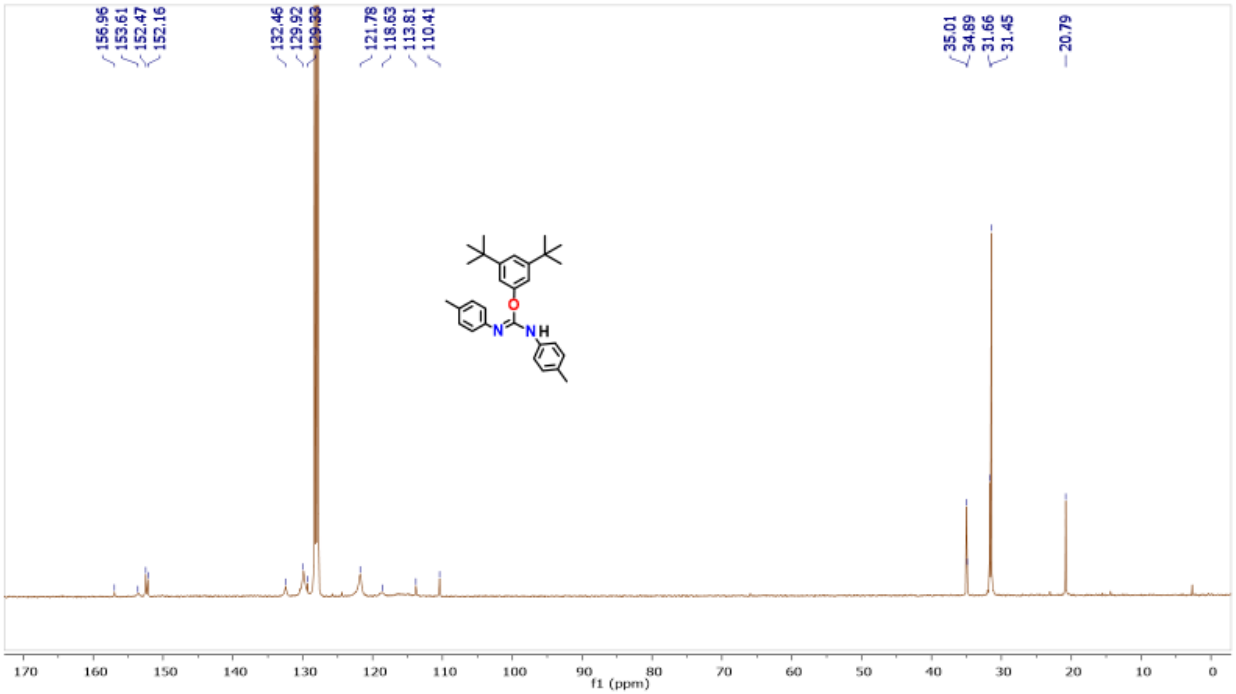

Figure S40. ^{13}C NMR of Entry p, Table 2 in the reaction mixture in C_6D_6.

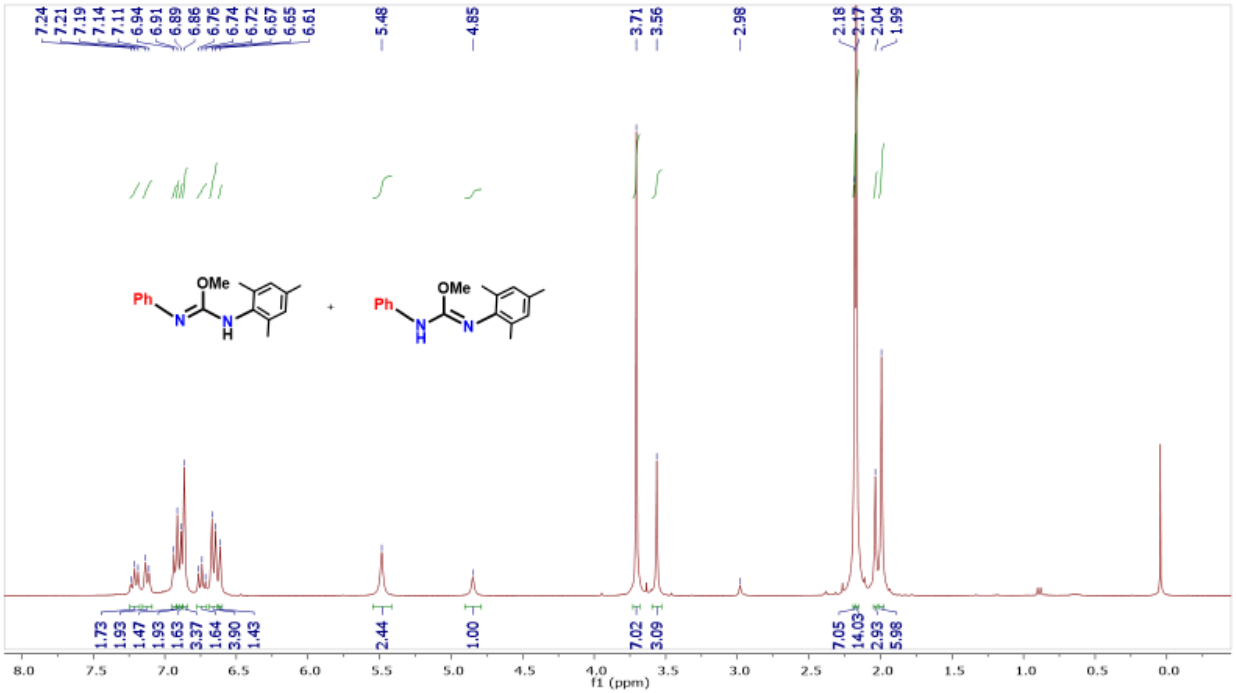

Figure S41. ^{1}H NMR of Entry 1, Table 3 in reaction mixture in C_6D_6.

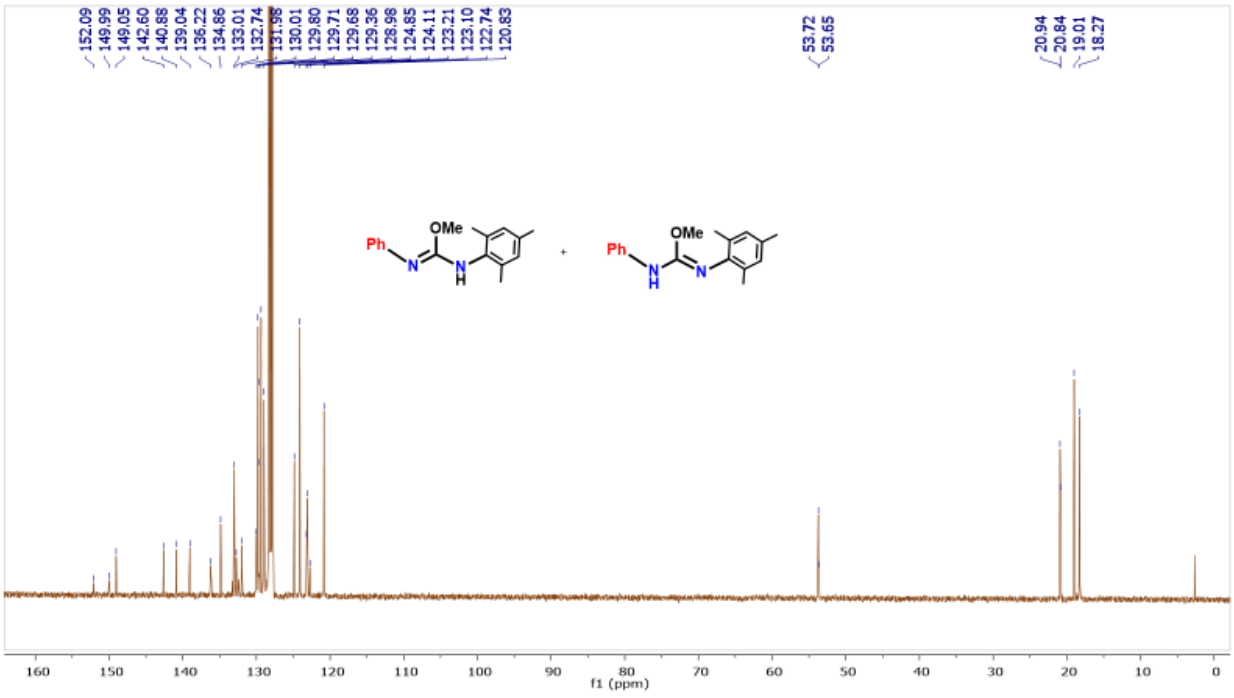

Figure S42. ^{13}C NMR of Entry 1, Table 3 in reaction mixture in C_6D_6.

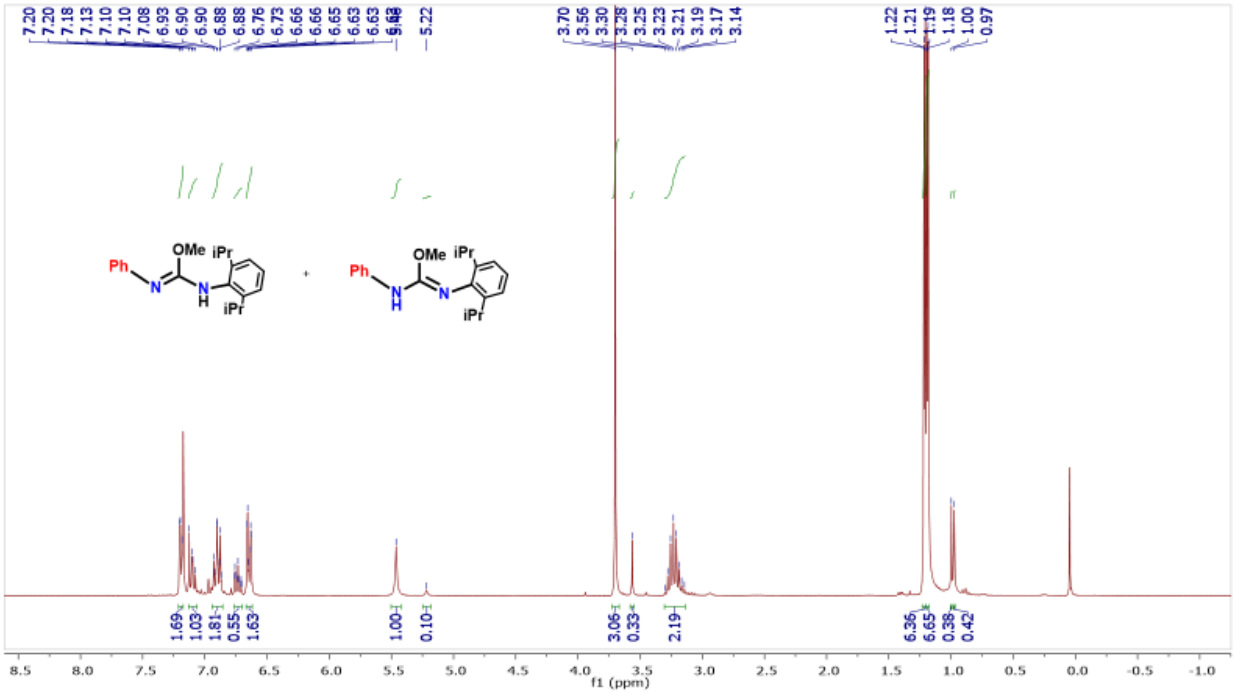

Figure S43. ^{1}H NMR of Entry 2, Table 3 in reaction mixture in C_6D_6.

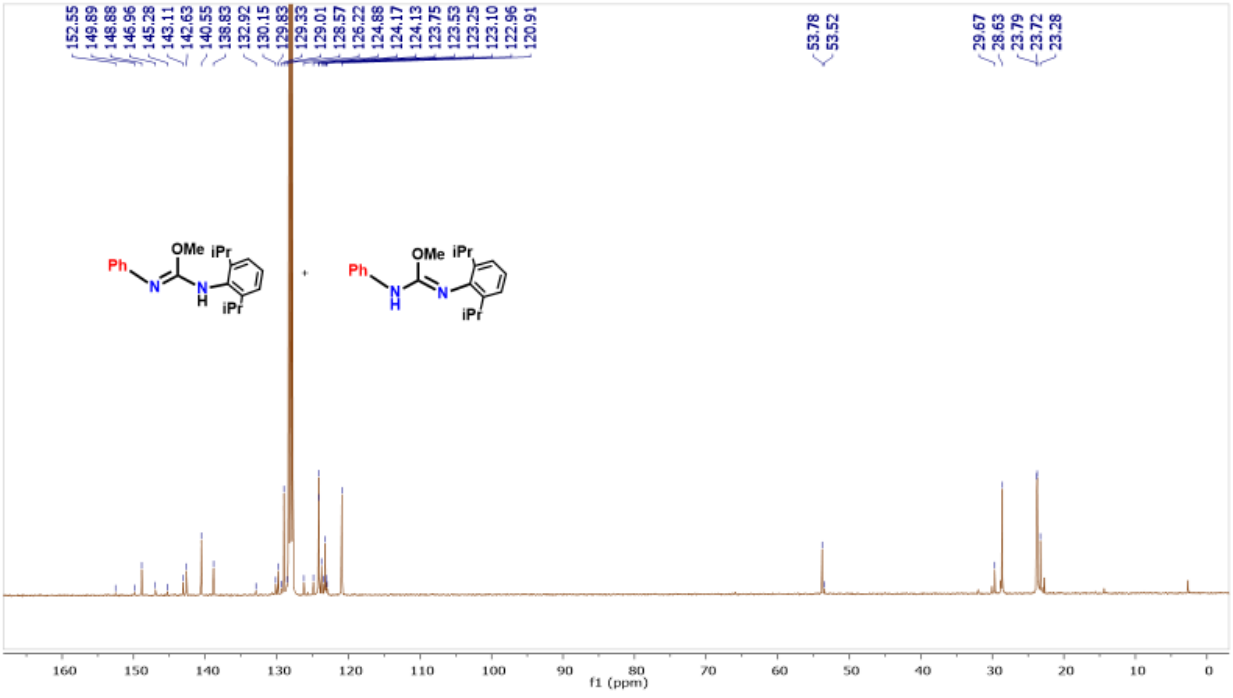

Figure S44. ^{13}C NMR of Entry 2, Table 3 in reaction mixture in C_6D_6.

2. Kinetic studies of isopropanol (^{i}PrOH) into DTC using Th-1. All the kinetic experiments were performed in the glovebox following a similar methodology. Inside a J. Young NMR tube a typical amount of complex **Th-1** (40 – 4.0 μmol), DTC (0.06 – 0.40 mmol), ^{i}PrOH (0.06 – 0.40 mmol), 1,3,5-trimethoxybenzene (59.5 μmol, as internal standard) from stock solutions were added and the total volume was made up to 0.55 mL with C_6D_6. The NMR tube was taken out of the glove box and freeze it until the ^{1}H NMR experiment began at 25 ºC. All the experiments were done by changing either one substrate or the catalyst while keeping the other reagents constant, and the data was collected every 33 or 60 seconds up to a half-hour. The product concentrations were measured by the area ratio of the isopropyl group for the product, a doublet at 1.21 ppm, and compared to the singlet at 6.18 ppm of the CH_{Ar} of the internal standard. Reaction rates were determined by the least-square fit of the initial product concentration versus time, and the plots were shown in Figures S39-S44.

Activation parameters including enthalpy ($\Delta H^{\neq}$), entropy ($\Delta S^{\neq}$), and activation energy (E_a) were calculated from kinetic data using Eyring and Arrhenius plots. In a typical sample, the J. Young tube was loaded with the desired amount of complex **Th-1** (1.5 μmol), DTC (0.2 mmol), ^{i}PrOH (0.2 mmol), 1,3,5-trimethoxybenzene (59.5 μmol, as internal standard) from stock solutions, diluted to a final volume of 0.55 mL with C_6D_6, and sealed. Then the sample was inserted into Bruker Advance 300 spectrometer, which had been previously set to the desired temperature. The data was collected every 19 or 33 seconds up to a half-hour. Reaction rates were determined by the least square fit of initial product concentration versus time, and Eyring and Arrhenius's plots were shown in Figures S45-S47. Enthalpy ($\Delta H^{\neq}$), entropy ($\Delta S^{\neq}$), and activation energy (E_a) were calculated from the slope and intercept of the least-square fit.

Deuterium labeling studies. All the KIE experiments were done in a similar method as the kinetic experiments. In a typical sample, the J. Young tube was loaded with the desired amount of complex **Th-1** (1.5 μmol), DTC (0.2 mmol), ^{i}PrOD (0.2 mmol), 1,3,5-trimethoxybenzene (59.5 μmol, as internal standard) from stock solutions, and diluted to a final volume of 0.55 mL with C_6D_6, and sealed. The NMR tube was frozen until the ^{1}H NMR experiment began at 25 ^{0}C. The KIE value was calculated from the ratio of the two slopes, and the plots are presented in Figures S48.

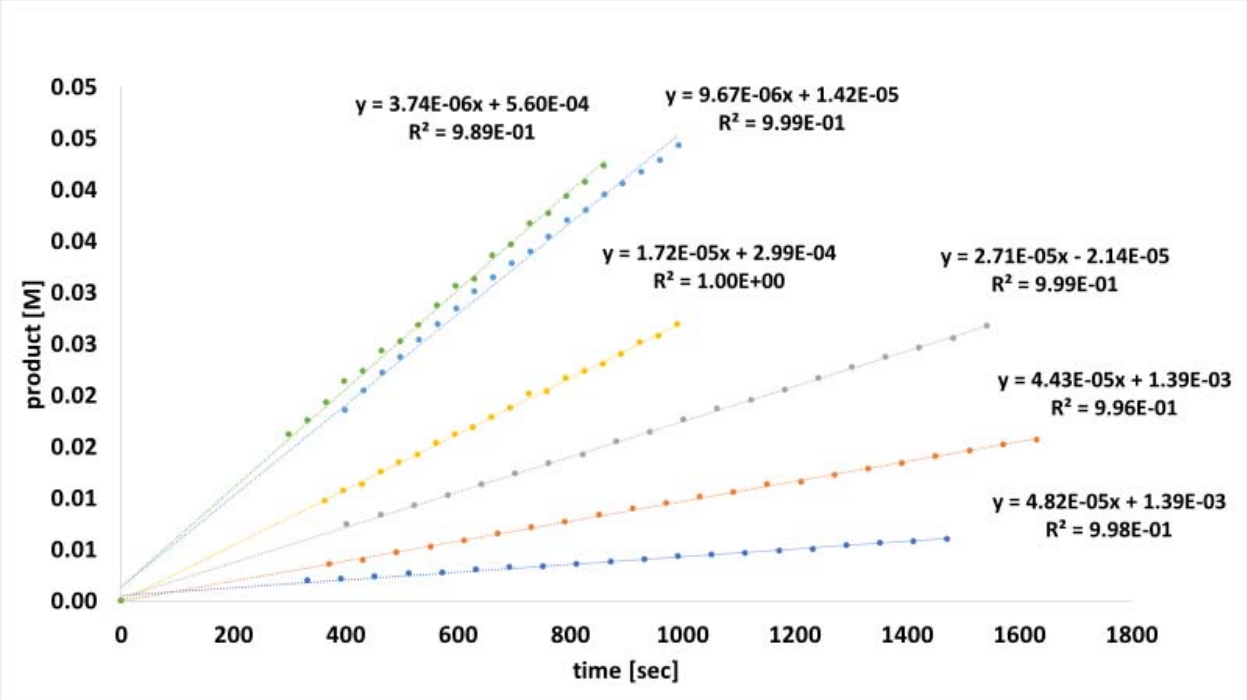

Figure S45. Initial reaction progress at different concentrations of complex **Th-1**. (0.727 mM (●), 1.364 mM (●), 1.818 mM (●), 3.636 mM (●), 5.455 mM (●) , 7.273 mM (●)).

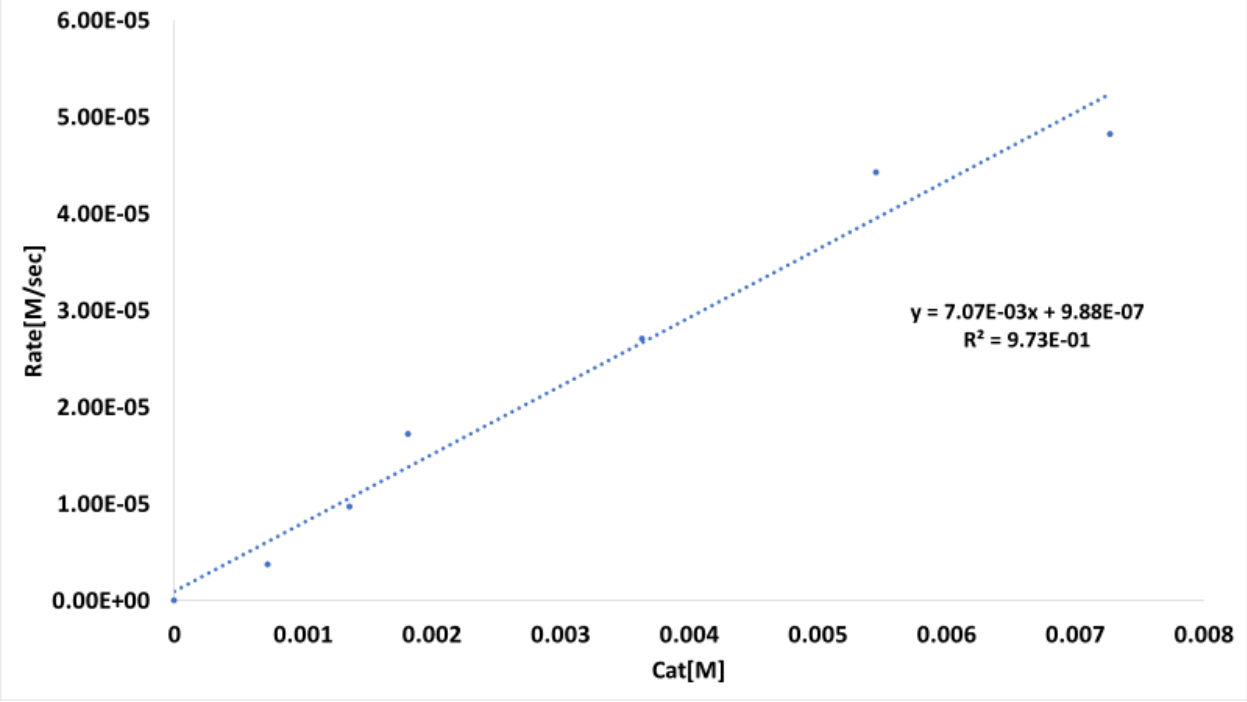

Figure S46. Plot of the initial reaction rate as a function of complex [**Th-1**] concentration.

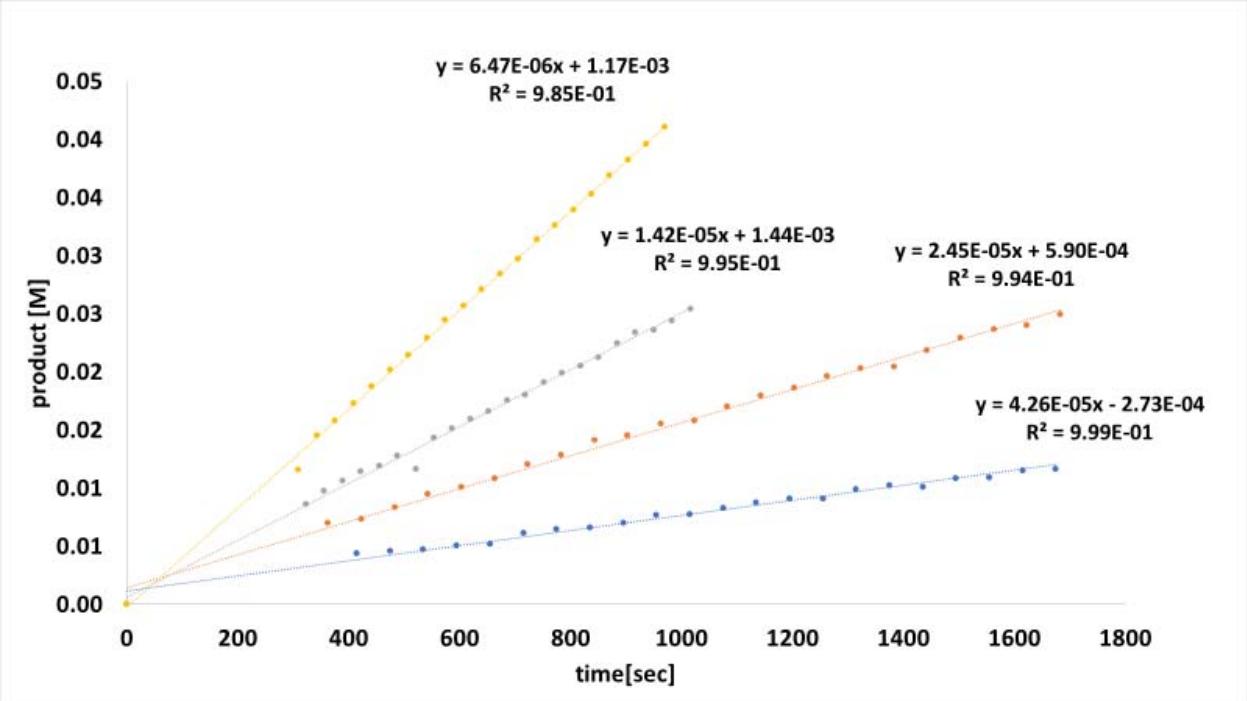

Figure S47. Initial reaction progress at different concentrations of DTC. (0.109 M (●), 0.273 M (●), 0.455 M (●), 0.909 M (●).

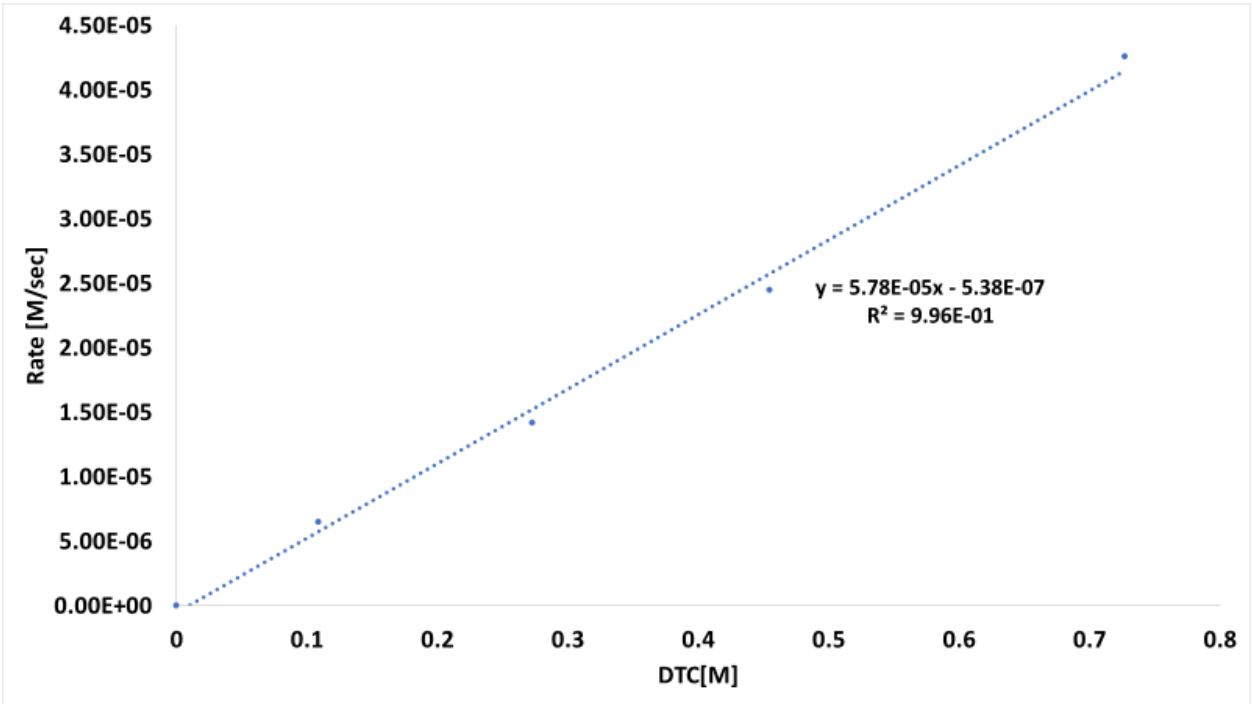

Figure S48. Plot of the initial reaction rate as a function of [DTC]

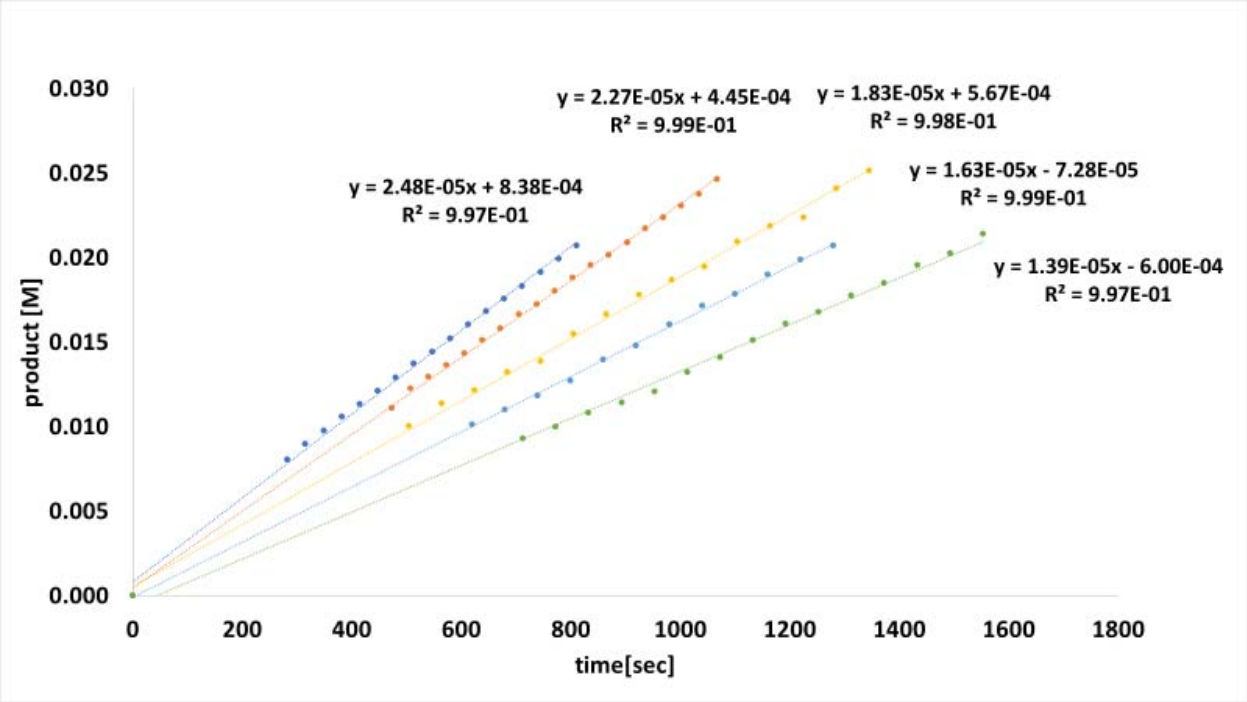

Figure S49. Initial reaction progress at different concentrations of ^{i}PrOH. (0.109 M (●), 0.273 M (●), 0.455 M (●), 0.545 M (●), 0.727 M (●)).

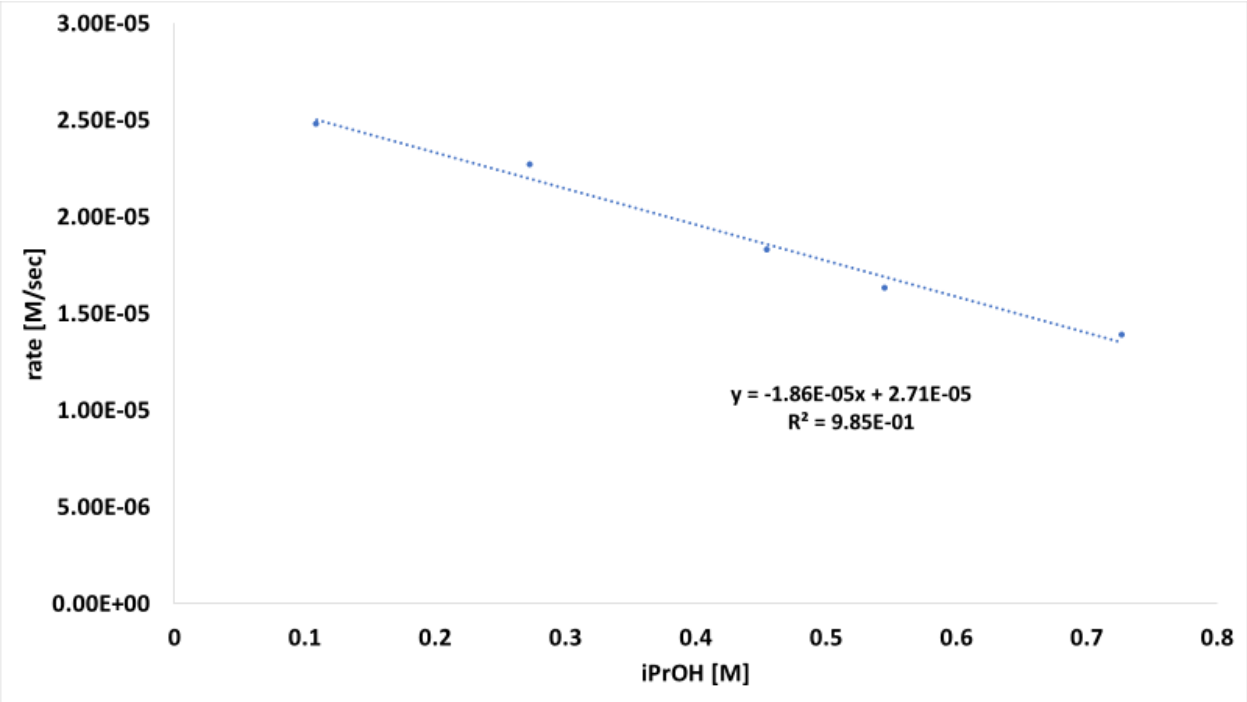

Figure S50. Plot of the initial reaction rate as a function of [^{i}PrOH]

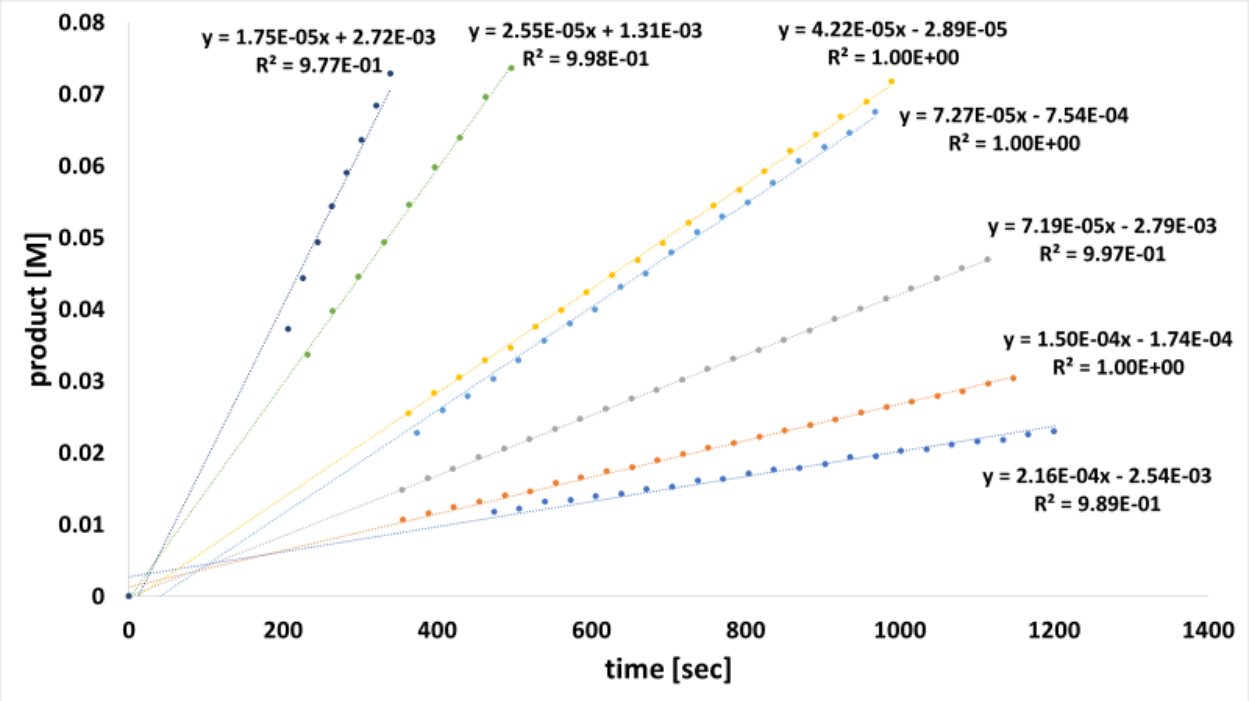

Figure S51. Initial reaction progress at different temperatures (21 (●), 25 (●), 30 (●), 35 (●), 40 (●), 45 (●) and 50 °C (●)) for the reaction between ^{i}PrOH and DTC using complex

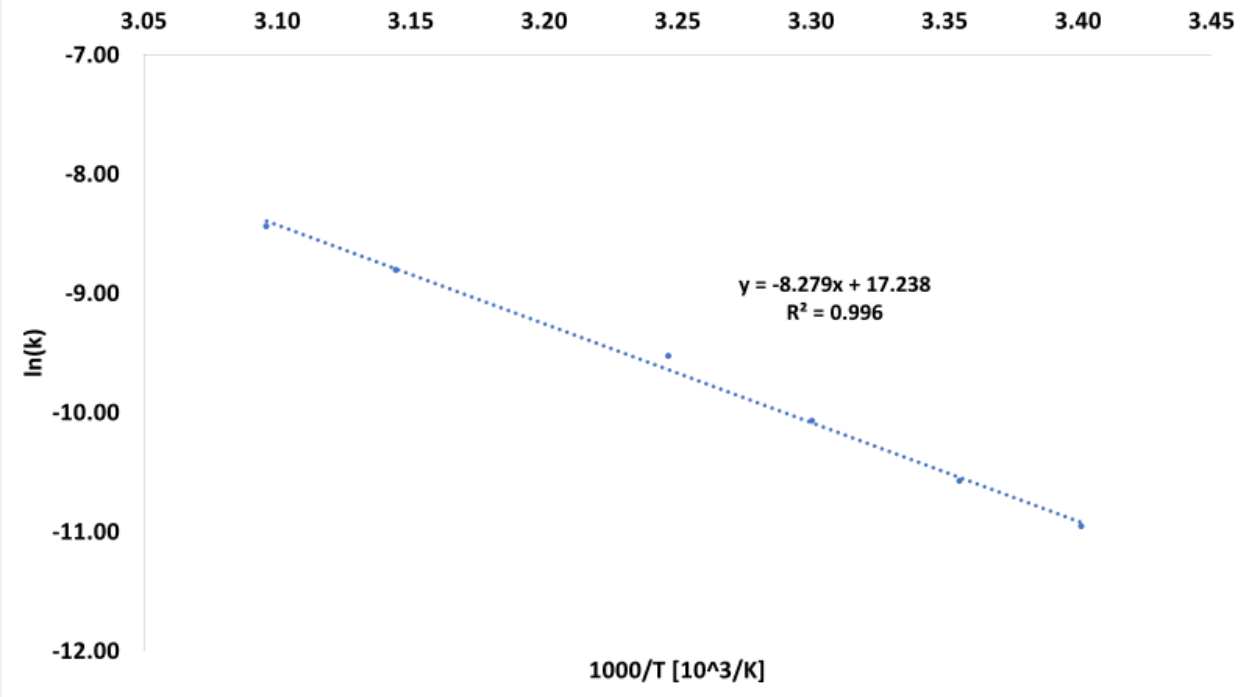

Figure S52. Arrhenius plot for the reaction between ^{i}PrOH and DTC using complex **Th-1** at different temperatures 21, 25, 30, 35, 40, 45 and 50 °C.

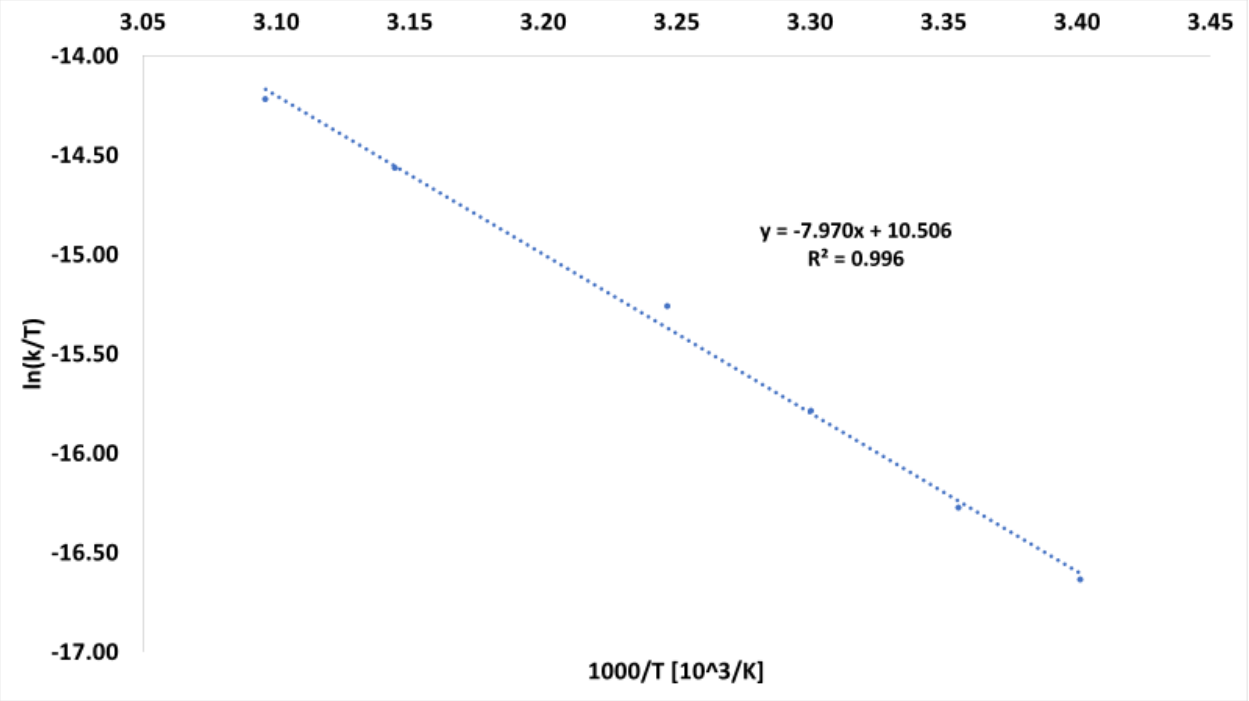

Figure S53. Eyring plot for the reaction between ^{i}PrOH and DTC using complex **Th-1** at different temperatures 21, 25, 30, 35, 40, 45 and 50 ºC.

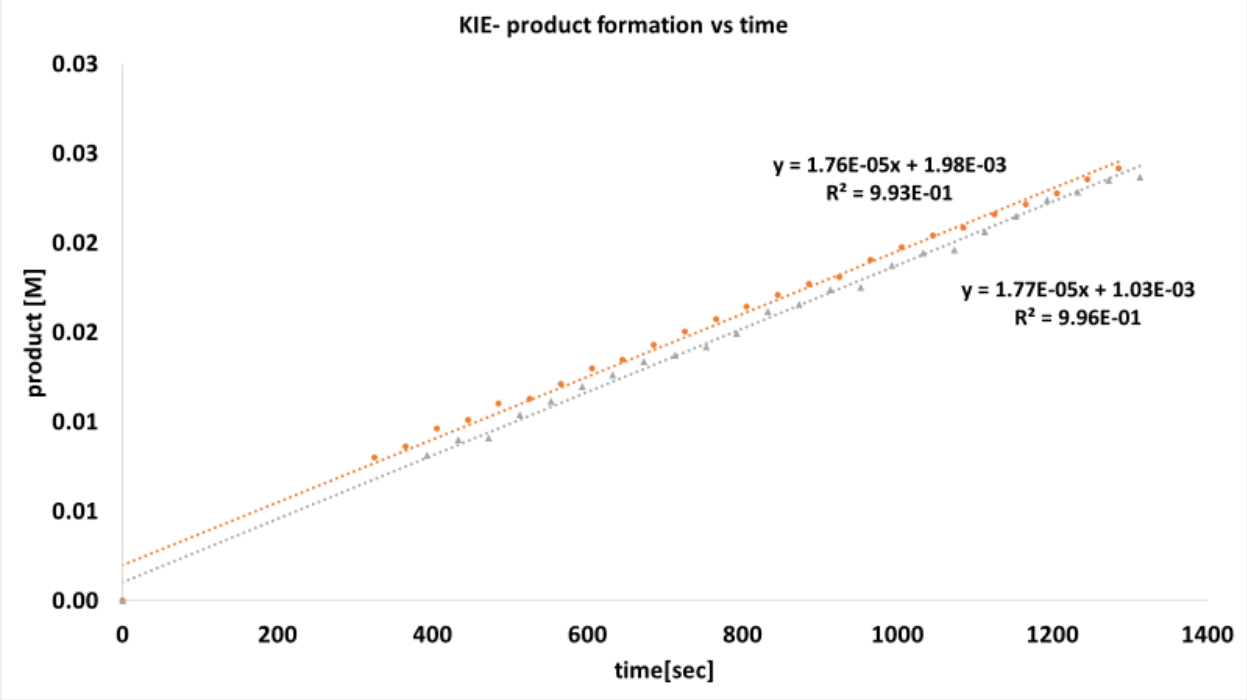

Figure S54. Initial reaction progress using, ^{i}PrOH (●), ^{i}PrOD (●).

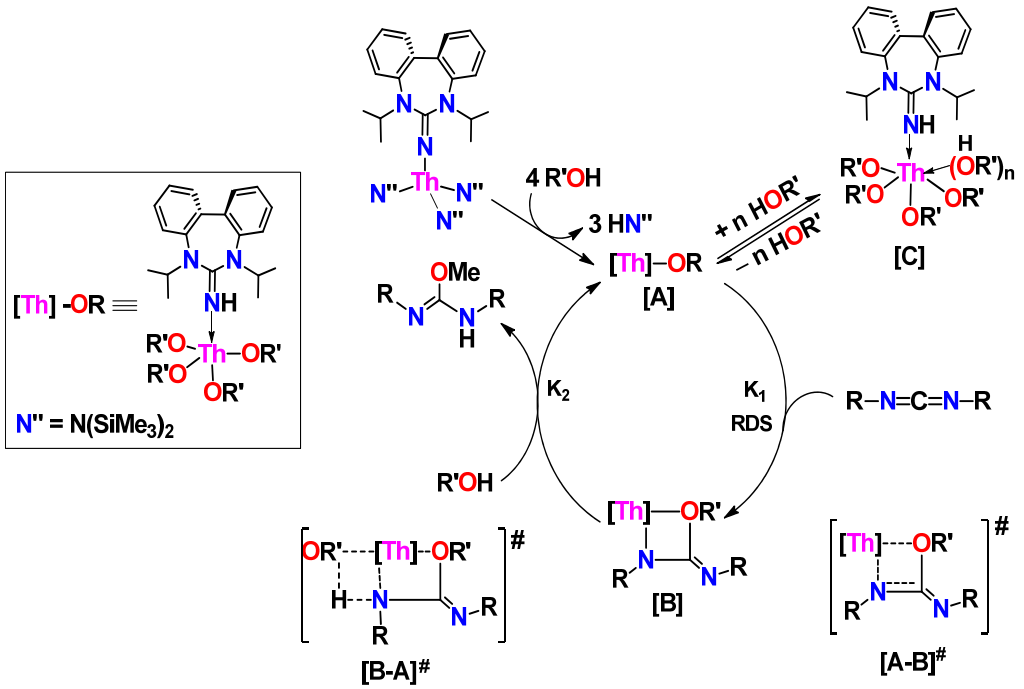

Scheme S3. A plausible mechanism of the actinide-mediated catalytic insertion of alcohol into carbodiimide mediated by complex **Th-1**.

According to the proposed mechanism (Scheme S3), the insertion of DTC into Th-O^{i}Pr bond is the rate-determining step (k_1) based on the experimental results. Therefore, we can assume a steady-state approximation giving the following rate equations:

$$\text{Eq.1}: \quad \frac{\partial p}{\partial t} = k_1 \cdot [Cat-A] \cdot [DTC]$$

While the first step is rapid and irreversible protonation of **Th-1** by iPrOH leading to the formation of **Cat-A** species. An equilibrium is must be considered as we noticed that increased amounts of alcohol slow down the reaction rate. Thus, suggesting the formation of spices (**C**) giving the following expression:

$$\text{Eq.2}: \quad K_{eq} = \frac{[C]}{[Cat-A] \cdot [i\,\mathrm{Pr}OH]}$$

Assuming that the total amount of the catalyst used in the reaction (**Th-1**) and present during the catalytic cycle is the sum of the active catalyst (**Cat-A**), and the alcohol saturated spices (**C**): [Cat-A] + [C] = [Th]. After substitution of [**Cat-A**] from equilibrium expression into rate equation, the following kinetic rate law is obtained:

$$\text{Eq.3}: \quad \frac{\partial p}{\partial t} = k_1 \cdot \frac{[Th] \cdot [DTC]}{(1 + K_{eq} \cdot [i\,\mathrm{Pr}OH])}$$

If K_{eq}[^{i}PrOH] is very large, giving the following equation:

$$\text{Eq.4}: \quad \frac{\partial p}{\partial t} = k_{obs} \cdot \frac{[Th] \cdot [DTC]}{[i\,\mathrm{Pr}OH]}$$

3. Stoichiometric reactions

All the stoichiometric experiments were performed in the glovebox following a similar methodology. A J. Young NMR tube was loaded with the typical amount of complex **Th-1** from a stock solution followed by the addition of the desired amount of ^{i}PrOH or DTC from a stock solution, and the total volume was made up to 0.55 mL with the appropriate solvent. The NMR tube was sealed taken out of the glovebox and monitored by ^{1}H NMR spectroscopy.

Th-1, The following complex was prepared according to a known procedure.[5]

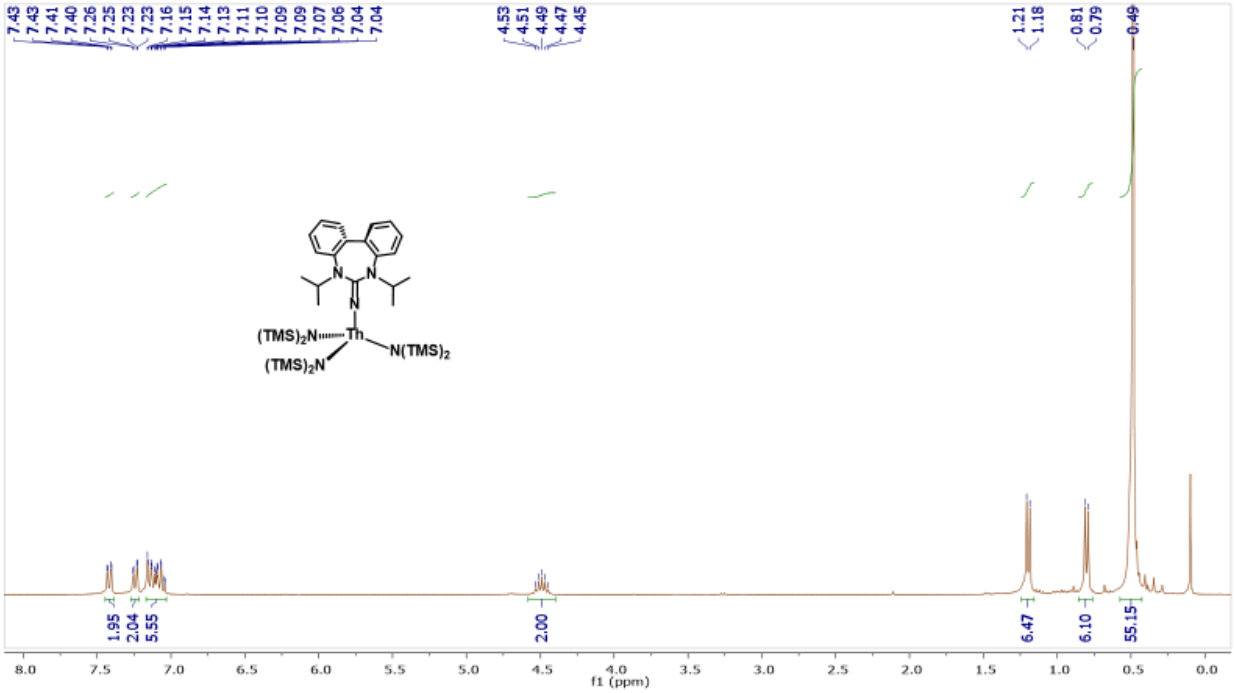

Figure S55. ^{1}H NMR spectra of **Th-1** in C_6D_6.

^{1}H NMR (300 MHz, C_6D_6) δ 7.42 (d, *J* = 5.6 Hz, 2H, Ar*H*), 7.24 (d, *J* = 7.4 Hz, 2H, Ar*H*), 7.17 – 7.10 (m, 2H, Ar*H*), 7.07 (m, 2H, Ar*H*), 4.54 – 4.41 (m, 2H, -*CH*$(CH_3)_2$), 1.20 (d, *J* = 6.3 Hz, 6H, -CH(*CH*$_3$)$_2$), 0.80 (d, *J* = 6.3 Hz, 6H, -CH(*CH*$_3$)$_2$), 0.49 (s, 54H, -N(TMS)$_2$).

L[1]H, The following ligand was prepared according to a known procedure.[4]

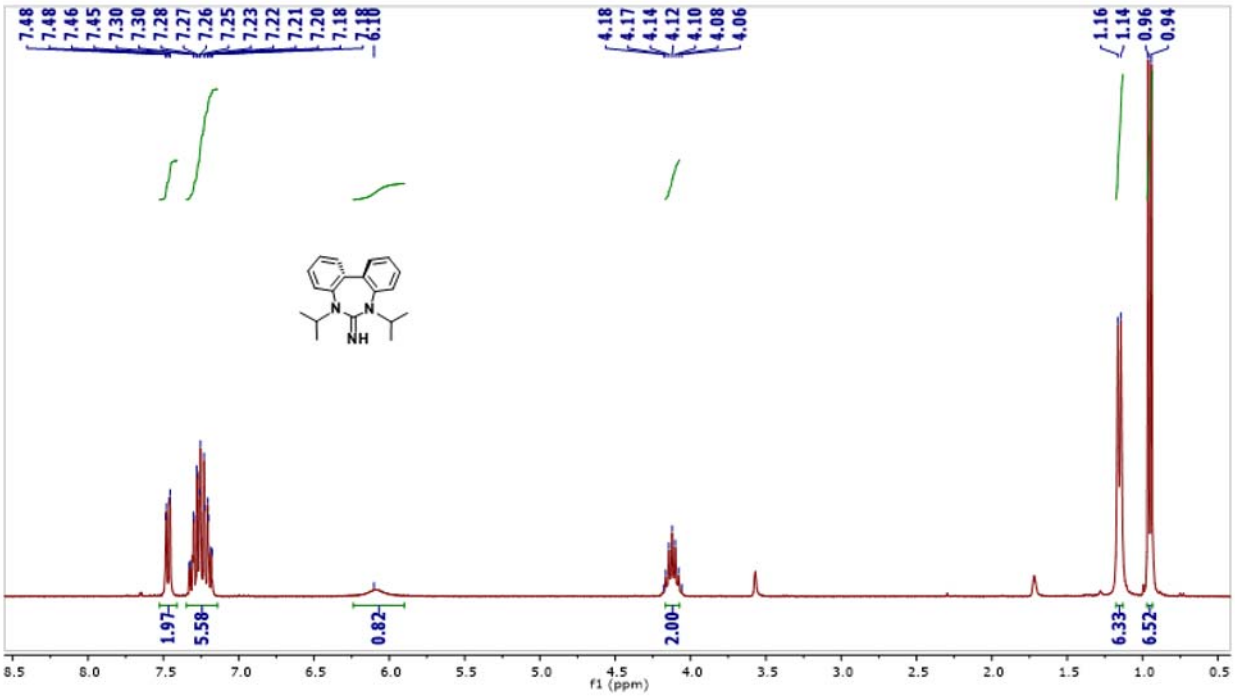

Figure S56. [1]H NMR spectra of **L[1]H** in THF-d.

[1]H NMR (300 MHz, THF) δ 7.47 (dd, *J* = 7.4, 1.5 Hz, 2H, Ar*H*), 7.35 – 7.14 (m, 6H, Ar*H*), 6.10 (s, 1H, -NH), 4.12 (septet, 2H, -*CH*(CH$_3$)$_2$), 1.15 (d, *J* = 6.4 Hz, 6H, -CH(*CH$_3$*)$_2$), 0.95 (d, *J* = 6.5 Hz, 6H, -CH(*CH$_3$*)$_2$).

Addition of *i*PrOH to complex **Th-1.**

8 equiv of *i*PrOH was added to a solution of 1 equiv complex **Th-1** and monitored by [1]H-NMR.

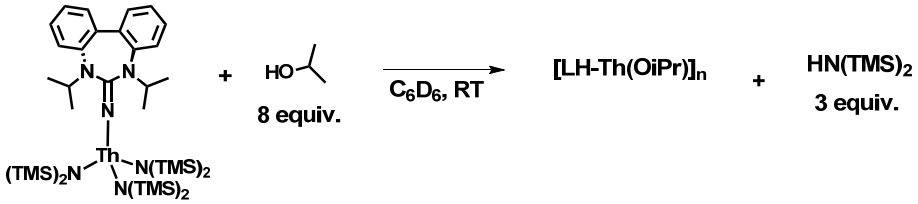

Scheme S4. The reaction of **Th-1** and eight equiv. of *i*PrOH.

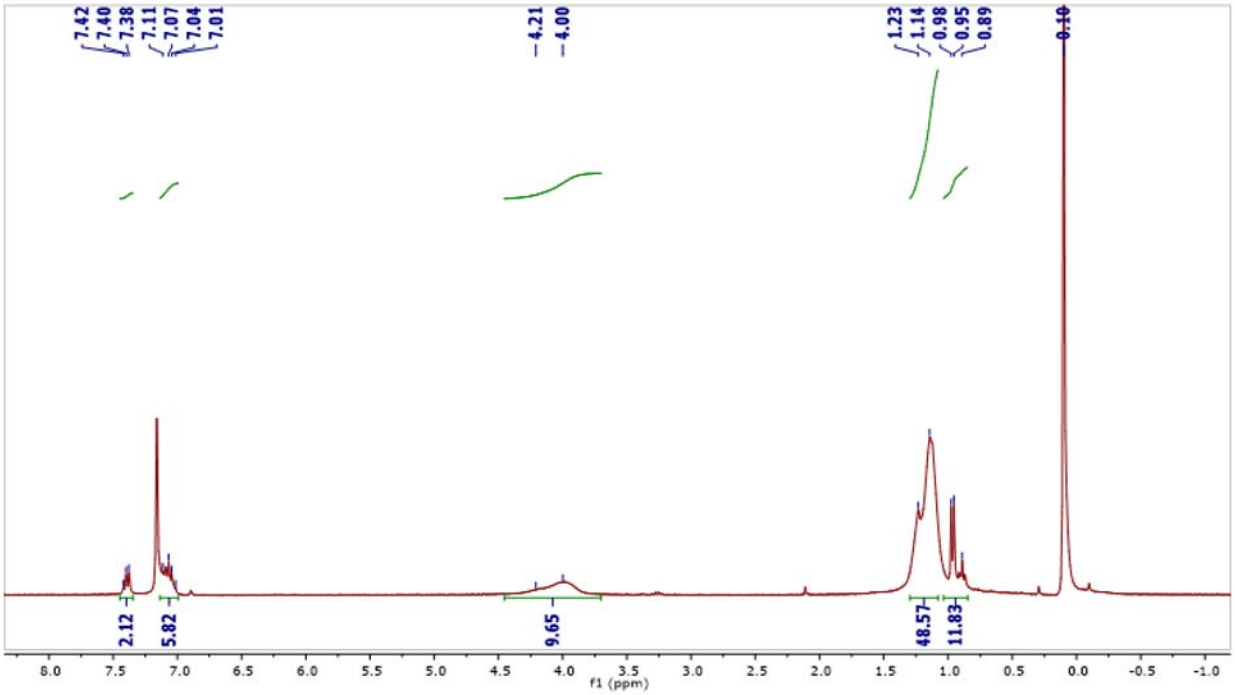

Figure S57. ^{1}H NMR of the reaction mixture of **Th-1** and 8 equiv. of ^{i}PrOH.

^{1}H NMR (300 MHz, C_6D_6) δ 7.45 – 7.34 (m, 2H, Ar*H*), 7.06 (m, 6H, Ar*H*), 4.21 – 4.00 (br, 10H, -*CH*$(CH_3)_2$, -O*CH*$(CH_3)_2$), 1.19 (br s, 48H, -OCH(*CH*$_3)_2$), 1.03 – 0.85 (m, 12H, -CH(*CH*$_3)_2$), 0.10 (s, 54H, -N(TMS)$_2$).

8 equiv of ^{i}PrOH was added to a solution of 1 equiv complex **Th-1** followed evaporation, and redissolving in C_6D_6 for monitored by ^{1}H-NMR.

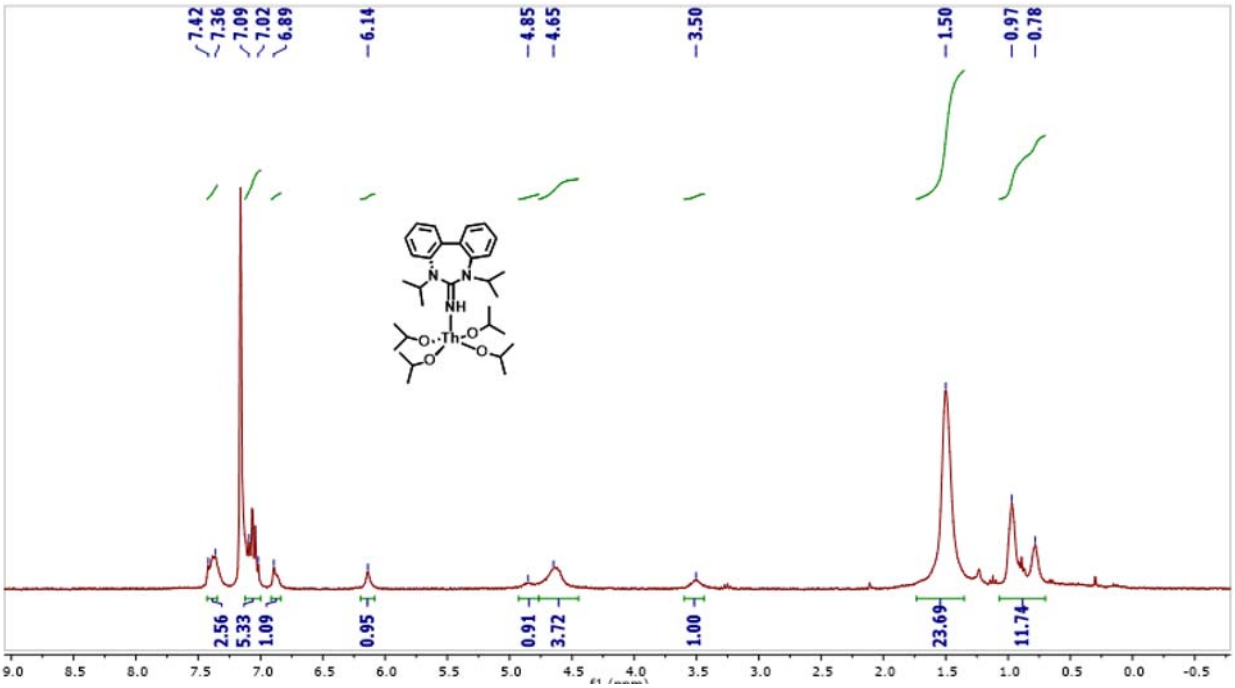

Figure S58. ^{1}H NMR of the reaction mixture of **Th-1** and 8 equiv. of ^{i}PrOH after evaporation.

^{1}H NMR (300 MHz, C_6D_6) δ 7.39 (m, 2H, ArH), 7.06 (m, 5H, ArH), 6.89 (m, 1H, ArH), 6.14 (s, 1H, -NH), 4.85 (s, 1H, -*CH*$(CH_3)_2$), 4.65 (s, 4H, -O*CH*$(CH_3)_2$), 3.50 (s, 1H, -*CH*$(CH_3)_2$), 1.50 (s, 24H, -OCH(*CH*$_3)_2$), 0.88 (m, 12H, -CH(*CH*$_3)_2$). MS (APCI): m/z 761.4160 (M+H)*-H.

8 equiv of ^{i}PrOH was added to a solution of 1 equiv complex **Th-1** followed by adding 4 equiv of DTC and monitored by ^{1}H-NMR.

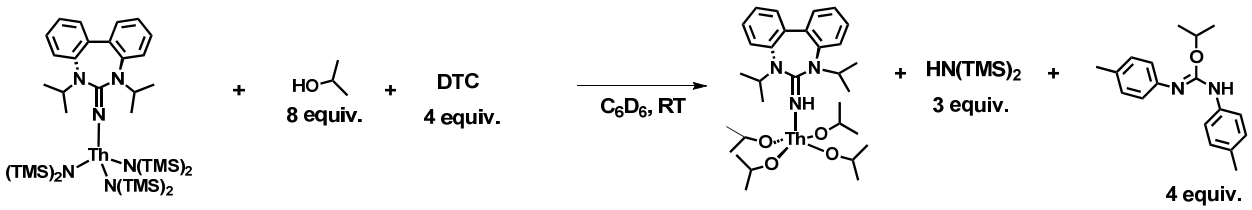

Scheme S5. Reaction of **Th-1** ,eight equiv of ^{i}PrOH, and 4 DTC.

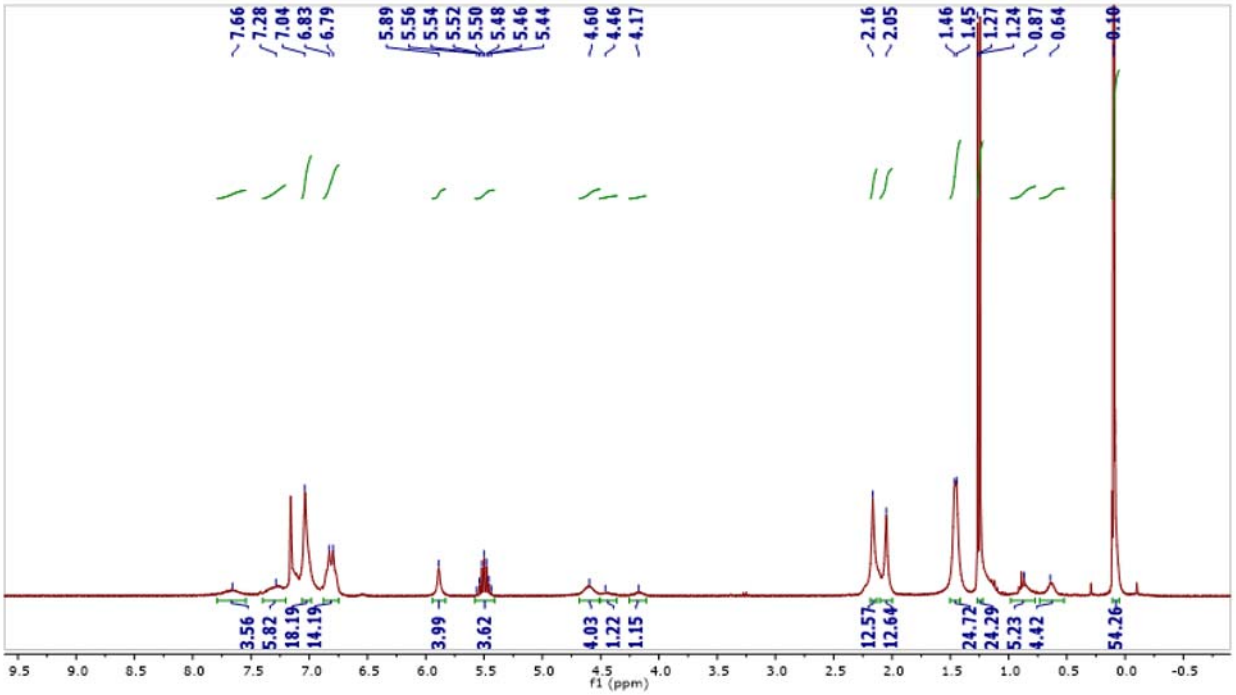

Figure S59. ^{1}H NMR of the reaction mixture of **Th-1** and 8 equiv of ^{i}PrOH and 4 equiv of DTC.

^{1}H NMR (300 MHz, C_6D_6) δ 7.66 (m, 2H, Ar*H*), 7.28 (m, 6H, Ar*H*), 7.04 (m, 18H, Ar*H*), 6.81 (m, 14H, Ar*H*), 5.89 (s, 4H), 5.58 – 5.41 (m, 4H), 4.60 (s, 4H), 4.46 (s, 1H), 4.17 (s, 1H), 2.16 (s, 12H), 2.05 (s, 12H), 1.45 (d, *J* = 5.4 Hz, 24H), 1.25 (d, *J* = 6.2 Hz, 24H), 0.87 (m, 6H), 0.64 (m, 6H), 0.10 (s, 54H).

8 equiv of ^{i}PrOD was added to a solution of 1 equiv complex **Th-1** followed evaporation and redissolving in Tol-d_8 for monitoring by ^{1}H-NMR.

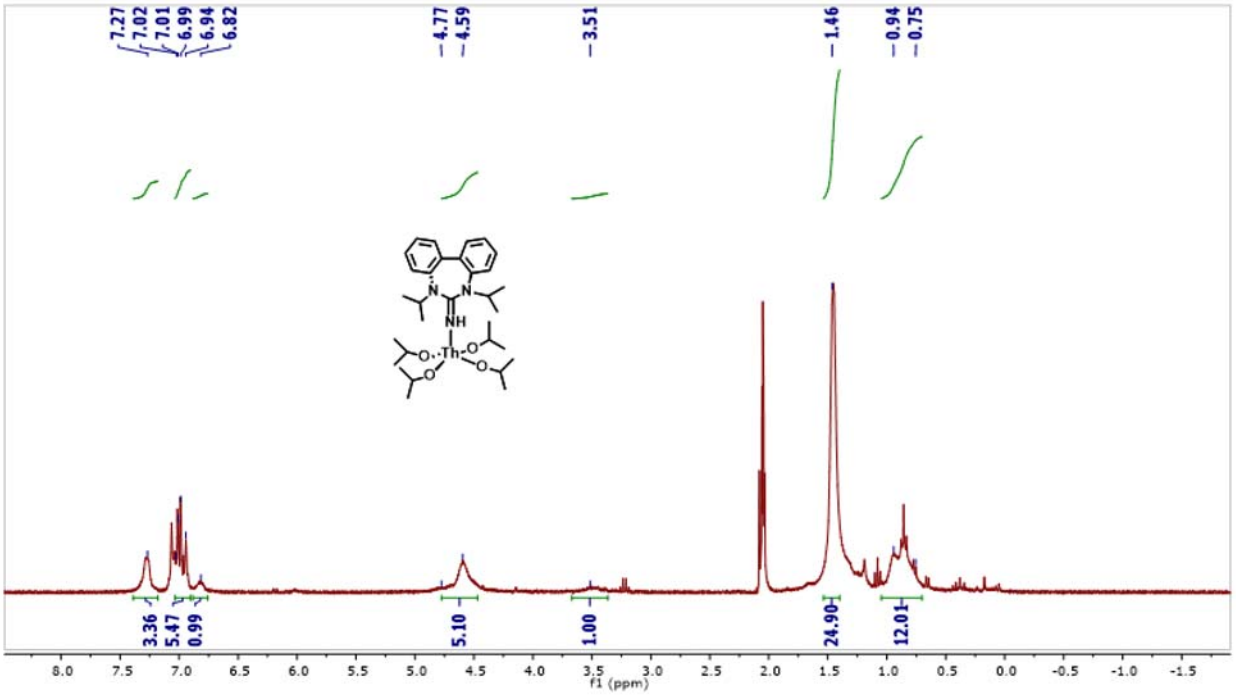

Figure S60. ^{1}H NMR of the reaction mixture of **Th-1** and 8 equiv of ^{i}PrOD followed evaporation, and redissolving in Tol-d_8 for monitored by ^{1}H-NMR.

^{1}H NMR (300 MHz, Tol) δ 7.27 (m, 2H, ArH), 6.99 (m, 5H, ArH), 6.82 (m, 1H, ArH), 4.68 (m, 5H, -O*CH*$(CH_3)_2$, -*CH*$(CH_3)_2$), 3.51 (m, 1H, -*CH*$(CH_3)_2$), 1.46 (br, 24H, -OCH(*CH*$_3)_2$), 0.85 (br, 12H, -CH(*CH*$_3)_2$).

8 equiv of ^{i}PrOH was added to a solution of 1 equiv complex **Th-1** followed evaporation and redissolving in Tol-d_8 for monitoring by ^{1}H-NMR at 90ºC.

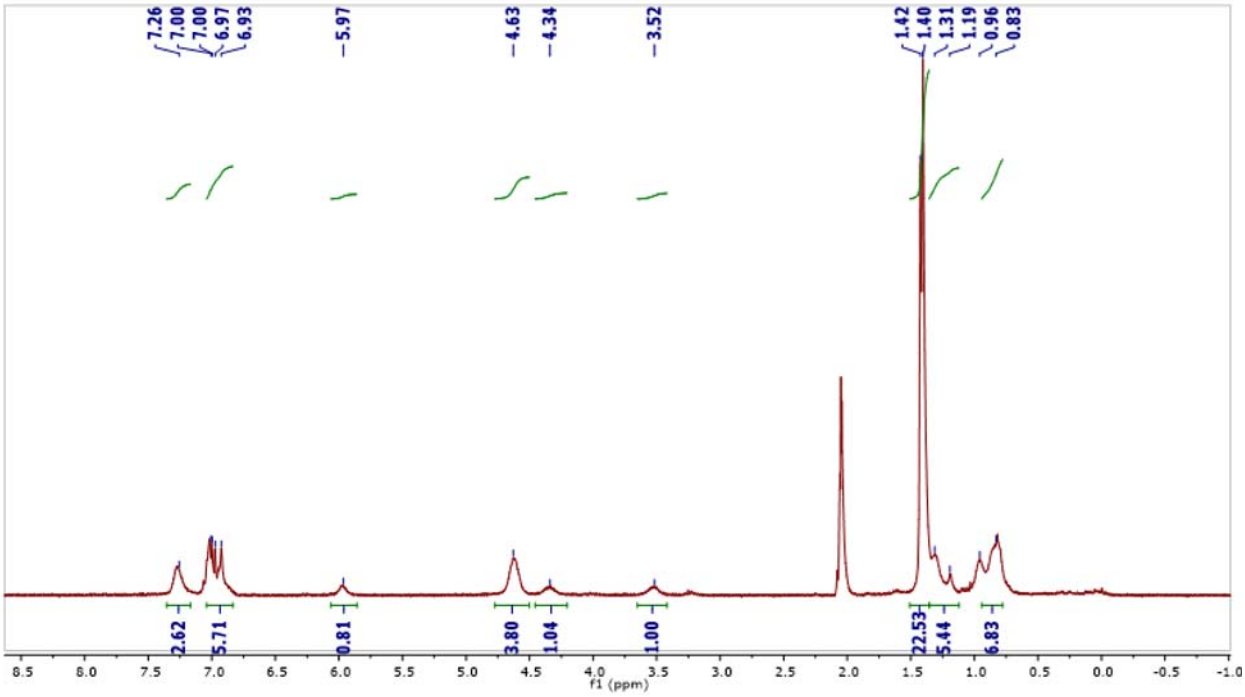

Figure S61. ^{1}H NMR of the reaction mixture of **Th-1** and 8 equiv of ^{i}PrOH followed evaporation, and redissolving in Tol-d for monitored by ^{1}H-NMR at 90ºC.

^{1}H NMR (300 MHz, Tol) δ 7.26 (m, 2H, Ar*H*), 6.97 (m, 5H, Ar*H*), 5.97 (s, 1H, -NH), 4.63 (m, 4H, -O*CH*(CH_3)$_2$), 4.34 (m, 1H, -*CH*(CH_3)$_2$), 3.52 (m, 1H, -*CH*(CH_3)$_2$), 1.41 (br d, 24H, -OCH(*CH_3*)$_2$), 1.25 (br d, 6H, -CH(*CH_3*)$_2$), 0.83 (br d, 6H, -CH(*CH_3*)$_2$).

4. IR experiments.

Free ligand spectrum, L^1H.

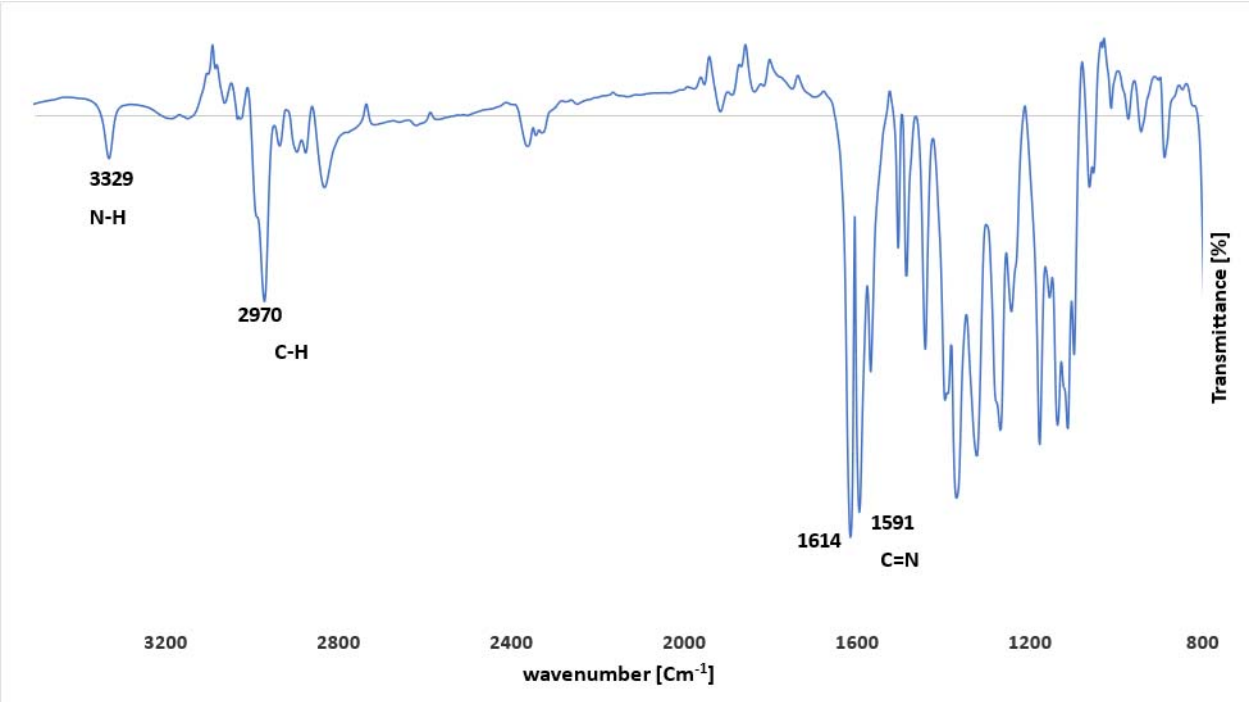

Figure S62. IR spectra of **L^1H**.

Figure S62 showes the free ligand IR spectrum, N-H strech, cm^{-1}. Methyl C-H strech, 2970, 2856 cm^{-1}. C=N strech, 1614 cm^{-1}.

IR spectrum of complex **Th-1**.

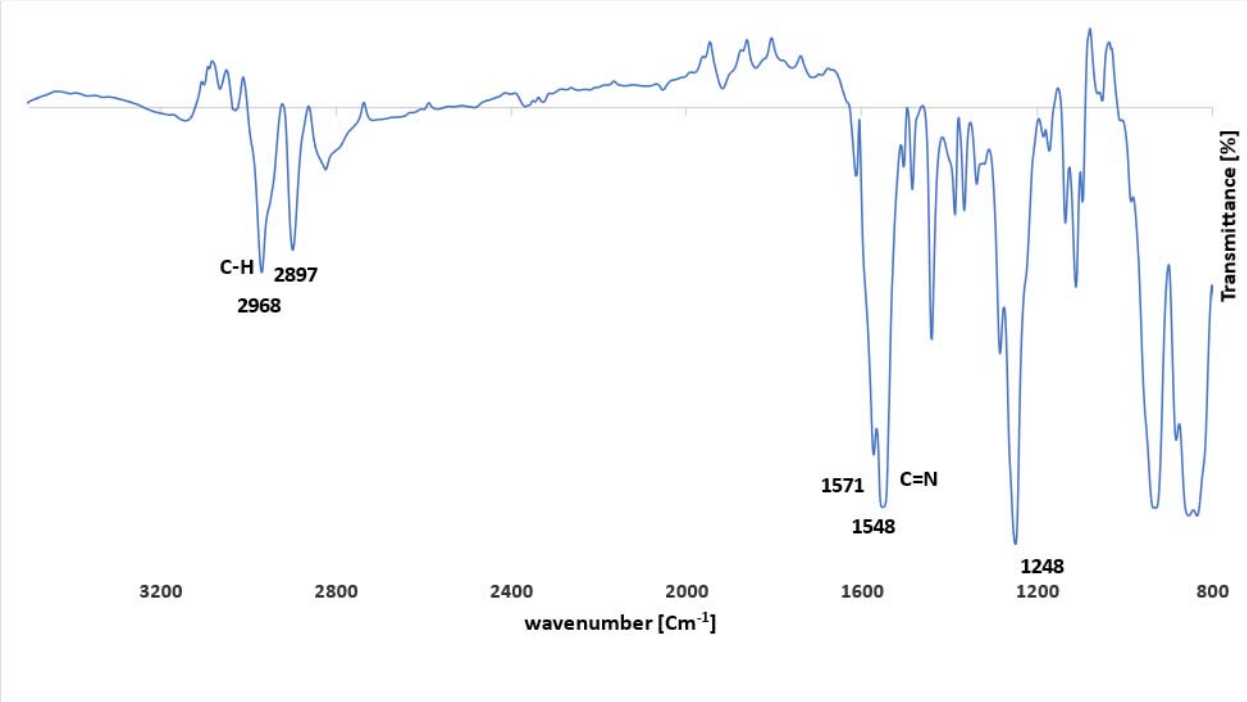

Figure S63. IR spectra of **Th-1.**

Figure S63 shows the **Th-1** IR spectrum, the absence of N-H stretch could be noticed. Methyl C-H stretch, 2968, 2897 cm^{-1}. C=N stretch weakened upon complexation and appears at 1571,1548 cm^{-1}.

IR overlay spectrum of **Th-1** complex reacted with 8 equiv of ^{i}PrOH for 30 min at room temperature, followed by solvent evaporation. The same procedure was performed with ^{i}PrOD. The IR spectra were recorded.

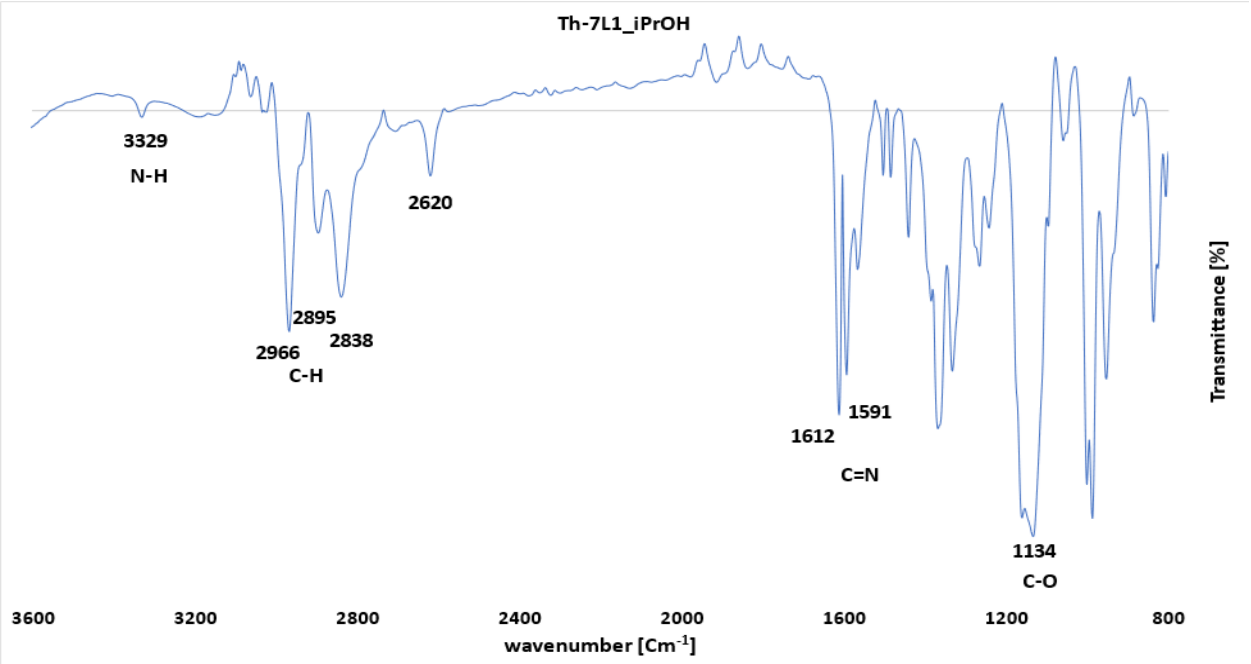

Figure S64. IR spectra of **Th-1** with ^{i}PrOH**.**

Figure S64 shows the IR spectrum of the reaction between **Th-1** and ^{i}PrOH Methyl C-H stretch, 2966, 2895, 2838 cm^{-1}. C=N stretch ,1612 ,1591 cm^{-1}. Strong C-O stretch 1134 cm^{-1}. The typical N-H steching of the free ligand appears at 3329. No signal at 2970 cm^{-1} of the C-H of the free ligand is observed sugesting that the ligand remain attached.

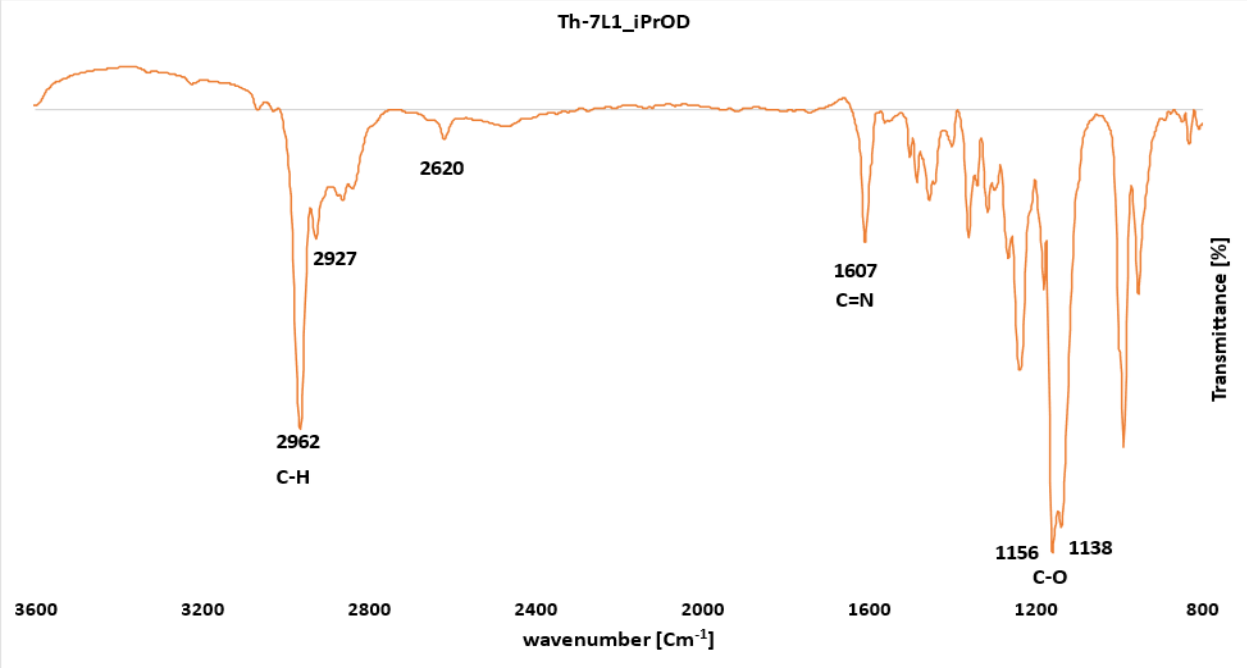

Figure S65. IR spectra of **Th-1** with iPrOD.

Figure S65 shows the IR spectrum of the reaction between **Th-1** and ^{i}PrOD No signal of N-D is observed or asignal at 2970 cm^{-1} of the C-H of the free ligand.

5. References

(1) Ali, A. R.; Ghosh, H.; Patel, B. K. A Greener Synthetic Protocol for the Preparation of Carbodiimide. *Tetrahedron Lett.* **2010**, *51* (7), 1019–1021.

(2) Peddarao, T.; Baishya, A.; Barman, M. K.; Kumar, A.; Nembenna, S. Metal-Free Access of Bulky N,N′-Diarylcarbodiimides and Their Reduction: Bulky N,N′-Diarylformamidines. *New J. Chem.* **2016**, *40* (9), 7627–7636.

(3) Dormond, A.; El Bouadili, A. A.; Moïse, C. Insertion of Carbonyl Compounds into Actinide-Carbon σ Bonds: Reactivity of $[(Me_3Si)_2N]_2MCH_2Si(Me_2)NSiMe_3$. *J. Chem. Soc., Chem. Commun.* **1985**, *288*, 914 – 916.

(4) Ghatak, T.; Drucker, S.; Fridman, N.; Eisen, M. S. Thorium Complexes Possessing Expanded Ring N-Heterocyclic Iminato Ligands: Synthesis and Applications. *Dalton. Trans.* **2017**, *46* (36), 12005–12009.

(5) Ghatak, T.; Makarov, K.; Fridman, N.; Eisen, M. S. Catalytic Regeneration of a Th–H Bond from a Th–O Bond through a Mild and Chemoselective Carbonyl Hydroboration. *Chem. Commun.* **2018**, *54* (78), 11001–11004.

(6) Saha, S.; Eisen, M. S. Catalytic Recycling of a Th–H Bond via Single or Double Hydroboration of Inactivated Imines or Nitriles. *ACS Catal.* **2019**, *9* (7), 5947–5956.

(7) Otwinowski, Z.; Minor, W. Processing of X-Ray Diffraction Data Collected in Oscillation Mode. *Methods in Enzymology* **1997**, *276*, 307 – 326.

(8) Farrugia, L. J. WinGX and ORTEP for Windows : An Update. *J. Appl. Crystallogr*. **2012**, *45* (4), 849–854.
(9) Sheldrick, G. M. Crystal Structure Refinement with SHELXL. *Acta Crystallogr. Sect. C Struct. Chem.* **2015**, *71*, 3 – 8.
(10) Liu, H.; Fridman, N.; Tamm, M.; Eisen, M. S. Catalytic Addition of Alcohols to Carbodiimides Mediated by Benzimidazolin-2-Iminato Actinide Complexes. *Organometallics* **2017**, *36* (23), 4600–4610.